

Regulation of glucocorticoid-induced leucine zipper (GILZ) in vascular inflammation

Dissertation
zur Erlangung des Grades
des Doktors der Naturwissenschaften
der Naturwissenschaftlich-Technischen Fakultät III
Chemie, Pharmazie, Bio- und Werkstoffwissenschaften
der Universität des Saarlandes

von

Rebecca T. Hahn

Saarbrücken
2015

Tag des Kolloquiums: 06.08.2015
Dekan: Univ.-Professor Dr.-Ing. Dirk Bähre
1. Berichterstatter: Prof. Dr. Alexandra K.Kiemer
2. Berichterstatter: Prof. Dr. Claus-Michael Lehr
Vorsitz: Prof. Dr. Marc Schneider
Akademischer Mitarbeiter: Dr. Sascha Tierling

Contents

ABBREVIATIONS	1
ABSTRACT	5
ZUSAMMENFASSUNG	6
1 INTRODUCTION	7
1.1 ATHEROSCLEROSIS	8
1.1.1 <i>General</i>	8
1.1.2 <i>Origin and progression</i>	8
1.1.3 <i>Therapeutic options</i>	10
1.2 SHEAR STRESS.....	12
1.2.1 <i>General</i>	12
1.2.2 <i>Mechanotransduction</i>	14
1.2.3 <i>Options of gene expression modification</i>	15
1.2.4 <i>Functions of Shear Stress</i>	17
1.3 GLUCOCORTICOID-INDUCED LEUCINE ZIPPER (GILZ)	19
1.3.1 <i>General</i>	19
1.3.2 <i>Regulation of GILZ</i>	20
1.3.3 <i>Functions of GILZ</i>	21
1.4 FURTHER REGULATORS OF INFLAMMATION.....	23
1.4.1 <i>Heme oxygenase 1 (HO1)</i>	23
1.4.2 <i>Dual specificity protein phosphatase 1 (DUSP1, MKP-1)</i>	24
1.4.3 <i>p38 mitogen-activated protein kinase (p38 MAPK)</i>	25
1.4.4 <i>Tristetraprolin (ZFP36, TTP)</i>	26
1.5 EPIGENETICS.....	27
1.5.1 <i>Imprinted genes H19 and IGF2</i>	28
1.6 AIM OF THIS WORK	30
2 MATERIALS AND METHODS	31
2.1 MATERIALS	32
2.2 HUMAN VESSELS	33
2.3 BACTERIAL CULTURE	33
2.3.1 <i>Bacterial strains and cultivation</i>	33
2.3.2 <i>Generation of competent bacteria using CaCl₂ method</i>	34
2.3.3 <i>Transformation</i>	34
2.3.4 <i>Isolation of plasmids</i>	34
2.3.5 <i>Determination of DNA concentration</i>	34
2.4 CELL CULTURE	35
2.4.1 <i>THP-1</i>	35

2.4.2	<i>Human umbilical vein endothelial cells (HUVEC)</i>	35
2.4.3	<i>Isolation of HUVEC</i>	35
2.4.4	<i>Cultivation of HUVEC</i>	36
2.4.5	<i>Freezing and thawing of HUVEC</i>	36
2.4.6	<i>Detection of mycoplasma</i>	36
2.5	TRANSFECTION	37
2.6	LUCIFERASE ASSAY	37
2.7	SHEAR STRESS	38
2.7.1	<i>Coating of glass slides</i>	38
2.7.2	<i>Flow experiments</i>	38
2.8	IMMUNOHISTOCHEMISTRY	40
2.9	RNA ANALYSIS	40
2.9.1	<i>RNA isolation by phenol chloroform extraction</i>	40
2.9.2	<i>DNase digestion</i>	41
2.9.3	<i>Determination of RNA concentration</i>	41
2.9.4	<i>Alu polymerase chain reaction (Alu PCR)</i>	41
2.9.5	<i>Agarose gel electrophoresis</i>	42
2.9.6	<i>Reverse transcription (RT)</i>	43
2.9.7	<i>Real-time RT-PCR</i>	43
2.10	DNA ANALYSIS	48
2.10.1	<i>DNA isolation</i>	48
2.10.2	<i>Determination of DNA concentration</i>	48
2.10.3	<i>Bisulfite treatment</i>	48
2.10.4	<i>PCR of bisulfite DNA</i>	49
2.10.5	<i>Exonuclease phosphatase treatment (ExoSAP)</i>	50
2.10.6	<i>Restriction digestion</i>	50
2.10.7	<i>Single nucleotide primer extension (SNuPE)</i>	51
2.11	PROTEIN ANALYSIS	52
2.11.1	<i>Protein isolation</i>	52
2.11.2	<i>Determination of protein concentration</i>	53
2.11.3	<i>SDS-polyacrylamide gel electrophoresis (SDS-Page)</i>	53
2.11.4	<i>Western Blot</i>	54
2.11.5	<i>Immunodetection</i>	54
2.12	STATISTICS	55
3	RESULTS	56
3.1	DOWNREGULATION OF GLUCOCORTICOID-INDUCED LEUCINE ZIPPER (<i>GILZ</i>) PROMOTES VASCULAR INFLAMMATION	57
3.1.1	<i>GILZ expression in degenerated vein bypasses</i>	57
3.1.2	<i>Localisation of GILZ in vessels</i>	59
3.1.3	<i>Inflammatory response in EC</i>	60

3.1.4	<i>Regulation of GILZ and ZFP36 by anti-inflammatory laminar shear stress.....</i>	63
3.1.5	<i>Mechanisms of GILZ downregulation in inflammation.....</i>	65
3.1.6	<i>Functional implications of GILZ downregulation.....</i>	69
3.2	LACK OF ENDOTHELIAL GLUCOCORTICOID-INDUCED LEUCINE ZIPPER (GILZ) INDUCTION UNDER ATHEROGENIC FLOW CONDITIONS	70
3.2.1	<i>Inflammatory activation of HUVEC by low and oscillatory flow</i>	70
3.2.2	<i>GILZ downregulation under inflammatory conditions</i>	71
3.2.3	<i>Mechanism of GILZ downregulation under oscillatory flow</i>	73
3.2.4	<i>Inflammatory activation in atherosclerotic clinical samples</i>	74
3.3	EPIGENETIC REGULATION BY SHEAR STRESS.....	75
3.3.1	<i>IGF2 and H19 under flow conditions</i>	75
3.3.2	<i>DNA Demethylation in HUVEC.....</i>	76
4	DISCUSSION.....	80
4.1	VALIDATION OF THE CELL CULTURE MODEL FOR SHEAR STRESS.....	81
4.1.1	<i>Shear stress models</i>	81
4.1.2	<i>Effects of shear stress</i>	81
4.2	GILZ DOWNREGULATION AT INFLAMMATORY CONDITIONS	83
4.3	MECHANISM OF GILZ REGULATION UNDER LAMINAR FLOW	84
4.3.1	<i>ZFP36 dependent GILZ downregulation</i>	85
4.3.2	<i>DUSP1 in atherosclerosis.....</i>	87
4.3.3	<i>Regulation of DUSP1 by shear stress</i>	88
4.4	MECHANISM OF GILZ REGULATION UNDER OSCILLATORY FLOW	89
4.5	FUNCTIONAL IMPLICATIONS OF GILZ DOWNREGULATION.....	90
4.6	REGULATION OF H19 AND IGF2 UNDER SHEAR STRESS.....	91
5	SUMMARY	93
5.1	SUMMARY	94
6	SUPPLEMENT	96
6.1	PLANS OF PARALLEL PLATE FLOW CHAMBERS.....	96
REFERENCES		98
PUBLICATIONS.....		122
ACKNOWLEDGEMENTS		123

Abbreviations

A	absorption
aa	amino acid
Amp	ampicillin
ANP	atrial natriuretic peptide
AP-1	activator protein-1
ApoB	apolipoprotein B
APS	ammonium persulfate
ARE	antioxidant responsive elements
atto	10^{-18}
aza	5-azacytidine
BAEC	bovine aortic endothelial cells
BHQ1	black hole quencher 1
bp	base pair
c	cellular
°C	degree Celsius
CCL2	chemokine (C-C motif) ligand 2 (monocyte chemoattractant protein 1, MCP1)
CCR2	C-C chemokine receptor 2
cDNA	complementary DNA
C/EBPb	CCAAT/enhancer binding protein-b
cm	centimeter
co	control
cox	cyclooxygenase
CpGs	CG dinucleotides
CREB	cyclic adenosine monophosphate response element-binding protein
C _T	threshold cycle
CTCF	CCCTC-binding factor
d	day
DAC	5-aza-2-deoxycytidine
dATP	deoxyadenosine triphosphate
dCTP	deoxycytidine triphosphate
dd	bidistilled
ddNTP	dideoxynucleosine triphosphate
DEPC	diethyl dicarbonate
dGTP	deoxyguanosine triphosphate
DMR	differentially methylated region
DMSO	dimethyl sulfoxide
dn	dominant negative
DNA	deoxyribonucleic acid
DNAse	deoxyribonuclease
DNMT	DNA (cytosine-5-)methyltransferase
dNTP	dideoxynucleosine triphosphate
dTTP	deoxythymidine triphosphate
DUSP1	dual specificity protein phosphatase 1 (mitogen-activated protein kinase phosphatase-1, MKP-1)
EC	endothelial cells
<i>E.coli</i>	<i>Escherichia coli</i>

EDTA	ethylene diamine tetraacetic acid
Egr-1	early growth response-1
eNOS	endothelial nitric oxide synthase
ERK	extracellular signal-regulated kinase
ESELE	E selectin
ExoSAP	exonuclease phosphatase treatment
f	femto (10^{-15})
FAK	focal adhesion kinase
6-FAM	6-carboxy-fluorescein
FCS	fetal calf serum
FHREs	forkhead responsive elements
Fox	forkhead box
FRET	fluorescence resonance energy transfer
g	gram
GFP	green fluorescent protein
GILZ	glucocorticoid-induced leucine zipper
GILZ-P	GILZ peptide
GR	glucocorticoid receptor
GREs	glucocorticoid responsive elements
GTPase	guanidine triphosphatase
h	hour
HAEC	human aortic endothelial cells
HAT	histone acetyltransferases
HDAC	histone deacetylase
HE	hematoxylin / eosin
HMG-CoA	3-hydroxy-3-methylglutaryl-coenzyme A
HO1	heme oxygenase 1
Hox	homeobox protein
HPLC	high performance liquid chromatography
HRMEC	human retinal microvascular endothelial cells
HuR	human antigen R
HUVEC	human umbilical vein endothelial cells
Hz	hertz
ICAM	intercellular adhesion molecule
IGF	insulin-like growth factor
IHC	immunhistochemistry
IκB	inhibitory protein kappa B
IL	interleukin
INF-γ	Interferon gamma
IP/RP-HPLC	ion pair reversed phase high performance liquid chromatography
JNK	c-Jun N-terminal kinase
kb	kilo bases = 1000 base pairs
kDa	kilodalton
KLF	Krüppel-like factor
l	liter
LB	Luria-Bertani
LDL	low density lipoprotein
lncRNAs	long non-coding RNAs
log	logarithm
LPS	lipopolysaccharide
LZ	leucine zipper

mA	milliampere
m	milli (10^{-3})
m	meter
M	molar
MAPK	mitogen-activated protein kinase
max.	maximal
MBD2	methyl CpG binding domain protein2
MIF	macrophage migration inhibitory factor
min	minute
miRNA	microRNA
MK	MAPK-activated protein kinase
mRNA	messenger RNA
MSK	mitogen- and stress activated protein kinase
MyD88	myeloid differentiation primary response 88
MΦ	macrophages
n	nano (10^{-9})
NAD(P)H	reduced nicotinamide adenine dinucleotide phosphate
NFAT	nuclear factor of activated T-cells
NF-κB	nuclear factor kappa B
NO	nitric oxide
NQO1	NAD(P)H dehydrogenase, quinone 1
Nrf2	nuclear factor erythroid 2-related factor 2
Nrf2-Keap1	nuclear factor erythroid 2-related factor 2 – Kelch-like erythroid cell-derived protein with CNC homology-associated protein 1
nt	nucleotides
NTD	N-terminal domain
oxLDL	oxidized LDL
p	pico (10^{-12})
Pa	pascal
PAGE	polyacrylamide gel electrophoresis
PBS	phosphate buffered saline
PBS ⁺	phosphate buffered saline ⁺
PBST	PBS with 0.1% [v/v] Tween 20
PCR	polymerase chain reaction
PDGF	platelet-derived growth factor
PECAM	platelet endothelial cell adhesion molecule
PER	proline and glutamic acid rich region
piRNAs	piwi-interacting RNAs
PKC	protein kinase C
PPAR γ	peroxisome proliferator-activated receptor γ
PVDF	polyvinylidene fluoride
Raf	rapidly accelerated fibrosarcoma
Ras	rat sarcoma
RBB	rockland blocking buffer
RNA	ribonucleic acid
RNAse	ribonuclease
ROS	reactive oxygen species
RT	reverse transcription
s	second
SDS	sodium dodecyl sulfate
SEM	standard error of the mean

Shc	Src homology 2 domain containing transforming protein
shRNA	small hairpin RNA
siRNA	small interfering RNA
SNuPE	single nucleotide primer extension
SOC	super optimal broth with glucose
SP1	specificity protein 1
SREBP-1	sterol regulatory element-binding protein-1
SSREs	shear stress responsive elements
STAT	signal transducer and activator of transcription
TAT-GILZ	transactivator of transcription–GILZ
TBE	tris-borat-EDTA buffer
TE	tris-EDTA
TEMED	tetramethylmethylenediamine
TGF	transforming growth factor beta
TLR	toll-like receptor
TNF- α	tumor necrosis factor alpha
TRE	12-O-tetradecanoylphorbol-13-acetate response element
Tris	tris(hydroxymethyl)aminomethane
TSC-22	stimulated clone-22
U	unit
3'UTR	3' untranslated region
UV	ultra violet
V	volt
VCAM	vascular cell adhesion molecule
VEGFR2	vascular endothelial growth factor receptor 2
VSMC	vascular smooth muscle cells
[v/v]	volume per volume
[w/v]	weight per volume
x g	fold gravitational force
Zeo	zeocin
ZFP36	zinc finger protein 36 ring finger protein, tristetraprolin (TTP)
μ	micro (10^{-6})

Abstract

Atherosclerosis represents a chronic cardiovascular disease, which is characterized by an inflammatory activation of the endothelium, with high prevalence and a major cause of morbidity and mortality. Low and disturbed vascular shear stress are risk factors for the development of atherosclerotic plaques, while laminar flow is important for physiological functions of the endothelium.

This work shows a downregulation of the glucocorticoid-induced leucine zipper (GILZ/TSC22D3) (*I*) in human inflamed vessels, (*II*) upon treatment of human endothelial cells (EC) with the inflammatory cytokine tumor necrosis factor alpha (TNF- α), and (*III*) in EC upon oscillatory flow. In contrast, anti-inflammatory laminar flow increased GILZ expression. Knockdown of GILZ in EC induced an inflammatory activation as indicated by enhanced nuclear factor kappa B (NF- κ B) activation.

The TNF-induced downregulation of GILZ is facilitated by induction of the mRNA binding protein tristetraprolin (TTP/ZFP36), which is also elevated in human inflamed vessels. Laminar flow antagonized GILZ downregulation by elevated mitogen kinase phosphatase (MKP-1/DUSP1) expression and subsequent ZFP36 downregulation. In human inflamed vessels, GILZ downregulation was also paralleled by diminished DUSP1 levels.

Taken together, our data show that the downregulation of GILZ in human EC promotes vascular inflammation. Upregulation of GILZ might therefore represent a therapeutic target for the treatment of the inflamed endothelium.

Zusammenfassung

Arteriosklerose wird als chronische, kardiovaskuläre Erkrankung charakterisiert durch entzündliche Prozesse im Endothel und zeigt hohe Prävalenz, Morbidität und Mortalität. Geringer und verwirbelter Shear Stress sind große Risikofaktoren für die Entstehung arteriosklerotischer Plaques, während laminarer Shear Stress die physiologischen Funktionen des Endothels stärkt.

Diese Arbeit zeigt eine Verringerung von glucocorticoid-induced leucine zipper (GILZ) (I) in humanen entzündeten Gefäßen, (II) in humanen Endothelzellen (EC) durch Behandlung mit dem inflammatorischen Zytokin tumor necrosis factor alpha (TNF- α) und (III) durch oszillierenden Fluß. Im Gegensatz dazu war die GILZ Expression durch anti-inflammatorischen laminaren Fluß erhöht und nach GILZ Knockdown zeigte die Aktivierung von nuclear factor kappa B (NF- κ B) eine inflammatorische Aktivierung in EC an.

Die TNF-induzierte Downregulation von GILZ erfolgte durch die Induktion des mRNA bindenden Protein Tristetraprolin (TTP/ZFP36) und der laminare Fluß wirkte der Downregulation von GILZ durch eine erhöhte mitogen kinase phosphatase (MKP-1/DUSP1) mit folgender verringrigerter ZFP36 Expression entgegen. In entzündeten Gefäßen liefen verringerte GILZ- und DUSP1-Level ebenfalls parallel mit erhöhter ZFP36 Expression.

Zusammenfassend wurde gezeigt, dass die Downregulation von GILZ in humanen EC die Gefäßentzündung steigert, wodurch die Hochregulation von GILZ ein neues Target für die Behandlung entzündeter Gefäße darstellen sollte.

1 Introduction

1.1 Atherosclerosis

1.1.1 General

Atherosclerosis is a chronic inflammatory cardiovascular disease of the arterial system. Leading to the end points of heart attack or stroke, it is the leading cause of death worldwide (Go *et al.*, 2013). There are behavioural risk factors like wrong nutrition, physical inactivity and smoking promoting the development of atherosclerosis. Also risk factors like chronic infections, autoimmune diseases, genetic predisposition and genetic materials damage are important aspects leading to obesity, high levels of cholesterol and other lipids, hypertension, diabetes mellitus and inflammatory activation (Frohlich & Al-Sarraf, 2013; Roy *et al.*, 2009; Wang *et al.*, 2013c; Patel & Blazing, 2013). Additionally, high risk factors for the development and progression of atherosclerotic plaques are low and disturbed shear stress (Cunningham & Gotlieb, 2005). For some years, atherosclerosis seemed to be a disease of the western lifestyle, but new results show that it already existed thousands of years ago (Thompson *et al.*, 2013).

Atherosclerosis is a chronic inflammatory disease characterized by an inflamed endothelium and an enclosure of lipids in the vessel wall, leading to the formation of deposits in the vessel wall also known as atherosclerotic plaques (Roy *et al.*, 2009). All variations of arteries show this pathology, whereas veins are not affected (Roy *et al.*, 2009). An exception is vein graft remodelling, where pieces of veins are localized at atherosusceptible regions after bypass surgeries, which is also characterized by inflammatory events, (Karper *et al.*, 2011; McPhee *et al.*, 2013). There are three areas in the body, which are mostly affected resulting in three clinical pictures: coronary artery disease, carotid artery disease, or peripheral arterial disease.

1.1.2 Origin and progression

Atherosclerosis has a complex, not completely understood mechanism, which is characterized by two processes: the accumulation of lipids respectively a shift in lipid profile and inflammation as well as an immune response especially in endothelial cells (EC). Therefore, molecules of both areas are used as biomarkers for risk prediction (e.g. low density lipoprotein (LDL) or C reactive protein) (Frohlich & Al-Sarraf, 2013; van Diepen *et al.*, 2013; Patel & Blazing, 2013).

After the “response to retention hypothesis”, the first step in the formation of atherosclerotic plaques (Figure 1), is the insudation of lipoproteins into the intima of the vessel wall (Williams & Tabas, 1998). LDL is modified to build an irreversible plaque because native LDL has no atherogenic properties and the insudation is reversible. The classical model is that reactive oxygen species are inducing the LDL modification (oxLDL), but there is also a new theory, which postulates that enzymatic modifications of LDL by proteases and cholesterylester hydrolases are necessary for an activation of the immune system and atherosclerosis progression (Torzewski & Bhakdi, 2013). Modified LDL is accumulated in the intima in hypercholesterolemic or dyslipidemic stages. On the one hand, it activates the endothelium resulting in an enhanced expression of adhesion molecules (e.g. intercellular adhesion molecule (ICAM), vascular cell adhesion molecule (VCAM), E-selectin), chemokines (e.g. monocyte chemoattractant protein1 (CCL2, MCP-1), interleukin-8 (IL-8)) and cytokines (e.g. TNF- α , IL-6), which attract inflammatory cells (e.g. monocytes, T cells) into the vessel wall and stimulate the differentiation of monocytes in macrophages (MΦ) (Figure 1 b). On the other hand, modified LDL is taken up by scavenger receptors into MΦ, which develop to foam cells, the major components of a plaque and promoters of inflammation by attraction of vascular smooth muscle cells (VSMC) and immune cells into the plaque. Each mentioned cell type stimulates the inflammatory response in the plaque *via* activation of transcription factors (e.g. nuclear factor kappa B (NF- κ B), c-Jun N-terminal kinases (JNKs)) and expression of further inflammatory mediators (van Diepen *et al.*, 2013). Proinflammatory cytokines also lead to an enhanced expression of TLR2 and TLR4 in atherosclerotic plaques (Edfeldt *et al.*, 2002), which promote the development of the disease (Schoneveld *et al.*, 2008). VSMC secrete collagen forming a fibrous cap between the lipid core and the intima to stabilize the plaque (Figure 1 c). The adaptive immune response is activated when T cells recognize peptide fragments of oxLDL, which are presented by antigen presenting cells. Furthermore, T cells promote VSMC apoptosis and stimulate the secretion of metalloproteinases by macropages to decrease the formation of the protective cap, which leads to a decrease of plaque stability. Inflammatory activation leads to plaque rupture (Figure 1 d) and a rapid formation of a thrombus, which promotes the closure of the artery (Patel & Blazing, 2013).

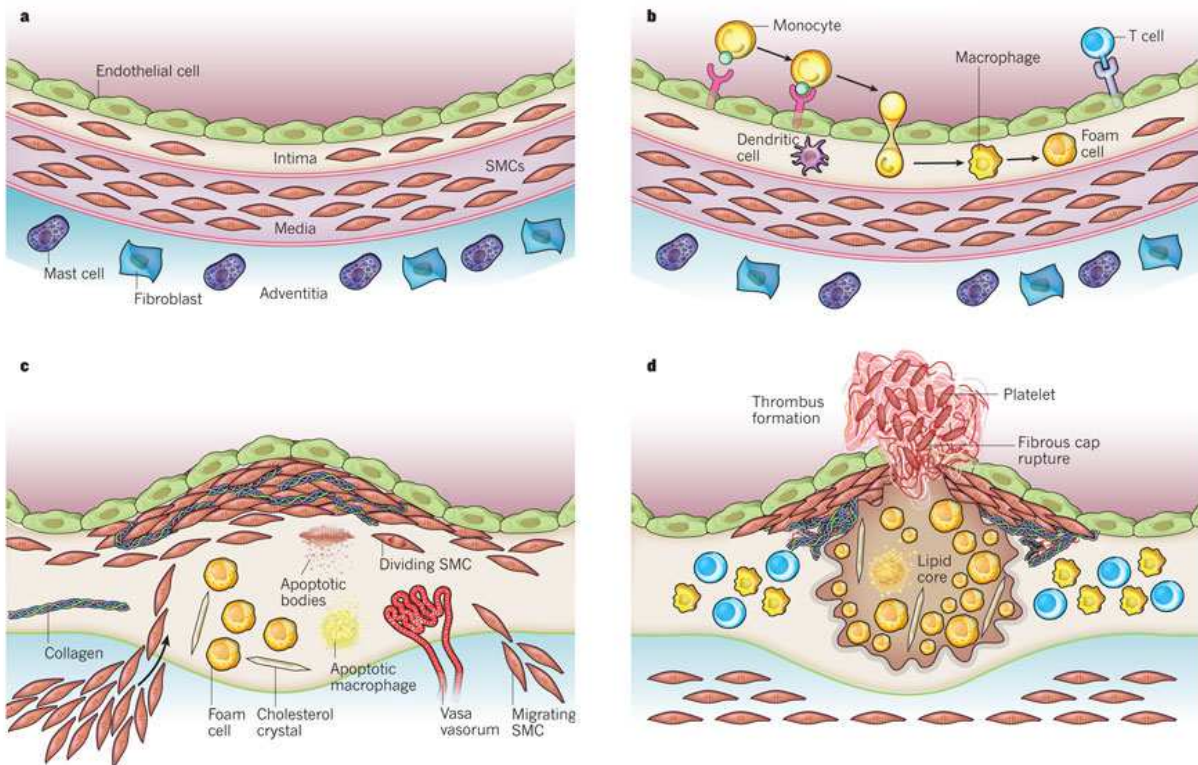


Figure 1: Development of an atherosclerotic plaque (Libby et al., 2011). See text for explanation.

1.1.3 Therapeutic options

Prevention is the major concern for a successful containment of atherosclerosis. First, it is required to change and control the behaviour, e.g. the type of ingested food, to do some exercise and to quit smoking. People with risk factors get some medication to ameliorate the prognosis, e.g. 3-hydroxy-3-methylglutaryl-coenzyme A (HMG-CoA) reductase inhibitors, nicotinic acid, anti-hypertensive drugs, or anticoagulants (Frohlich & Al-Sarraf, 2013).

The last possibilities to prevent further cardiovascular damage through occlusion of an artery are stenting or coronary artery bypass grafting (Figure 2) (Wang et al., 2013a, Kutty & Nair, 2008). There are already many possibilities to control atherosclerosis, but nothing with lasting effect.

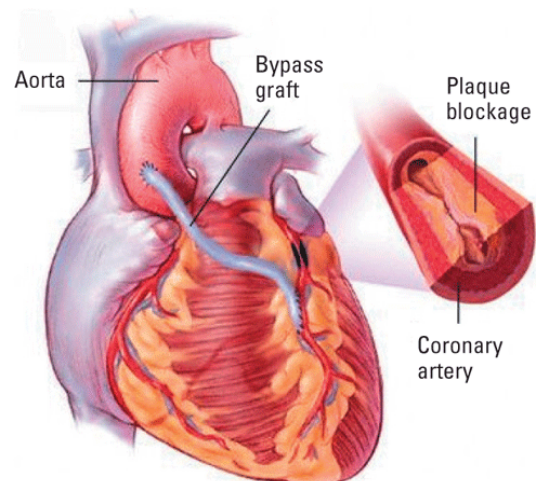


Figure 2: Bypass graft after surgery of a blockage in a coronary artery (<http://www.kalpkizi.gen.tr/bypass-b.gif>)

Therefore, this disease is still in the focus of current research. Cyclooxygenase-(cox)-inhibitors, i.e. acetylsalicylic acid, are potent widely used drugs to protect against heart failure. Beside from their anticoagulant effect, their anti-inflammatory properties seem to be important for their beneficial effect. Furthermore, other selective anti-inflammatory drugs, like cytokines (IL-1 β , C-C chemokine receptor 2 (CCR2)), leukotrienes or selective phospholipase A2 inhibitors as well as glucocorticoids and the anti-proliferative drug methotrexate are studied in clinical trials for their potential antiatherosclerotic effects. Others, like TNF- α inhibitors, seem to be not effective (Patel & Blazing, 2013).

The key role of the immune answer in this disease also implicates the possibility of a vaccination against immune players. Although, there are different approaches like passive immunization against such as oxidized phospholipids (Hansson & Nilsson, 2009), active immunization using apolipoprotein B (ApoB)-100 peptides as antigen (Chyu & Shah, 2014), or anti-cytokine auto-vaccinations (Uyttenhove & Van, 2012). A new approach is the treatment by gene targeting including small interfering RNA (siRNA), microRNA (miRNA) or epigenetics, which are directed against hyperlipidemia or inflammation on the whole, in the liver, or in the plaque (Makinen & Yla-Herttula, 2013). There are different experimental substances, which inhibit several stages of atherosclerosis, like benzylidenethiazole analogs against monocyte migration, incretins against foam cell formation, or specific antioxidants targeting LDL oxidation. Triglycerides, adhesion molecules or the neovascularisation, which is correlated with plaque progression, may act as new targets. Additionally, the application of stem cells seems to be a possibility to antagonize this disease. Major technological advances lead to a lot of computational and nanotechnological approaches for diagnosis and treatment of atherosclerosis (Wang *et al.*, 2013c).

1.2 Shear stress

1.2.1 General

Shear stress (τ) is a general force produced by the flow of a fluid along a surface. Transmitted to the body, the biomechanical force is induced by the blood stream and acts on EC in the vessel wall. The unit of shear stress is dynes per square centimeter (dynes/cm²) (10 dynes/cm² = 1 pascal (Pa)) (Cunningham & Gotlieb, 2005). The formula describing shear stress results from a combination of Newton fluids and the law of Hagen Poisseuille, with some adaptations: Blood has no constant viscosity and therefore it is not a real Newton fluid. Furthermore, vessels are elastic, not a rigid pipe. Therefore, shear stress is calculated with the following formula in arteries:

$$\tau = \frac{4\mu Q}{\pi r^3} \quad (\text{Cunningham \& Gotlieb, 2005})$$

Q = blood flow rate

r = radius of the vessel wall

μ = viscosity of blood

For experimental conditions the formula has to be adapted to the different geometry of the chamber (2.7.2) used as follows:

$$\tau = \frac{6Q\mu}{bh^2} \quad (\text{Frangos et al., 1988})$$

τ = shear stress [dynes/cm²]

Q = flow rate [cm³/s]

μ = viscosity (0.01 dynes*s/cm²) (Frangos et al., 1988)

b = channel width (1.9 cm)

h = channel high

Shear stress in biological systems is classified into different types:

- laminar, pulsatile
- turbulent, disturbed, nonlaminar
- low
- oscillatory

Normally, laminar shear stress is located in straight vessels and typically varies in arteries from 5 to 20 dynes/cm². Still, pressure conditions alternate to a great extent depending on blood pressure and pulse, therefore, laminar shear stress alters also beyond the given values. *In vivo*, laminar flow has a pulsatile character resulting of pulsatile blood pressure. In contrast, in curvatures and bifurcations, turbulences are existent in fluid resulting in low (< 5 dynes/cm²) and disturbed shear stress (Cunningham & Gotlieb, 2005) (Figure 3).

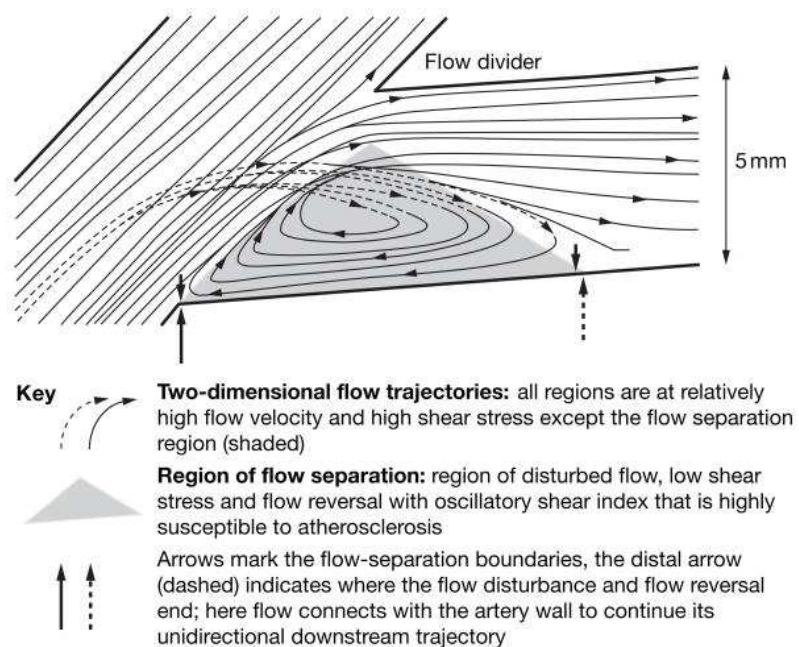


Figure 3: Flow simulation in a bifurcated artery (Davies, 2009)

Turbulences also originate, when the fluid velocity is enhanced. The beginning of turbulence is calculated by the Reynolds number, which characterizes the stability of flow. Oscillatory flow is no natural type of flow and does not exist in the body. In fact, it is an experimental cell culture model, which is employed to evaluate the disturbed type of flow. Oscillatory flow is generated by the change of flow direction, normally

with a frequency of 1 Hz (± 5 dynes/cm 2) (Ali *et al.*, 2009). In every type of flow, a force imposes directly on the endothelium and has effects on the EC (Davies, 2009).

1.2.2 Mechanotransduction

The mechanism resulting of imposed forces on the endothelium is called mechanotransduction (Davies, 1995; Davies, 2009). Mechanotransduction is dividable into four steps, but the temporal relation between the different steps is poorly understood so far:

- Physical deformation
- Intracellular transmission of stress
- Conversion of mechanical force to chemical activity
- Downstream biochemical signaling with feedback

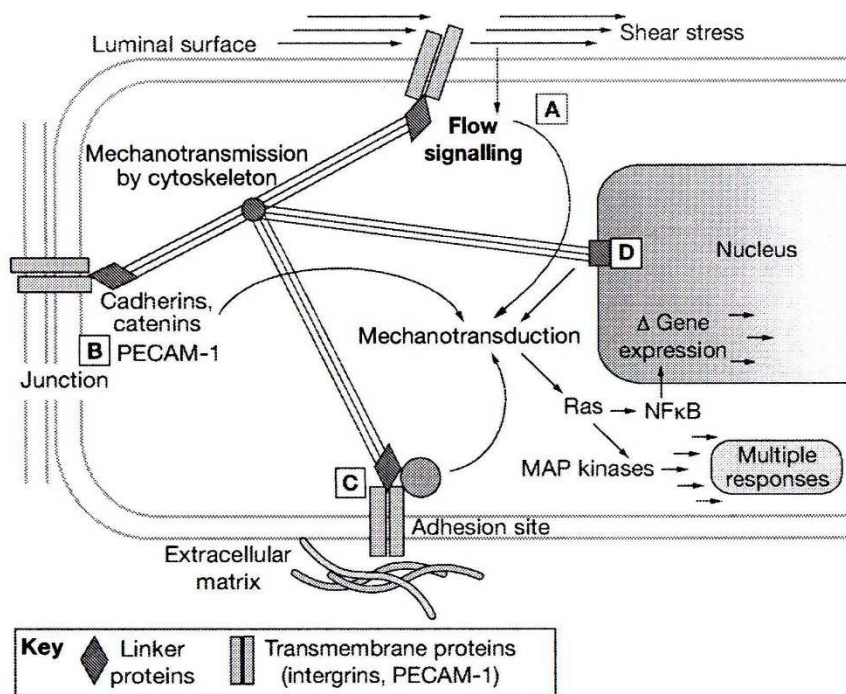


Figure 4: The decentralized model of endothelial mechanotransduction by shear stress (Davies, 2009). See text for explanation. PECAM-1 (platelet endothelial cell adhesion molecule-1), NF-κB (nuclear factor-κB), MAP kinases (mitogen-activated protein kinases)

The flow effectuates a physical deformation of the luminal cell surface and activates local membrane structures, such as ion channels and G-proteins, changes in phospholipid mechanism and membrane fluidity. Highly charged glycocalix and primary

cilia are located on the cell surface and are established as important factors of the mechanism (Hierck *et al.*, 2008; Yao *et al.*, 2007). The force is also transferred by transmembrane located integrins to the cytoskeleton, which plays a central role in mechanotransduction (Wang *et al.*, 1993). The intracellular transmission is carried out by cytoskeletal deformation and leads to the conversion to chemical activity resulting in modification of gene expression (see 1.2.3). Figure 4 shows a possible activation pathway of the small GTPase Ras (rat sarcoma), which influences different kinases or transcription factors, such as NF- κ B to modulate gene expression (Davies *et al.*, 1997).

But not all of these steps are always required. An early ion response, such as a calcium influx resulting in enhanced calcium concentration and changed cell activation is also possible (Cunningham & Gotlieb, 2005). Further, nuclear deformation by the cytoskeleton may immediately lead to a modified cell signaling *via* lamins (Figure 4).

1.2.3 Options of gene expression modification

Shear stress is known to have many possibilities to modulate the gene expression and function of EC. In several studies, 10-20 signaling pathways were identified, which play a role, with MAPK-pathways, NF- κ B and endothelial nitric oxide synthase (eNOS)- nitric oxide (NO) pathways being most often described (Frueh *et al.*, 2013):

- Activation of signaling molecules
e.g. heterotrimeric G proteins, tyrosine phosphorylation of proteins such as Src homology 2 domain containing transforming protein (Shc), c (cellular) -src tyrosine kinase, and focal adhesion kinase (FAK), activation of MAPK, protein kinase C (PKC), and JNK, release of reactive oxygen species (ROS), production of NO (Tzima, 2006)
- Activation of transcription factors
e.g. c-fos, c-jun, c-myc, NF- κ B, Krüppel-like factor 2 (KLF2), nuclear factor erythroid 2-related factor 2 (Nrf2) (Tzima, 2006; Boon & Horrevoets, 2009), 10 different transcription factors are acknowledged as yet (Frueh *et al.*, 2013)

- Regulation via binding to shear stress responsive elements (SSREs) in promotersequence

SSREs are regulatory elements or cis-elements in the promoter region of a gene to modulate its gene expression. There are sequences for positive regulation as well as negative regulation identified (Malek & Izumo, 1995; Malek & Izumo, 1995; Miyakawa *et al.*, 2004). GAGACC was first identified in 1993 and since then, it has been identified in many different genes (Resnick *et al.*, 1993; Silberman *et al.*, 2009). In most SSRE-regulated genes, more than one SSRE was identified, which seems to be more powerful (Houston *et al.*, 1999; Resnick *et al.*, 2003).

Positive regulating SSREs are: GAGACC (Resnick *et al.*, 1993), TGACTCC (12-O-tetradecanoylphorbol-13-acetate response element (TRE) (CCL2)) (Shyy *et al.*, 1995), GAGACCCCC (platelet-derived growth factor (PDGF)-B), GGGGCGGGGCG-(PDGF-A, TF) (Resnick *et al.*, 2003).

Negative regulating SSREs are: CTTT (Barbie-Box), GAGAG / GGGAG (GAGA-Box) (Miyakawa *et al.*, 2004), TGACTCAG, TGGGCGGGGC (Resnick *et al.*, 2003).

There are also several transcription factors identified, which are involved in shear stress gene regulation, such as NF- κ B, activator protein-1 (AP-1), early growth response-1 (Egr-1), sterol regulatory element-binding protein-1 (SREBP-1) or specificity protein 1 (SP1) (Malek & Izumo, 1995; Xing *et al.*, 2006; Resnick *et al.*, 2003; Nagel *et al.*, 1999). Additionally, the nuclear factor erythroid 2-related factor 2 – Kelch-like erythroid cell-derived protein with CNC homology-associated protein 1 (Nrf2-Keap1) system regulates cytoprotective gene expression via antioxidant responsive elements (ARE), with several ARE-regulated genes induced by laminar shear stress (Dai *et al.*, 2007; Chen *et al.*, 2003).

- Epigenetic regulation (Zhou *et al.*, 2011; Zhou *et al.*, 2014)

(general epigenetic informations see in chapter 1.5)

There are three different possibilities for flow-induced epigenetic regulation: DNA-methylation, histone modification and binding of miRNA.

Estrogen receptor- β is described to have a higher DNA methylation state in artherosclerotic lesions (Post *et al.*, 1999). Recently, Homeobox protein A5

(HoxA5) and KLF3 were shown as novel mechanosensitive transcription factors regulated by DNA methylation in response to flow (Dunn *et al.*, 2014). DNA methylation with DNA (cytosine-5)-methyltransferase 1 (DNMT1) as key protein is postulated being a new important regulation mechanism for pathophysiological stimuli due to disturbed flow (Zhou *et al.*, 2014).

Histone deacetylases 1-7 (HDAC1-7) are activated in EC by laminar or oscillatory flow (Chen *et al.*, 2013).

There is a lot of data on miRNAs and flow-related gene expression. More than 50 miRNAs are already described to be flow-responsive (Weber *et al.*, 2010a; Weber *et al.*, 2010b; Wu *et al.*, 2011; Ni *et al.*, 2011; Qin *et al.*, 2010; Fang *et al.*, 2010; Marin *et al.*, 2013; Wei *et al.*, 2013; Son *et al.*, 2013; Hergenreider *et al.*, 2012; Holliday *et al.*, 2011).

1.2.4 Functions of Shear Stress

Shear stress has many different functions, and so far, there have been approximately 1000-2000 mechanosensitive genes identified (Frueh *et al.*, 2013). Very much of them are involved in the pathogenesis of atherosclerosis (Dolan *et al.*, 2013; Gimbrone, Jr. & Garcia-Cardena, 2013). Generally, atherosclerotic plaques are localized in curvatures or bifurcations of vessels where static conditions as well as low and oscillatory shear stress occur. These inflammatory conditions promote the formation of atherosclerotic lesions by modification of gene and protein expression. In straight vessels the laminar blood flow is known as a main atheroprotective factor, which is important for the physiological function of the endothelium and acts anti-inflammatory (Cunningham & Gotlieb, 2005) (Figure 5). Whereas long time (> 24 h) laminar flow is atheroprotective, while short time laminar flow activates the endothelium in an inflammatory manner (Boon & Horrevoets, 2009; Chlupac *et al.*, 2014). Besides laminar shear stress as a physical inhibitor of vascular inflammation, other regulators antagonizing vascular inflammation are as yet poorly investigated.

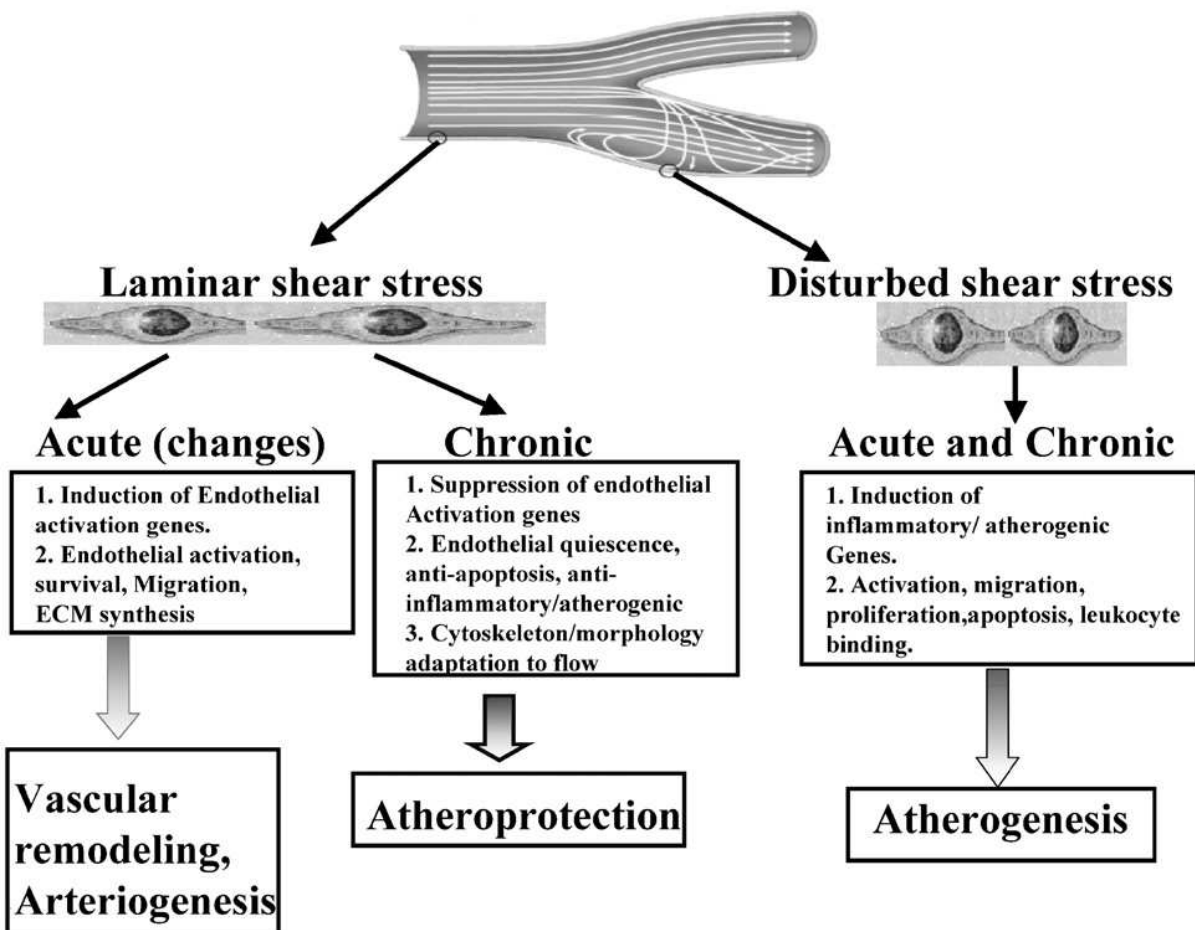


Figure 5: The heterogeneous response of the endothelium to various shear stress patterns (Resnick *et al.*, 2003). ECM (extra cellular matrix)

Atheroprotective shear stress promotes anti-inflammatory, antithrombotic, anticoagulative, and antioxidative properties of EC, and supports homeostasis, barrier function as well as wound healing of the endothelium (Cunningham & Gotlieb, 2005). On the other hand, atheroprone shear stress increases oxidation, leukocyte adhesion, permeability of the endothelium and inflammation in EC (Gimbrone, Jr. & Garcia-Cardena, 2013; LaMack *et al.*, 2005; Himborg *et al.*, 2004).

A central atheroprotective mediator is the vasodilator NO, which is induced by laminar shear stress, as well as activation of eNOS (Rubanyi *et al.*, 1986; Davis *et al.*, 2004; Dimmeler *et al.*, 1999). Additionally, an important factor of atherosclerosis is the production of ROS performed in part by reduced nicotinamide adenine dinucleotide phosphate (NAD(P)H), which is decreased by laminar and increased by oscillatory flow (De Keulenaer *et al.*, 1998). Heme oxygenase 1 (HO1), another enzyme exhibiting antioxidative and antiatherosclerotic action (Stocker & Perrella, 2006) is strongly activated by laminar shear stress (Zakkar *et al.*, 2008). Thrombomodulin is

increased in response to laminar flow of 15 dynes/cm² modulating the coagulation state (Takada *et al.*, 1994). Furthermore, laminar flow leads to the inhibition of signal transducer and activator of transcription (STAT) 3, followed by an inflammatory response as well as an activation of peroxisome proliferator-activated receptor γ (PPAR γ) (Ni *et al.*, 2003; Liu *et al.*, 2005; Liu *et al.*, 2004).

Inducing monocyte adherence and transmigration *in vivo*, low shear stress was considered to be inflammatory (Walpolo *et al.*, 1993). Additionally, IL-6, an activator of B- and T-lymphocytes (Jirik *et al.*, 1989), is upregulated under low flow (Shaik *et al.*, 2009). Leukocyte adhesion is determined by the expression of adhesion molecules and chemokines. The adhesion molecules ICAM, VCAM, and E/P-selectin are induced by low and non-uniform shear stress in combination or absence of TNF- α treatment (Cicha *et al.*, 2009; Chiu *et al.*, 2004; Walpolo *et al.*, 1995; Chappell *et al.*, 1998). CCL2 and IL-8 promote leucocyte adhesion under low flow (2 dynes/cm²) (Gerszten *et al.*, 1999). For CCL2, an upregulation was shown under oscillatory flow, which was dependent on increased transglutaminase activity (Matlung *et al.*, 2012; Cheng *et al.*, 2007). IL-8 is induced by low flow and decreased under laminar shear stress (Hastings *et al.*, 2007; Shaik *et al.*, 2009). A further player of inflammation is TLR2, which is enhanced by disturbed shear (Mullick *et al.*, 2008). Additionally, its TNF- α -induced activation is diminished by laminar, but not by disturbed flow (Dunzendorfer *et al.*, 2004).

Shear stress is not only a regulator of endothelial cell function, it also plays an important role in mechanical-transcriptional coupling and in regulation of the VSMC phenotype (Hastings *et al.*, 2007).

1.3 Glucocorticoid-induced leucine zipper (GILZ)

1.3.1 General

GILZ (TSC22D3) is an anti-inflammatory protein induced by glucocorticoids, which was identified in 1997 in murine T-lymphocytes (D'Adamio *et al.*, 1997). Over the years, it was found out to be also expressed in various human cell types, e.g. MΦ, dendritic cells, B-lymphocytes, epithelial, and endothelial cells (Ayroldi & Riccardi, 2009; Hahn *et al.*, 2014; Hoppstädter *et al.*, 2012; Cheng *et al.*, 2013).

Murine and human GILZ have a high similarity (97% in the coding region) (Cannarile *et al.*, 2001), with murine GILZ containing 137 aa (17 kDa) (D'Adamio *et al.*, 1997), and the human GILZ protein consisting of 135 aa (15 kDa). GILZ belongs to the leucine zipper (LZ) family because of its highly conserved LZ domain (abcdef) in the central position (76 - 97) of the molecule, which is characterized by a heptad repeat of leucine residues, which are found in position d (Figure 6). This domain, also known as transforming growth factor beta (TGF- β)-stimulated clone-22 (TSC-22), has a great homology compared to other members of this family. Furthermore, this region is responsible for homodimerization, while the other two domains of GILZ are responsible for protein-protein interactions between GILZ and transcriptional as well as signaling molecules (Fan & Morand, 2012). One of these domains, which is located in front of the LZ domain is the N-terminal domain (NTD), and the C-terminal domain behind it is also known as proline and glutamic acid rich region (PER) (Di Marco *et al.*, 2007; Kester *et al.*, 1999).

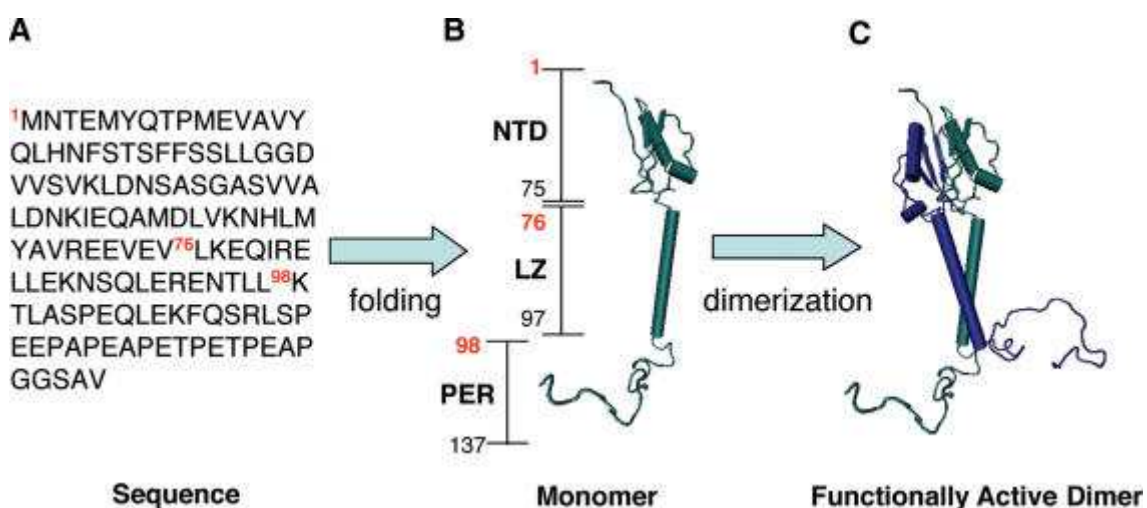


Figure 6: GILZ protein sequence, domains, and activation by dimerisation (Di Marco *et al.*, 2007). NTD = N-terminal domain, LZ = leucine zipper, PER = proline and glutamic acid region

1.3.2 Regulation of GILZ

Important for the regulation of GILZ are transcription factor binding sites in its promoter (Asselin-Labat *et al.*, 2004), including six *glucocorticoid responsive elements* (GREs), putative binding sites for STAT6, for nuclear factor of activated T cells (NFAT), for Oct-1, for c-myc, for forkhead responsive elements (FHREs), for cyclic adenosine monophosphate response element-binding protein (CREB), and an estrogen-response sequence (Ayroldi & Riccardi, 2009).

Further inducers of GILZ are IL-10 in MΦ and mast cells, IL-4 and IL-13 in monocytes, IL-15 in natural killer cells, TGF- β in dendritic cells, erythropoietin and stem factor in primary erythroid progenitors, as well as vasopressin and aldosterone in mammalian kidney epithelial cells (Berrebi *et al.*, 2003; Godot *et al.*, 2006; Cohen *et al.*, 2006; Perez *et al.*, 2005; Soundararajan *et al.*, 2005; Kolbus *et al.*, 2003). Additionally, GILZ was induced in T-lymphocytes upon IL-2 withdrawal, leading to the dephosphorylation of transcription factor forkhead box O3 (Fox O3) binding to the FHREs identified in the GILZ promoter (Asselin-Labat *et al.*, 2004). Moreover, laminar shear stress of 25 dynes/cm² for 6 h and 24 h was also shown to induce GILZ (McCormick *et al.*, 2001).

A decreased GILZ expression was described for anti-CD3 activation in T-lymphocytes, for B-cell receptor activation in B-cells, by estrogens in MCF-7 human breast cancer cells and by IL-1, TNF- α , and interferon- γ (INF- γ) in epithelial cells (Ayroldi *et al.*, 2001; Glynne *et al.*, 2000; Tynan *et al.*, 2004; Eddleston *et al.*, 2007). For MΦ, different TLR ligands i.e. lipopolysaccharide (LPS) for TLR4 or PAM₃CSK₄ for TLR2, were identified as GILZ downregulators (Hoppstädter *et al.*, 2012). TLRs diminished GILZ levels in a myeloid differentiation primary response 88 (MyD88) dependent fashion *via* a mRNA binding protein tristetraprolin (TTP / ZFP36) induced mRNA destabilization (Hoppstädter *et al.*, 2012).

1.3.3 Functions of GILZ

GILZ protein is known to act *via* binding to other proteins. The building of GILZ homodimer is described to inhibit NF- κ B by binding to its p65 subunit leading to a diminished cytokine transcription (Ayroldi & Riccardi, 2009; Cheng *et al.*, 2013; Hahn *et al.*, 2014; Di Marco *et al.*, 2007; Berrebi *et al.*, 2003). Some other transcription factors were also identified as targets of the GILZ monomer, e.g. AP-1, Raf-1 and Ras (extracellular signal-regulated kinase (ERK)) and AKT pathways (Ayroldi & Riccardi, 2009). AP-1 is inhibited by interaction of the GILZ N-terminal 60-amino acid region with the AP-1 subunits c-Jun and c-Fos (Mittelstadt & Ashwell, 2001; Ayroldi *et al.*, 2002). Additionally, GILZ functions as a transcriptional repressor and binds to binding sites in the promoter of PPAR- γ 2 (Shi *et al.*, 2003). Effects of GILZ are summarized in Figure 7.

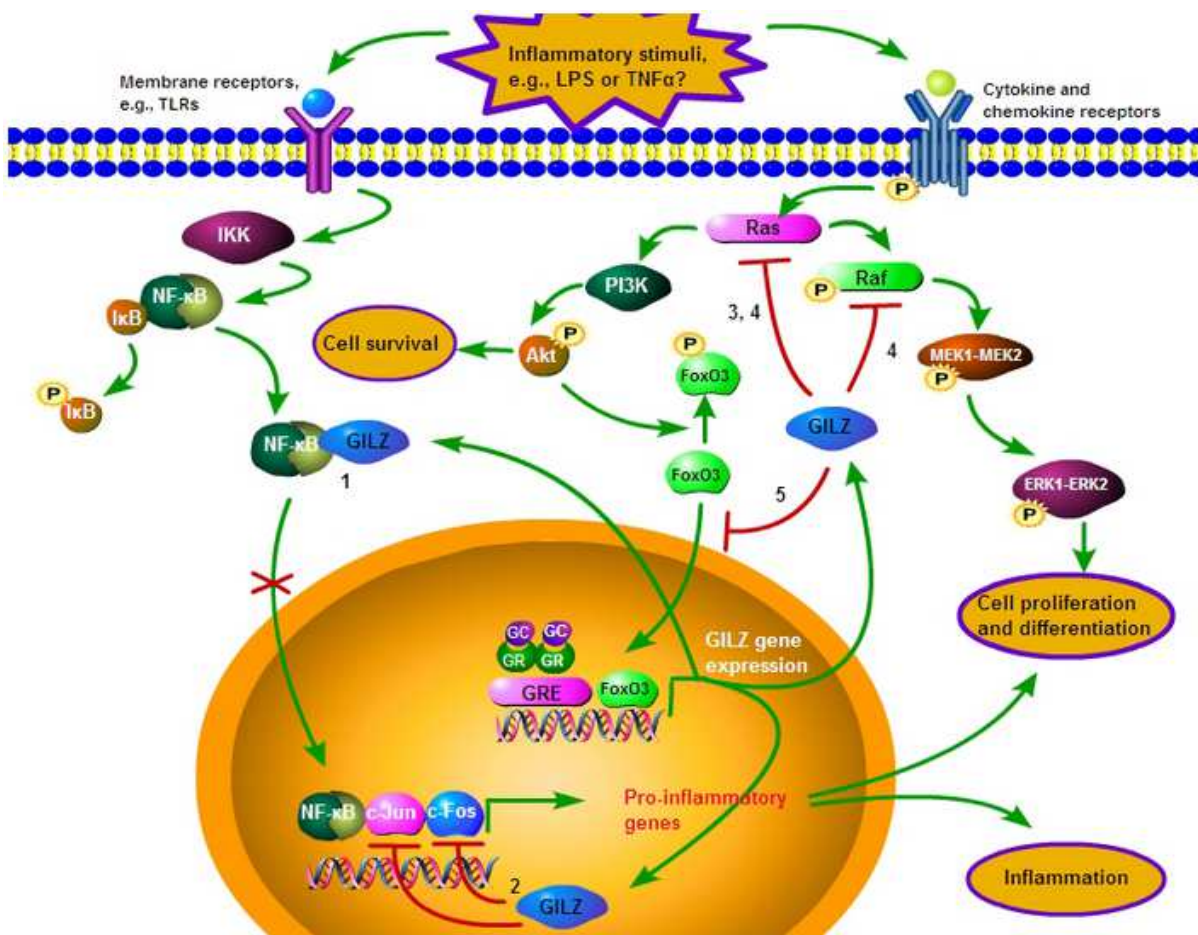


Figure 7: Effects of GILZ on immune signaling pathways (Fan & Morand, 2012). See text for details. GILZ: glucocorticoid induced leucine zipper, TLRs: toll-like receptors, LPS: lipopolysaccharide, TNF- α : tumor necrosis factor α , I κ B: inhibitory protein κ B, IKK: I κ B kinase, NF- κ B: nuclear factor- κ B, PI3K: phosphatidylinositol 3-kinase, PKB: protein kinase B, MEK: mitogen/extracellular signal-regulated kinase, ERK: extracellular-signal-regulated kinase, FoxO3: forkhead box O3, GC: glucocorticoids, GR: glucocorticoid receptor, GRE: glucocorticoid responsive element

Besides other important functions in cell proliferation and renal sodium transport, the anti-inflammatory effects of GILZ, mostly mediated *via* NF- κ B inhibition, are of special interest (Ayroldi & Riccardi, 2009). GILZ induction is pivotal for the anti-inflammatory and immunosuppressive actions of glucocorticoids (Ayroldi *et al.*, 2014; Berrebi *et al.*, 2003; Fan & Morand, 2012). As an example, GILZ modulates T-lymphocyte activation (Ayroldi & Riccardi, 2009; Cohen *et al.*, 2006; Libert & Dejager, 2014). Rheumatoid arthritis is a chronic inflammatory disease, which is treated with glucocorticoids suggesting GILZ as guarantor of efficacy (Beaulieu *et al.*, 2010; Eades *et al.*, 2014). Furthermore, GILZ downregulation is postulated in different inflammatory diseases, like chronic rhinosinusitis, tuberculosis or Crohn's disease (Berrebi *et al.*, 2003; Zhang *et al.*, 2009). In mice, dinitrobenzene sulfonic acid-induced colitis was significantly inhibited by over-expression of GILZ in T-cells (Cannarile *et al.*, 2009).

Recently, upregulation of GILZ was described to remedy the immune tolerance to allergens in respiratory allergies (Karaki *et al.*, 2014). In EC, induction of GILZ expression inhibits inflammatory leukocyte recruitment (Cheng *et al.*, 2013).

Additionally, two different approaches has been described using GILZ as an anti-inflammatory drug to mediate the anti-inflammatory effects of glucocorticoids without the detrimental effects (Ayroldi *et al.*, 2014). The fusion protein transactivator of transcription–GILZ (TAT-GILZ) regulated apoptosis of thymocytes in mice (Delfino *et al.*, 2004). Injection of TAT-GILZ inhibited Th1-induced colitis in mice (Cannarile *et al.*, 2009) and protected against LPS-induced endotoxemia (Pinheiro *et al.*, 2013). Immunomodulatory GILZ peptide (GILZ-P), a proline-rich segment in the carboxyl terminus of GILZ, improved experimental autoimmune encephalomyelitis in mice and activated p65 in THP-1(Srinivasan & Janardhanam, 2011; Srinivasan *et al.*, 2014).

1.4 Further regulators of inflammation

The inflammatory activation of the endothelium plays a central role for the progression of atherosclerosis (see 1.1.2) (van Diepen *et al.*, 2013). In the following, some inflammation related players, which are important for this work, are described.

1.4.1 Heme oxygenase 1 (HO1)

HO1 was first described as enzyme of the heme catabolism, which catalyzes the degradation of heme in biliverdin-IX, divalent iron, and carbon monoxide (Tehnunen *et al.*, 1968). HO1 is induced by its substrate heme and by various stressors, such as UV light, heat shock, lipopolysaccharide, heavy metals, reactive oxygen species and hyperoxia, whereby it has cell protective properties (Immenschuh & Ramadori, 2000; Han *et al.*, 2009). Furthermore, it is also activated by anti-inflammatory stimuli, such as atrial natriuretic peptide (ANP) in Kupffer- and endothelial cells (Kiemer *et al.*, 2003b; Kiemer *et al.*, 2003a) and laminar shear stress in the endothelium (Zakkar *et al.*, 2008). Especially the generated carbon monoxide is an anti-inflammatory, antiapoptotic, and vasodilatory mediator with antiatherosclerotic potential (Siow *et al.*, 1999; Stocker & Perrella, 2006).

1.4.2 Dual specificity protein phosphatase 1 (DUSP1, MKP-1)

DUSP1 is the first identified of at least 10 known MKPs of mammalian cells and also known as hVH1, CL100, 3CH134 or Erp (Keyse, 2000; Wancket *et al.*, 2012). The 40 kDa enzyme was first reported in 1992 and is known to be widely expressed (Charles *et al.*, 1992; Wancket *et al.*, 2012). It is a negative regulator of mitogen activated protein kinases (MAPKs), and inhibits all of them, p38, JNK as well as ERK, by dephosphorylation of their phosphotyrosine and phosphothreonine residues (Alessi *et al.*, 1993; Liu *et al.*, 1995; Raingeaud *et al.*, 1995) leading to an anti-inflammatory response (Figure 8) (Wancket *et al.*, 2012). A suppression of ZFP36 by an DUSP1 inhibited p38 MAPK pathway was recently described for MΦ and epithelial cells (Huotari *et al.*, 2012).

Activation of DUSP1 is normally mediated by anti-inflammatory stimuli, such as glucocorticoids (Fürst *et al.*, 2007), ANP (Kiemer *et al.*, 2002a) and laminar shear stress (Zakkar *et al.*, 2008). Negative regulation is possible by cytokines like IFN- γ (Wancket *et al.*, 2012; Lawan *et al.*, 2013).

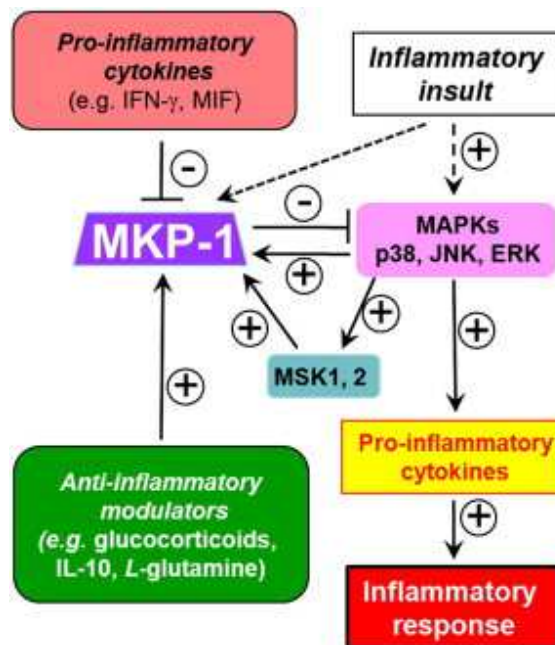


Figure 8: Immunomodulatory regulation of inflammation by modulating MKP-1 (DUSP1) expression (Wancket *et al.*, 2012). IFN- γ : interferon- γ , MIF: macrophage migration inhibitory factor, MSK: mitogen- and stress-activated protein kinase, JNK: c-Jun N-terminal kinase, IL-10: interleukin-10

Several translational and posttranslational mechanisms are possible for the regulation of DUSP1 (Lawan *et al.*, 2013; Lin *et al.*, 2003; Wancket *et al.*, 2012). MAPKs

themselves enhance DUSP1, resulting in a negative feedback loop (Lawan *et al.*, 2013). Binding of transcription factor CCAAT/enhancer binding protein-b (C/EBPb) was shown for DUSP1 induction in MΦ (Cho *et al.*, 2008). Expression of DUSP1 is regulated *via* mRNA stability by the mRNA binding proteins human antigen R (HuR) and ZFP36 (Emmons *et al.*, 2008; Kuwano *et al.*, 2008). Posttranslational modifications were identified such as proteasome dependent degradation (Lin *et al.*, 2003) or DUSP1 acetylation (Cao *et al.*, 2008). Also, epigenetic expression regulation is possible *via* miRNAs (e.g. miRNA-101) (Zhu *et al.*, 2010) or DNA methylation (Chen *et al.*, 2012a).

For DUSP1, many different functions are known. It plays a role in the immune system, central nervous system, musculoskeletal system, infections, and different types of cancer (Lawan *et al.*, 2013; Wancket *et al.*, 2012). The role of DUSP1 in the pathophysiology of atherosclerotic plaques is controversially discussed, as both, anti-inflammatory (Fürst *et al.*, 2005; Kim *et al.*, 2012; Zakkar *et al.*, 2008e) as well as pro-atherosclerotic actions have been suggested (Imaiizumi *et al.*, 2010; Shen *et al.*, 2010).

1.4.3 p38 mitogen-activated protein kinase (p38 MAPK)

p38 MAPK belongs to the group of highly conserved serine/threonine protein kinases (Su & Karin, 1996). p38 is almost ubiquitarily found, whereby 4 different isoforms are known (α , β , γ , δ), which are variably expressed in different cells (Hale *et al.*, 1999). Activation occurs in response to several stimuli, such as inflammatory cytokines (e.g. TNF- α), UV radiation, osmotic stress or LPS (Kierner *et al.*, 2002a; Raingeaud *et al.*, 1995), leading to the activation of GTPases (e.g. Ras, Rac) and a phosphorylation cascade of MAPK kinase kinase and MAPK kinase. The cascade ends in the phosphorylation of threonine and tyrosine residues in the conserved Thr-Xaa-Tyr motif, which is located in a regulatory loop between the kinase subdomains VII and VIII (Whitmarsh & Davis, 1996). p38 itself regulates gene expression through different mechanisms, such as activation of transcription factors or other protein kinases, or modulating the stability and translation of mRNA by phosphorylation of mRNA binding proteins, e.g. ZFP36, by MAPK-activated protein kinase (MK)-2, a downstream target of p38 MAPK (Stoecklin *et al.*, 2004; Clark *et al.*, 2003; Herlaar & Brown, 1999; Chen *et al.*, 2001). Furthermore, p38 has many important functions in tissue ho-

moeostasis as well as in multiple pathologies from inflammation and the immune response to heart, cancer, and neurodegenerative diseases (Cuadrado & Nebreda, 2010).

1.4.4 Tristetraprolin (ZFP36, TTP)

Tristetraprolin belongs to the Cys-Cys-Cys-His-tandem-zincfinger-protein family. Its function is the destabilisation of mRNA by binding to adenosine-uridine-rich-elements (AUUUA) in the 3' untranslated region (3`UTR) leading to deadenylation and degradation of the bound mRNA (Blackshear, 2002; Carballo *et al.*, 1998). Normally, adenosine-uridine-rich-elements are located in mRNAs of inflammatory cytokines such as TNF- α , IL-8, and IL-6, resulting in an anti-inflammatory action of ZFP36 (Aslam & Zaheer, 2011; Lai *et al.*, 1999; Lai *et al.*, 2006; Balakathiresan *et al.*, 2009; Zhao *et al.*, 2011). In the meantime, numerous targets are genome-wide identified (Mukherjee *et al.*, 2014). Furthermore, cytokine production is inhibited by ZFP36 *via* binding of p65 (Schichl *et al.*, 2009). An important regulator of ZFP36 is the p38 MAPK, which inhibits the activation of ZFP36 and degradation of cytokine mRNA by phosphorylation of MK2 (Aslam & Zaheer, 2011; Lai *et al.*, 1999; Stoecklin *et al.*, 2004).

Recently, inflammatory actions of ZFP36 were also detected. In stimulated M Φ , GILZ was actively downregulated *via* *GILZ* mRNA destabilization mediated by the mRNA binding protein ZFP36 (Hoppstädter *et al.*, 2012). Additionally, ZFP36 is expressed in EC and foam cells of atherosclerotic lesions (Zhang *et al.*, 2013). Moreover, ZFP36 expression is inhibited downstream of the anti-inflammatory DUSP1 (Huotari *et al.*, 2012), a potent inhibitor of p38 MAPK (Kiemer *et al.*, 2002a).

1.5 Epigenetics

Epigenetic modifications are covalent or noncovalent alterations of DNA resulting in a modified gene expression, which can be classified into the following three categories (Figure 9) (Chen *et al.*, 2013).

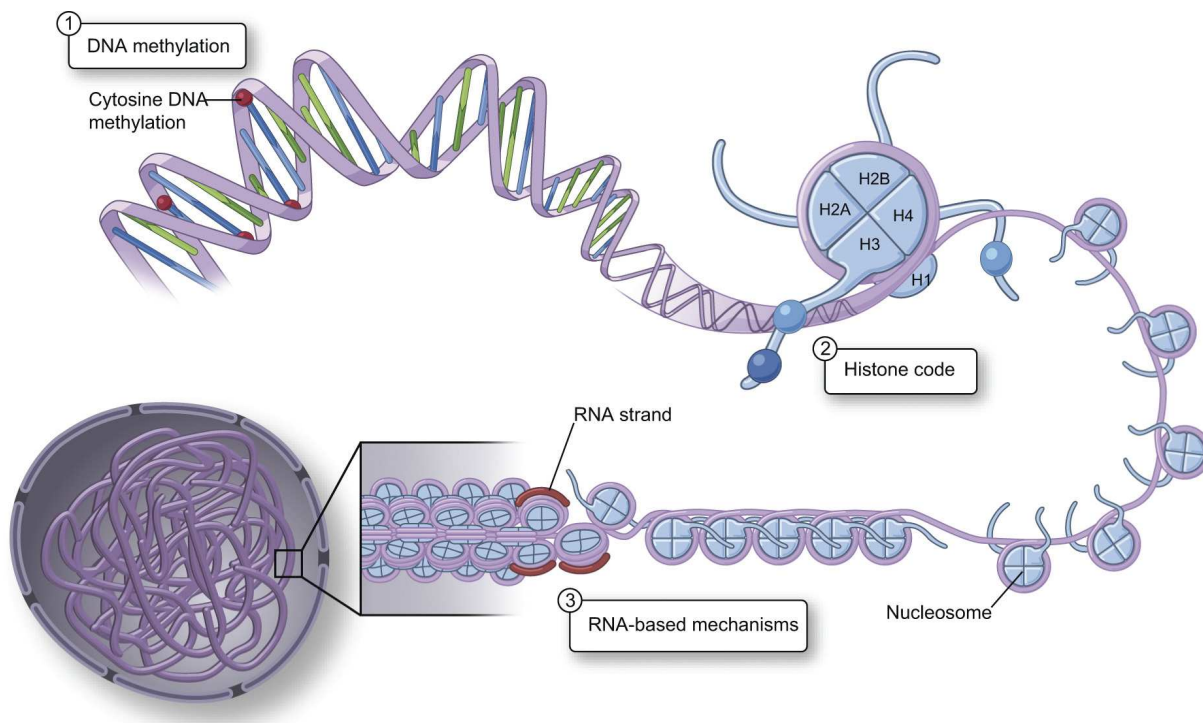


Figure 9: Three fundamental mechanisms of epigenetic gene regulation (Yan *et al.*, 2010). See text for details.

DNA methylation

DNA methylation results by addition of a methyl group from S-adenyl methionine to the fifth carbon of a cytosine to form 5-methylcytosine in the context of CpG dinucleotides (Moore *et al.*, 2013). CpGs are normally unmethylated and thus hypermethylation of CpG islands leads to the stable silencing of gene expression. So-called CpG islands are clusters of more than 200 bp with high CG content in promoters of genes. Methylation and demethylation of DNA are both enzymatic processes. Demethylation of methylated DNA induces the gene expression as well as binding of proteins to the methylated CpG (Chen *et al.*, 2013; Zhou *et al.*, 2014).

The importance of this modification in vascular functions has been reported for DNA methylation of eNOS and vascular endothelial growth factor receptor 2 (VEGFR2)

promoters, which are bound and suppressed by methyl CpG binding domain protein2 (MBD2) (Rao *et al.*, 2011).

Histone modification

Histones are enzymatically modified at their N-terminal regions. This process influences the accessibility of the DNA to the transcriptional machinery (Kouzarides, 2007). Generally, acetylation, methylation, phosphorylation, or ubiquitylation are used to activate the transcription and methylation, ubiquitination, sumoylation, deimination, and proline isomerisation is used to reduce the transcription (Zhou *et al.*, 2014). The best studied actors are histone acetyltransferases (HAT) and HDAC, which both are known to be dysregulated in cardiovascular diseases (Wang *et al.*, 2014).

RNA-based mechanisms

Noncoding RNAs (NcRNAs) are divided into five classes dependent on its structure and length: microRNAs (miRNAs), small interfering RNAs (siRNAs), piwi-interacting RNAs (piRNAs), small nucleolar RNAs and long non-coding RNAs (lncRNAs) (Mattick, 2009; Stefani & Slack, 2008). lncRNAs and miRNA are well-known, whereas lncRNA consist of about 200 contrarily to the miRNA, which are single-stranded RNAs of 18–22 nucleotides and represent a novel class of gene regulators. As endogenous mediators, miRNA are located in introns of genes and contemporaneously transcribed with the respective mRNA. Target RNAs are mostly bound within their 3`UTR by miRNAs, which results in the degradation of the mRNA or translational repression by a perfect or imperfect complement (Winter *et al.*, 2009; Zhou *et al.*, 2014). As an example, miRNA-126 decreases VCAM expression, suggesting an importance in vascular inflammation (Harris *et al.*, 2008).

1.5.1 Imprinted genes *H19* and *IGF2*

Genomic imprinting is an effect widely based on DNA methylation (Feil & Khosla, 1999). The human genome contains a cluster of imprinted genes on chromosome 11 (Lin *et al.*, 1999) including important examples of imprinted genes: the non translated *H19* RNA and the insulin-like growth factor (*IGF2*), which are reciprocally expressed. *H19* is only expressed by the maternal allele (Rachmilewitz *et al.*, 1992) and *IGF2* is paternally expressed (Giannoukakis *et al.*, 1993). Both promoters are regulated by

the same enhancers, but on different parental chromosomes (Leighton *et al.*, 1995). On the maternal allele, *H19* is expressed and *IGF2* is imprinted by blocking the enhancer activity to the *IGF2* promoter by the binding of insulator factor CTCF (CCCTC-binding factor) to the unmethylated imprinting control region. On the paternal region, this region is methylated, whereby binding of CTCF is not possible, resulting in a silencing of *H19* (Figure 10) (Gabory *et al.*, 2006).

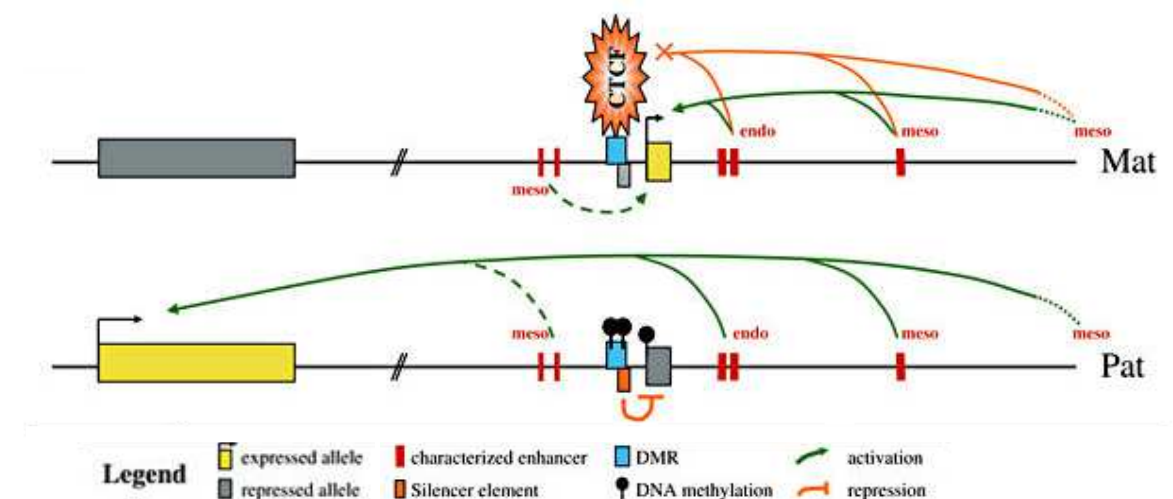


Figure 10: Imprinting mechanisms of *H19* and *IGF2* (Gabory *et al.*, 2006). See text for details.
meso: mesodermal enhancers, endo: endodermal enhancers, Mat: maternal allele, Pat: paternal allele, CTCF: CCCTC-binding factor, DMR: differentially methylated region

Both genes are mainly prenatally expressed and strongly downregulated after birth in most tissues (Weber *et al.*, 2001). Expression is also known for various tumors suggesting a role in tumorigenesis and a few other diseases (Kessler *et al.*, 2013; Taniguchi *et al.*, 1995; Matouk *et al.*, 2013; Bergman *et al.*, 2013; Engstrom *et al.*, 1998). While the growth factor *IGF2* is widely accepted as tumorigenic protein, the non-translated *H19* is discussed to be either a tumor promoter or a tumor suppressor. Both genes are also connected to atherosclerosis by playing a role in proliferation of VSMCs (Han *et al.*, 1996; Li *et al.*, 2009; Zaina & Nilsson, 2003; Zaina *et al.*, 2002). Additionally, *H19* was reported to be upregulated in the inflammatory disease rheumatoid arthritis (Stuhlmuller *et al.*, 2003), whereby in chondrocytes, TNF- α leads to a decrease of *H19* (Steck *et al.*, 2012).

1.6 Aim of this work

Atherosclerosis is a widely spread, cardiovascular disease with a major cause of morbidity and mortality. The molecular mechanisms of this disease, especially in the context of different kinds of shear stress, are as yet not completely understood. Inflammation is known to be one of the main factors in atherosclerosis development, which is especially characterized by the inflammatory activation of the endothelium. The anti-inflammatory protein GILZ, which mediate the anti-inflammatory actions of glucocorticoids, is known to be involved in different inflammatory processes.

The aim of this work was to elucidate the role of GILZ in endothelial inflammation.

Therefore, following aspects were clarified:

- (I) The downregulation of the GILZ expression in human degenerated veins and atherosclerotic arteries compared to healthy vessels
- (II) The differentially up- and downregulation of the GILZ expression at anti- and inflammatory conditions, especially at shear stress conditions, in endothelial cells
- (III) The mechanism of GILZ regulation
- (IV) Functional implications of GILZ downregulation

2 Materials and methods

2.1 Materials

Endothelial cell growth medium was purchased from Promocell (Heidelberg, Germany), RPMI-1640, Earle's medium 199, fetal calf serum gold (FCS), trypsine and penicilline/streptomycine were obtained from PAA (Cölbe, Germany). Collagenase A from *Clostridium histolyticum* and collagen (sterile, lyophilizate, from rat tail tendon) were bought from Roche Deutschland Holding GmbH (Grenzach-Wyhlen, Germany), dissolved, and diluted after manufacturer's instructions.

RNA later and Qiazol were from Qiagen (Hilden, Germany). Kanamycin, tumor necrosis factor alpha (TNF- α), dexamethasone, and ampicillin were purchased from Sigma-Aldrich Chemie GmbH (München, Germany), SB203580 from Jena Bioscience (Jena, Germany) and LPS as well as Pam₃CSK₄ from Invivogen (San Diego, CA, USA). siGILZ (siGENOME SMARTpool) and siControl (siGenome) were from Dharmacon (Nidderau, Germany). pGL4.32[*luc2P/NF-κB-RE/Hygro*] containing 5 repetitive elements of the NF-κB consensus sequence GGGAAATTCC was obtained from Promega (Heidelberg, Germany). pcDNA3-p38 α -dn was a gift from Prof. Dr. Jian-Dong Li, University of Rochester Medical Center, USA (Shuto *et al.*, 2001).

The parallel flow chamber was modified after (Frangos *et al.*, 1988) and manufactured by upag AG (Vollersode, Germany). The peristaltic pump (403U/VM4 purple/white, 040.3K1V.M4E, 0.85-17 ml/min) was obtained from Watson Marlow (Rommerskirchen, Germany). Silicon tubes were purchased from VWR (Darmstadt, Germany) and silicon mats for gasket construction were from rfQ Medizintechnik (Tuttlingen, Germany).

For Western blot analyses, anti-GILZ (sc-26518) and anti-MKP-1 (sc-1199) antibodies were purchased from SantaCruz (Heidelberg, Germany), anti-TTP (T5327) and anti-tubulin (T9026) were obtained from Sigma (Taufkirchen, Germany), and anti-TLR2 (Cat # 3268-1) from Epitomics (Burlingame, USA). The IRdye-labeled secondary antibodies goat anti-mouse, goat anti-rabbit, and donkey anti-goat were from LI-COR Biosciences (Bad Homburg, Germany), and anti-GILZ antibody for IHC (FL-134) was obtained from SantaCruz (Heidelberg, Germany).

All primers and probes were purchased from Eurofins MWG Operon (Ebersfeld, Germany). 5 x HOT FIREPol® EvaGreen® qPCR Mix Plus was from Solis BioDyne (Tartu, Estonia). Taq-Polymerase (5 U/ μ l), 10x *Taq* buffer and the dNTP mix (dATP,

dCTP, dGTP and dTTP, 10 mM each) were obtained from Genscript (Piscataway, NJ, USA).

Other materials were purchased from Merck (Darmstadt, Germany), Sigma (Taufkirchen, Germany), VWR (Darmstadt, Germany), or Roth (Karlsruhe, Germany) unless otherwise noted.

2.2 Human vessels

Human healthy saphenous veins and radial arteries as well as pieces of atherosclerotic aortas and degenerated aortocoronary saphenous vein bypass grafts were obtained from patients undergoing coronary bypass surgeries. During operation, vessels were immediately transferred into RNA stabilization solution (*RNA later*, Qiagen, Hilden, Germany), stored at 4°C, and after some days transferred to -20°C. Samples were obtained from Prof. Dr. Hanno Huwer (SHG Klinik Völklingen, Germany) with the consent of patients and with permission of the local ethics committee (ref #102/09).

2.3 Bacterial culture

2.3.1 Bacterial strains and cultivation

The following *Escherichia coli* strains were used as host organism for plasmids:

Escherichia coli (*E. coli*) TOP10 (Invitrogen, Carlsbad, CA, USA), genotype F- mcrA Δ(mrr-hsdRMS-mcrBC) φ80lacZΔM15 ΔlacX74 nupG recA1 araD139 Δ(ara-leu)7697 galE15 galK16 rpsL(Str^R) endA1 λ⁻

Escherichia coli (*E. coli*) GT116 (Invivogen, San Diego, CA, USA), genotype F- mcrA Δ(mrr-hsdRMS-mcrBC) φ80lacZΔM15 ΔlacX74 recA1 endA1 Δdcm ΔsbcC-sbcD

E. coli GT116 was used to produce the shTTP plasmid because of enhanced compatibility with hairpin structures and cultivated in low salt LB_{Zeo}-medium.

Bacteria were grown in LB_{Amp}-medium (Luria Bertani, Version Miller with 10% [w/v] NaCl, pH 7.5) (bacto-tryptone 10% [w/v], yeast extract 5% [w/v], NaCl 10% [w/v], ampicillin 100 µg/ml) or low salt LB_{Zeo}-medium (Luria Bertani, pH 7.5) (bacto-tryptone 10% [w/v], yeast extract 5% [w/v], NaCl 2.5% [w/v], zeocin 25 µg/ml) at 37°C and 5% CO₂. For selection of single clones, LB_{Amp}- and low salt LB_{Zeo}-agar (medium containing 30% [w/v] agar) were used.

2.3.2 Generation of competent bacteria using CaCl₂ method

5 ml of an overnight culture was transferred into 100 ml LB-medium and rotated at 37°C until absorption of A_{650 nm}= 0.4 was achieved. After 30 min incubation on ice, bacteria were centrifuged (2,000 × g, 4°C 5 min) and resuspended in 2.5 ml cold CaCl₂ solution (75 mM CaCl₂, 15% glycerol). 10 ml CaCl₂ solution were added, mixed and 30 min incubated on ice. Bacteria were centrifuged again, resuspended in 2.5 ml cold CaCl₂ solution, and frozen in 100 µl aliquots.

2.3.3 Transformation

10-150 ng of a plasmid were added to 100 µl competent bacteria, mixed, and incubated on ice for 20 min. After heat shock for 80 s at 42°C, bacteria were incubated again on ice for 2 min. Afterwards, 900 µl prewarmed SOC medium (trypton 20 g/L, yeast extract 5 g/L, NaCl 0.5 g/L, KCl 0.2 g/L, MgCl₂ 10 mM, glucose 20 mM) was added and shaken 1.5 h at 37°C. After plating, bacteria were incubated overnight.

2.3.4 Isolation of plasmids

Isolation of plasmids from overnight culture was prepared using QIAprep Spin Mini-prep or Midiprep kit (Qiagen, Hilden, Germany) according to the manufacturer's instructions.

2.3.5 Determination of DNA concentration

Concentration of plasmids was measured by determining the extinction at 260 nm. The purity was checked by an additional measurement at 280 nm, which is an indicator for protein contaminations. The ratio 260/280 should be 1.8 for DNA. Measure-

ments were performed with a BioMate UV-Vis spectrophotometer (ThermoElectron, Oberhausen, Germany). 50 µg/ml DNA equates an extinction of 1 at 260 nm.

2.4 Cell culture

2.4.1 THP-1

This human leukemic monocytic cell line was cultivated in RPMI-1640 with 10% [v/v].

2.4.2 Human umbilical vein endothelial cells (HUVEC)

HUVEC are primary cells, which were obtained by isolation of human umbilical veins. The umbilical cords were transferred into PBS⁺ immediately after birth (*phosphate buffered saline*⁺) (NaCl 8.0 g/L, KCl 0.20 g/L, Na₂HPO₄ 1.15 g/L, KH₂PO₄ 0.20 g/L, MgCl₂·6H₂O 0.10 g/L, CaCl₂·2H₂O 0.10 g/L) containing 1% [v/v] penicilline (10,000 U/ml)/streptomycine (10 mg/ml) and stored at 4°C (Klinikum Saarbrücken, Germany). The isolation of HUVEC was carried out up to 10 days after childbirth.

2.4.3 Isolation of HUVEC

Earle's medium 199 and endothelial cell growth-medium were always used containing 10% [v/v] FCS Gold, 1% [v/v] penicilline (10,000 U/ml)/streptomycine (10 mg/ml), 0.1% [v/v] kanamycin (50 mg/ml) unless otherwise noted.

The isolation of HUVEC was performed under sterile conditions by digestion of umbilical veins with 0.1 g/L collagenase A at 37°C after Jaffe *et al.* (1973). To stop the digestion, veins were rinsed with Earle's medium 199. After centrifugation (10 min, 200 x g) cells were resuspended in 5 ml endothelial cell growth-medium, and cultivated at 37°C and 5% CO₂ in a 25 cm² cell culture flask. After one day cells were washed three times with PBS (*phosphate buffered saline*) (NaCl 7.20 g/L, KH₂PO₄ 0.43 g/L, Na₂HPO₄ 1.48 g/L) and cultivated until confluence.

2.4.4 Cultivation of HUVEC

After reaching confluence, cells were passaged to a new cell culture flask or plate: cells were washed three times with PBS and 1 ml or 2 ml trypsine-EDTA-solution was added (in a 25 cm² or 75 cm² flask). After 2 min incubation at 37°C, the trypsine was inactivated with 25 ml Earle's medium 199. The suspension was centrifuged (10 min, 175 x g) and the pellet completely resuspended in endothelial cell growth-medium. Subsequently, cells were splitted 1:3 or 1:4, and 1 part seeded into new 75 cm² cell culture flasks, in 6-well plates, or 1.5 parts on glass slides in 4-well plates. Experiments were performed in passage three. If necessary, determination of cell count was performed *via* a Neubauer improved hemocytometer.

Cells were harvested after the experiments in 1 ml Qiazol to isolate RNA, DNA, and proteins simultaneously.

2.4.5 Freezing and thawing of HUVEC

freezing:

Confluent cells in passage one were used for freezing. HUVEC were washed and trypsinized as outlined above. After centrifugation, cells of a 75 cm² flask were resuspended in 3 ml ice cold freezing medium (50% [v/v] Earle's medium 199, 20% [v/v] endothelial cell growth-medium, 20% [v/v] FCS Gold, 10% [v/v] DMSO). After filling into cryovials, cells were frozen at -20°C for one day. Afterwards, they were transferred into -80°C for one week and then into liquid nitrogen at -196°C.

thawing:

To reduce cytotoxic effects of DMSO, cryovials were thawed 2-3 min at 37°C and the suspension was rapidly transferred into 20 ml prewarmed Earle's medium 199. After centrifugation (10 min, 200 x g), cells were resuspended in endothelial cell growth-medium and converted into a new 75 cm² cell culture flask.

2.4.6 Detection of mycoplasma

To exclude contaminations with *mycoplasma*, HUVEC were once tested with the Venor®GeM mycoplasma detection kit (Minerva Biolabs, Berlin) according to the manu-

facturer's instructions. It is based on the amplification of mycoplasma DNA with a detection limit of 1-5 fg.

2.5 Transfection

Before transfection with either siRNA or plasmids, HUVEC were grown until 80% confluence. Electroporation was performed using the Amaxa® Nucleofector™ Kit (Lonza, Basel, Switzerland) according to the manufacturer's instructions.

For GILZ knockdown, 100 pmol/L siGILZ or siControl were transfected for 20 h.

The luciferase assay was carried out by transfection of 100 pmol/L siRNA and 1.5 µg pGL4.32[Luc2P/NF-κB-RE/Hygro] for 20 h. Plasmid was obtained from Indou Awissi Kpebane (Pharmaceutical Biology, Saarland University).

Overexpression of dominant negative (dn) p38 α MAPK was performed by nucleofection of 2 µg of pcDNA3-p38 α -dn or pcDNA3-empty for 24 h by Dr. Kerstin Hirschfelder (Pharmaceutical Biology Saarland University).

For ZFP36 (TTP) knockdown, 1 µg shTTP plasmid (Fechir *et al.*, 2005) or 1 µg psiRNA-LucGL3 plasmid (Invivogen) as control were transfected for 24 h. The shTTP plasmid was created by cloning of siRNA against ZFP36 5`-ACCTCACAAAGACTGAGCTATGTCGGATCAAGAGTCCGACATAGCTCAGTCTTG-TTT-3 into the BbsI sites of psiRNA-h7SKGFPzeo by Dr. Jessica Hoppstädter (Pharmaceutical Biology, Saarland University) and produced with *E. coli* GT116.

As transfection control, the pmaxGFP™ plasmid (Lonza, Basel, Switzerland) was used. The green color of cells based on the green fluorescent protein (GFP) was detected via fluorescence microscopy. Except for the Luciferase assay (see below), cells were seeded into 6 well plates after transfection.

2.6 Luciferase assay

HUVEC were transfected as outlined above and seeded into white 96 well plates with white bottom (PerkinElmer, Rodgau-Jüdesheim, Germany). Cells were harvested with 1x passive lysis buffer (Promega, Heidelberg, Germany) and stored at -80°C at least for 1 h. A Wallac Victor² multilabel counter with the software Wallac 1420 (Wal-

Iac/PerkinElmer, Rodgau-Juedesheim, Germany) was used for the measurement of the luminescence after adding of 50 µl luciferase substrate buffer (tricine 20 mM, MgCO₃ Mg(OH)₂ x 5 H₂O 2.67 mM, MgSO₄ x 7 H₂O 1.07 mM, EDTA 100 µM, DTT 33.3 mM, ATP 530 µM, coenzym A 0.213 mg/ml, D-luciferin 470 mM) to 25 µl of cell lysate.

2.7 Shear Stress

2.7.1 Coating of glass slides

Sterilized glass slides (76 x 26 x 1 mm, Roth) with exact identical thickness were incubated for 40 min in 1 ml collagen solution (30 µg/ml in 0.2% acetic acid) in 4-well plates, whereas the reverse surface was coated. While washing twice with PBS, glass slides were turned in the wells. After drying for 30 min, cells were seeded onto the glass slides.

2.7.2 Flow experiments

The level of laminar shear stress is determined by the flow rate. Calculation of the flow rate was performed with the following formula:

$$\tau = \frac{6Q\mu}{bh^2} \quad (\text{Frangos et al., 1988})$$

τ = shear stress [dynes/cm²]

Q = flow rate [cm³/s]

μ = viscosity (0.01 dynes*s/cm²) (Frangos et al., 1988)

b = channel width (1.9 cm)

h = channel height (= thickness of the middle part of the chamber (1.15 mm) – thickness of the glass slide)

The calculated flow rate was adjusted by controlling the pump drive and the tube diameter in the pump before each experiment. Afterwards, glass slides with confluent HUVEC were integrated in the parallel plate flow chambers (Figure 11), which were

then connected to the peristaltic pump and were filled with endothelial cell growth-medium (Figure 12).

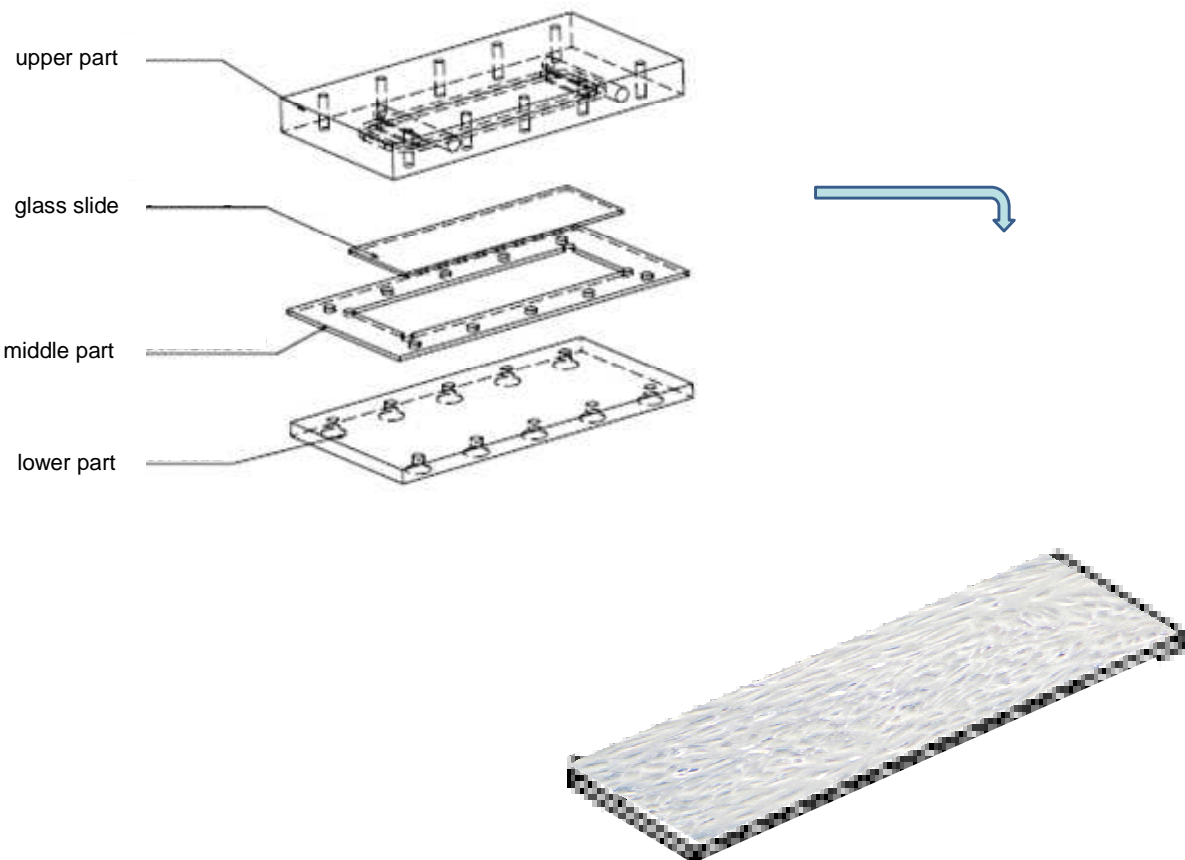


Figure 11: Setup of one parallel plate flow chamber with glass slide. Chamber was modified after (Frangos *et al.*, 1988) and manufactured by Upag AG after plans shown in the supplement (Vollersode, Germany). Technical drawing and assistance were kindly performed by Christian and Alexander Hahn.

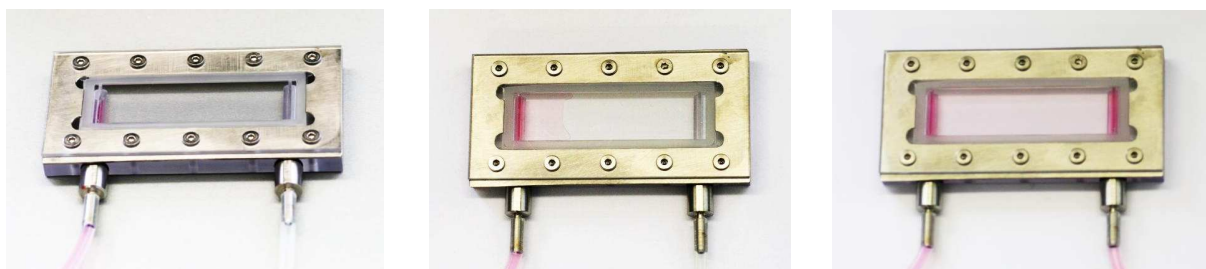


Figure 12: Filling of the parallel plate flow chamber

HUVEC cultivated on collagen coated glass slides were exposed either to laminar shear stress of 20 dynes/cm² (laminar), to low laminar shear stress of 2 dynes/cm²

(low), or to oscillatory shear stress (oscillatory) for 24 h in this parallel plate flow chamber. All types of flow were generated by a peristaltic pump (403U/VM purple/white, Watson Marlow). Laminar flow rates were regulated to fit a shear stress of 20 or 2 dynes/cm² as outlined above and the flow was unidirectionally. For oscillatory shear stress the direction of flow was changed with a frequency of 1/s using an electronic control unit (timer-module Ne555 (obtained from Mathias Sander, Experimental Physics, Prof. Dr. Ott, Saarland University)).

TNF- α (10 ng/ml) was added to the flow medium during a short stop in the flow. After 5 min of laminar flow to distribute the TNF- α in the medium, laminar or oscillatory flow was continued for another 2 h or 3.5 h. Untreated cells were similarly flowed. Cells were harvested in 1 ml Qiazol.

2.8 Immunohistochemistry

Sections of murine femoral arteries, healthy radial arteries and healthy saphenous veins were fixed in 4% formalin. Paraffin-embedded slides with cut samples were stained for GILZ with the CSA II Kit (Dako, Hamburg, Germany) according to (Tybl *et al.*, 2011). The GILZ antibody was used in a concentration of 1:10,000 overnight at 4°C.

2.9 RNA analysis

To protect the RNA from degradation by RNases, chloroform treated reaction tubes were used. Tips, H₂O, and buffer were decontaminated with UV light.

2.9.1 RNA isolation by phenol chloroform extraction

To isolate RNA, a single step method after (Chomczynski & Sacchi, 1987) was used.

HUVEC

After washing with PBS, cells were harvested in 1 ml Qiazol and frozen at -80°C at least for 1 h. Lysates were defrosted at room temperature, 250 μ l chloroform was added and vortexed for 15 s until turbidity. The mixture was incubated for 3 min at

room temperature, centrifuged (15 min, 4°C, 17,000 x g) and 400 µl supernant was transferred into a new reaction tube. RNA was precipitated by adding 100% isopropanol at -20°C over night. The lower- and the interphase were used for DNA and protein isolation (2.10 and 2.11).

On the following day, the suspension was centrifuged (10 min, 4°C, 17,000 x g), washed with ice-cold 75% ethanol ([v/v] in 0.1% DEPC-H₂O), dried at 55°C, and dissolved in 20 µl 0.1% DEPC-H₂O.

Human vessels

Samples, stored in *RNA later*, provided at -20°C were defrosted and ends of pieces (max. 0.3 mm length) were cut off. After transferring into Qiazol, samples were disintegrated for 2 min at 18,000 rpm using an Ultra-Turrax® (IKA, Staufen, Germany) and stored at -80°C. Isolation of RNA was performed as described above.

2.9.2 DNase digestion

To exclude any contamination with genomic DNA, RNA was digested with the Ambion DNA free kit (Ambion # 1906, Applied Biosystems, Darmstadt, Germany) according to the manufacturer's guidelines.

2.9.3 Determination of RNA concentration

The measurement was performed with a BioMate UV-Vis spectrophotometer (ThermoElectron, Ulm, Germany) at the absorption maximum of 260 nm. 40 µg/ml RNA equates an extinction of 1.

2.9.4 Alu polymerase chain reaction (Alu PCR)

To check the DNA digestion and detect any contaminations of DNA in the RNA, an Alu PCR was carried out, which amplifies repetitive *Alu* sequences in a PCR reaction (Mullis & Falloona, 1987). These sequences are found in a large number in the human genome (5% of DNA) and contain about 300 bp. The primer A1S 5'-TCA TGT CGA CGC GAG ACT CCA TCT CAA A-3` was used. The reaction mixture was prepared on ice, added to 100 ng of RNA, and the reaction was performed in a Thermo-cycler PX2 (ThermoElectron, Ulm, Germany). As a positive control, 500 ng of ge-

nomic DNA of THP-1 cells (obtained by Dr. Kerstin Hirschfelder, Pharmaceutical Biology, Saarland University) were used.

reaction mixture (one sample):

Primer A1S (50 µM)	0.5 µl
10x <i>Taq</i> buffer	2.5 µl
dNTPs (10 mM each)	0.5 µl
<i>Taq</i> polymerase (5 U/µl)	0.5 µl
RNA	100 ng
H ₂ O	ad 25 µl

reaction conditions:

denaturation	94°C	5 min	
denaturation	94°C	1 min	
annealing	56°C	1 min	
elongation	72°C	2 min	
final elongation	72°C	10 min	30 cycles

The detection of amplified product was done using agarose electrophoresis on a 1.5% agarose gel. If no product was detected, reverse transcription was carried out. If a product was detected, DNase digestion and Alu PCR were repeated.

2.9.5 Agarose gel electrophoresis

The basic principle of agarose gel electrophoresis is the migration of charged particles in an electric field. The gel contains 0.5 – 2% [w/v] agarose depending on the size of detectable DNA fragments supplemented with 0.04% [v/v] ethidium bromide. After mixing with 6x loading dye (18% [w/v] ficoll type 400, 0.5 M EDTA, 60 ml 10x TBE (tris-borat-EDTA buffer: tris base 10.8 g/L, boric acid 3.5 g/L, Na₂EDTA 0.74 g/L), 0.25 % [w/v] bromophenol blue, 0.25% [w/v] xylencyanol, H₂O_{dd} ad 100 ml) samples were loaded onto a gel in TBE buffer and separated at 100 V. For the determination of DNA sizes, a 50 bp DNA ladder (Fermentas, St. Leon-Rot, Germany) or a 1 kb DNA ladder (Invitrogen, Karlsruhe, Germany) was additionally loaded onto

the gel. Fluorescence detection of intercalated ethidium bromide at 312 nm was performed with an UV transilluminator (White Top Light Transilluminator) with the software ArgusX1 (Biostep, Jahnsdorf, Germany).

2.9.6 Reverse transcription (RT)

0.25 - 1 µg of RNA in 10 µl H₂O were denatured at 65°C for 5 min, put on ice, and transcribed into complementary DNA (cDNA) using the High Capacity cDNA Reverse Transcription Kit (Applied Biosystems, Darmstadt, Germany) with the oligo dT Primer 5`-TTT TTT TTT TTT TTT TTT-3` and RNaseOUT™ ribonuclease inhibitor (Invitrogen, Karlsruhe, Germany). RNA was incubated with the mixture for 10 min at 25°C and then 2 h at 37°C. After inactivation of the reverse transcriptase for 5 s at 85°C, samples were diluted with 80 µl H₂O on ice. A reaction without enzyme served as negative control for real-time RT-PCR.

reaction mixture (one sample):

10x RT buffer	2 µl
25x dNTP-mix (100 mM, 25 mM each)	0.8 µl
Oligo dT(10 µM)	2 µl
RNaseOUT™ Ribonuclease Inhibitor (40 U/µl)	0.25 µl
MultiScribe reverse transcriptase (4 U/µl)	1 µl
H ₂ O	3.95 µl

2.9.7 Real-time RT-PCR

Real-time RT-PCR is a special form of the PCR reaction, whereas DNA quantification is performed during the amplification (Kubista *et al.*, 2006; Mullis *et al.*, 1986). Quantification is carried out by two different principles, both of them measuring the emerging fluorescence. The first method is the determination by fluorescence resonance energy transfer (FRET), where the target specific probe is dually labelled (5'-end: 6-carboxy-fluorescein (6-FAM), 3'-end: black hole quencher 1 (BHQ1)). The second method is the fluorescent dye EvaGreen® (SolisBioDyne, Tartu, Estonia), which intercalates into the emerging DNA amplicates.

2.9.7.1 Real-time RT-PCR with dual labelled probe

The conditions for PCR reactions and mixtures are listed in Table 3. The reaction mixture was assembled on ice and filled in 96 well plates. 5 µl sample, standard, negative control from reverse transcription or H₂O was added, each in triplicate. Used primers and probes are given in Table 1 and

Table 2. Reaction and quantification were performed with an iCycler iQ5 and the iQ5 package software (Biorad, München, Germany). Quantification occurred by analysis of the C_T (threshold cycle) value. The concentration of probes was then calculated by the software related to the standard curve. Values were normalized to the house keeping gene ACTB (β-actin). The standard deviation of triplicates was less than 0.5 and the efficiency of the reactions was between 95% and 105%.

standard dilution series

For quantification of cDNA and determination of the PCR efficiency, a dilution series with 7 dilutions (starting point: 20 attomol/µl, in TE buffer) of the plasmid pGEM®-T Easy (Promega, Heidelberg, Germany) with the appropriate insert. Glycerol stocks of bacteria with the appropriate plasmids were provided by Prof. Dr. Alexandra K. Kiemer (Pharmaceutical Biology, Saarland University) or cloned during my diploma thesis. Calculation of required amount of plasmid:

$$c \text{ (target DNA)[attomol/µl]} = c(\text{plasmid})[\mu\text{g/ml}] * 1.515[\text{pmol/µl}] / N[\text{bp}]$$

N = number of base pairs of vector and insert

primers and probes

Sequences for primers and probes (Table 1 and Table 2) were obtained from Prof. Dr. Alexandra K. Kiemer (Pharmaceutical Biology, Saarland University) or designed with the program Primer3 (<http://frodo.wi.mit.edu/primer3/>).

Table 1: primer sequences for real-time RT-PCR

mRNA	primer sense (5' → 3')	primer antisense (5' → 3')
<i>ACTB</i>	TGC GTG ACA TTA AGG AGA AG	GTC AGG CAG CTC GTA GCT CT
<i>IL-8</i>	TGC CAG TGA AAC TTC AAG CA	ATT GCA TCT GGC AAC CCT AC
<i>IL-6</i>	AAT AAT AAT GGA AAG TGG CTA TGC	AAT GCC ATT TAT TGG TAT AAA AAC
<i>TLR2</i>	GCA AGC TGC GGA AGA TAA TG	CGC AGC TCT CAG ATT TAC CC
<i>CCL2</i>	TTG ATG TTT TAA GTT TAT CTT TCA TGG	CAG GGG TAG AAC TGT GGT TCA
<i>GILZ</i>	TCT GCT TGG AGG GGA TGT GG	ACT TGT GGG GAT TCG GGA GC
<i>ICAM</i>	GAA GTG GCC CTC CAT AGA CA	TCA AGG GTT GGG GTC AGT AG
<i>VCAM</i>	CGA GAC CAC CCC AGA ATC TA	CTG TGG TGC TGC AAG TCA AT
<i>E-selectin</i>	AGC CCA GAG CCT TCA GTG TA	CCC TGC ATG TCA CAG CTT TA

Table 2: probe sequences for real-time RT-PCR

mRNA	probe (5' → 3')
<i>ACTB</i>	6-FAM-(CAC GGC TGC TTC CAG CTC CTC)BHQ-1
<i>IL-8</i>	6-FAM-(CAGACCCACACAATACATGAAGTGGTGA)BHQ-1
<i>IL-6</i>	6-FAM-(TCC TTT GTT TCA GAG CCA GAT CAT TTC T)BHQ-1
<i>TLR2</i>	6-FAM-(ATG GAC GAG GCT CAG CGG GAA G)BHQ-1
<i>CCL2</i>	6-FAM-(AGA TAC AGA GAC TTG GGG AAA TTG CTT TTC)BHQ-1
<i>GILZ</i>	6-FAM-(CAG GAT GCT CAC ATT TAA GTT TTA CAT GCC C)BHQ-1
<i>ICAM</i>	6-FAM-(AAC ACA AAG GCC CAC ACT TC)BHQ-1
<i>VCAM</i>	6-FAM-(GCT CAG ATT GGT GAC TCC GT)BHQ-1
<i>E-selectin</i>	6-FAM-(CAT CTG GGA ATT GGG ACA AC)BHQ-1

Table 3: PCR conditions for real-time RT-PCR

mRNA	probe	dNTPs	MgCl ₂	annealing
<i>ACTB</i>	1.5 pmol	200 μM	5 mM	60°C
<i>IL-8</i>	2.5 pmol	200 μM	4 mM	60°C
<i>IL-6</i>	2.5 pmol	200 μM	3 mM	57°C
<i>GILZ</i>	1.5 pmol	200 μM	4 mM	60°C
<i>CCL2</i>	1.5 pmol	200 μM	4 mM	59°C
<i>TLR2</i>	2.5 pmol	800 μM	6 mM	60°C
<i>ICAM</i>	2.5 pmol	200 μM	3 mM	58°C
<i>VCAM</i>	2.5 pmol	200 μM	4 mM	58°C
<i>E-selectin</i>	1.5 pmol	200 μM	4 mM	58°C

reaction mixture (one sample):

primer sense (50 µM)	0.25 µl
primer anti-sense (50 µM)	0.25 µl
10x <i>Taq</i> buffer	2.5 µl
MgCl ₂	x
dNTPs(10 mM, each)	x
probe (1 pmol/µl)	x
<i>Taq</i> polymerase (5 U/µl)	0.5 µl
H ₂ O	ad 25 µl

reaction conditions:

denaturation	95°C	08:00 min	45 cycles
denaturation	95°C	00:15 min	
annealing	x	00:15 min	
elongation	72°C	00:15 min	
final elongationf	25°C	00:30 min	

2.9.7.2 Real-time RT-PCR with EvaGreen®

cDNA was diluted 1:5 and used as standard dilution series. EvaGreen® Mix (Solis-BioDyne, Tartu, Estonia) was used according to the manufacturer's guidelines with a mixture as given in Table 4. Also primer sequences are given in Table 4. The reaction mixture was assembled on ice and filled in 96 well plates. 5 µl sample, standard, negative control from reverse transcription or H₂O was added, each in triplicate. Reaction and quantification was performed with an iCycler iQ5 and the iQ5 package software (Biorad, München, Germany). Quantification was done by analysis of the C_T values after the Livak method (ΔC_T method) (Livak & Schmittgen, 2001) (*Applications Guide* of iCycler iQ5):

$$\frac{2^{C_T(\text{actin,treated}) - C_T(\text{gene,treated})}}{2^{C_T(\text{actin,co}) - C_T(\text{gene,co})}}$$

Values were normalized to the house keeping gene ACTB (β-actin). The standard deviation of triplicates was less than 0.5 and the efficiency of the reactions was between 95% and 105%.

Table 4: primer sequences for real-time RT-PCR with EvaGreen®

mRNA	primer sense (5' → 3')	primer antisense (5' → 3')
DUSP1	CAG CTG CTG CAG TTT GAG TC	AGG TAG CTC AGC GCA CTG TT
HO1	CGA GAC GGC TTC AAG CTG GT	AAG ACT GGG CTC TCC TTG TT
H19	TTC AAA GCC TCC ACG ACT CT	CTG AGA CTC AAG GCC GTC TC
IGF2	GGA CTT GAG TCC CTG AAC CA	TGA AAA TTC CCG TGA GAA GG
CTCF	GAA CCC ATT CAG GGG AAA AGC	TCG CAA GTG GAC ACC CAA ATC
TLR2	GGG GTC CTG TGC CAC CGT TTC	CCC AGT AGG CAT CCC GCT CAC
ZFP36	TCG CCA CCC CAA ATA CAA G	TCG GCT AGG GTT GTG GAT G
ACTB	TGC GTG ACA TTA AGG AGA AG	GTC AGG CAG CTC GTA GCT CT

DUSP1 and HO1 primer sequences are published in (Zakkar *et al.*, 2008).

Table 5: PCR conditions for real-time RT-PCR with EvaGreen®

mRNA	primers	annealing
DUSP1	0.6 µl	56°C
HO1	0.3 µl	56°C
H19	0.4 µl	60°C
IGF2	0.5 µl	56°C
CTCF	0.4 µl	58°C
TLR2	0.3 µl	65°C
ZFP36	0.5 µl	60°C
ACTB	0.4 µl	60°C

reaction mixture (one sample):

primer sense (10 µM)	x
primer antisense (10 µM)	x
EvaGreen® mix	4 µl
H ₂ O	ad 20 µl

reaction conditions:

denaturation	95°C	30:00 min	
denaturation	94°C	00:30 min	
annealing	x	00:30 min	40 cycles
elongation	72°C	00:30 min	
melting curve	55°C	00:07 min	40 cycles

2.10 DNA analysis

2.10.1 DNA isolation

DNA was isolated from the Qiazol lysates (2.9.1) after the supernatant with RNA was completely removed. DNA was precipitated by addition of 300 µl 100% [v/v] ethanol, washed with ice cold 70% [v/v] ethanol, and solved in 50 µl H₂O.

After isolation, DNA analysis was carried out in cooperation with Dr. Sascha Tierling in the Institute of Genetics/Epigenetics (Prof. Dr. Walter, Saarland University).

2.10.2 Determination of DNA concentration

In addition to the method described in 2.3.5, DNA was determined using a Nanodrop instrument at 260 nm (Thermo Fisher Scientific, Waltham, MA, USA).

2.10.3 Bisulfite treatment

Bisulfite treatment is a method to convert unmethylated cytosines of DNA into uracils. 500 ng DNA were mixed with 187 µl sodium-bisulfite solution (1.9 g NaHSO₃, 750 µl 2 M NaOH, 2.5 ml H₂O) and 73 µl scavenger solution (98.7 mg (+ -)-6 hydroxy-2, 5, 7, 8-tetramethylchromane-2-carboxylic acid C₁₄H₁₈O₄, 2.5 ml Dioxan). The reaction was performed with a master cycler (Eppendorf AG, Hamburg, Germany).

reaction conditions:

denaturation	99°C	15 min
sulfonation and desamination	50°C	30 min
denaturation	99°C	5 min
sulfonation and desamination	50°C	1.5 h
denaturation	99°C	5 min
sulfonation and desamination	50°C	1.5 h

After addition of 150 µl H₂O, samples were centrifuged (15,500 x g, 24 min) through a filter unit (Centrifugal Filters Ultracel, MilliporeTM, Darmstadt, Germany), which was desulfonated with 500 µl 0.3 M NaOH (incubation 10 min, centrifugation 15,500 x g, 17 min) and washed with 500 µl TE buffer (15,500 x g, 17 min). Elution of DNA was

carried out with 50 µl prewarmed (50°C) TE buffer on the turned filter unit using centrifugation (4,000 x g, 25 min). Samples were stored at 4°C.

2.10.4 PCR of bisulfite DNA

2 µl of bisulfite DNA was merged with the reaction mixture (Table 6 and Table 7) and the reaction was carried out in a Thermal Cycler (Applied Biosystems, Darmstadt, Germany). During PCR, methylated CG sequences were amplified as CG and unmethylated CG, which were converted into UG by bisulfite treatment, were amplified as TG.

Table 6: primers of bisulfite DNA

gene	primer sense (5' → 3')	primer antisense (5' → 3')
DUSP1p	GAA AAG GGG TAT AAG AGT ATG T	CTA CCA ACT AAA ACT AAC CTC C
DUSP1ed	GTT TTG GTT TTG AGT AAG TTT GAT G	TAA CCC TCA AAA TAA TTA AAA CAA TTA A
DUSP1eu	GTT ATT GGG ATT TAG GGT A	CTA AAC TAA AAA CCT CCA AC
H19	GGG TTT GGG AGA GTT TGT GAG GT	AAC ACA AAA AAC CCC TTC CTA CCA

Table 7: conditions for the PCR of bisulfite DNA

gene	cycles	annealing
DUSP1p	36	54°C
DUSP1ed	42	52°C
DUSP1eu	40	56°C
H19	45	57.6°C

reaction mixture (one sample) (DUSP1)

primer sense (10 µM)	0.5 µl
primer anti-sense (10 µM)	0.5 µl
10x buffer B (Solis BioDyne)	3 µl
MgCl ₂ (25 mM, Qiagen)	3 µl
dNTPs (10 mM, 2.5 µM each, Sigma)	2.4 µl
<i>Hot fire pol</i> (50 U/µl, Solis BioDyne)	0.5 µl
H ₂ O	18.1 µl

reaction mixture (one sample) (H19)

primer sense (10 µM)	0.5 µl
primer anti-sense (10 µM)	0.5 µl
10x reaction buffer (Qiagen)	3 µl
MgCl ₂ (25 mM, Qiagen)	3 µl
dNTPs(10 mM, 2.5 µM each, Sigma)	2.4 µl
<i>Hot Star Taq</i> (5 U/µl, Solis BioDyne)	0.3 µl
H ₂ O	21.3 µl

reaction conditions:

denaturation	95°C	30 min	
denaturation	95°C	1 min	
annealing	x	1 min	
elongation	72°C	45 s	
final elongation	55°C	10 min	x cycles

A possible contamination in the bisulfite treatment was controlled using agarose gel electrophoresis with an 1.2% [w/v] agarose gel in 0.5% TBE (2.9.5).

2.10.5 Exonuclease phosphatase treatment (ExoSAP)

Degradation of remaining primers and dNTPs, which were used in the PCR of bisulfite DNA, was done by addition of 1 µl Exonuclease I/SAP shrimp alkaline phosphatase (1 U / 9 U, USB Corporation, Cleveland, Ohio, USA) to 5 µl PCR product and incubation at 37°C for 30 min. For enzyme inactivation, samples were incubated at 80°C for 15 min.

2.10.6 Restriction digestion

A restriction digestion was performed in order to enhance the SNuPE signal during the H19 promoter analysis.

10 µl of the product were digested with 0.5 µl Tsp509I (New England Biolabs GmbH, Frankfurt, Germany) at 37°C for 30 min. Restriction enzyme inactivation was performed at 80°C for 20 min. The products (182 bp and 146 bp) were controlled on a 1.2% [w/v] agarose gel in 0.5% TBE (2.9.5).

2.10.7 Single nucleotide primer extension (SNuPE)

The reaction mixture was added to the ExoSAP product (see below) and the reaction was performed with SNuPE primers as indicated below (Table 8). For DUSP1ed primers, it was necessary to have two different preparations, because of a poor HPLC signal separation. Additionally, primer 2 of DUSP1eu needs ddGTP and ddATP instead of ddCTP and ddTTP, because the primer lies on the reverse strand. The primers are located in front of a possibly methylated CpG region (Table 9). Within the reaction, primers are elongated with the corresponding base (methylated CpG → cytosine, unmethylated CpG → thymine).

Table 8: SNuPE primers

gene	primer 1 (5' → 3')	primer 2 (5' → 3')
DUSP1p	AGA GGG AGG AG	TAA GGT AGG TGG TA
DUSP1ed	TTG TAT TTG GGT AGT G	CAA CAT ATC CTT AC (reverse)
DUSP1eu	TTG GAT TTT GTT TT	AGG GTT GTG GT
H19	TGT TAG TAG AGT G	GTG ATT AGT ATA AGT T

Table 9: positions of analyzed cytosins in GRCh37/hg19

gene	localisation	position (primer 1)	position (primer 2)
DUSP1, chromosome 5, reverse strand			
DUSP1p	promoter	C at position nt 172,198,585	C at position nt 172,198,562
DUSP1ed	enhancer region downstream	C at position nt 172,196,754	C at position nt 172,196,740
DUSP1eu	enhancer region upstream	C at position nt 172,199,333	C at position nt 172,199,291
H19, chromosome 11, reverse strand			
H19	promoter	C at position nt 1,998,506	C at position nt 1,998,376

reaction mixture (one sample):

primer 1 (30 µM)	2.4 µl
primer 2 (30 µM)	2.4 µl
10x buffer C (Solis BioDyne)	2 µl
MgCl ₂ (25 mM, Qiagen)	1.6 µl
ddCTP (1 mM, Larova)	1 µl
ddTTP (1 mM, Larova)	1 µl
<i>Termi Pol</i> (50 U/µl, Solis BioDyne)	1 µl
H ₂ O	2.6 µl

reaction conditions:

denaturation	96°C	2 min	50 cycles
denaturation	96°C	30 s	
annealing	50°C	30 s	
elongation	60°C	1 min	

SNuPE products were analyzed using ion pair reversed phase high performance liquid chromatography (IP/RP-HPLC) with an HPLC WAVE 3000TM (Transgenomic), a DNAsep-Column at 50°C, and a flow rate of 0.9 ml/min. The principle of the analysis is the separation of elongated primers (first: cytosine – guanine – adenine – thymine) based on size, charge, and hydrophobicity.

2.11 Protein analysis

2.11.1 Protein isolation

Two methods for protein isolation were used.

- Proteins were isolated from Qiazol lysates (2.9.1, 2.10.1) from the supernant after DNA precipitation. Precipitation of proteins was done with 600 µl of supernant, mixed with 1.4 ml acetone. After incubation of 10 min and centrifugation (10 min, top speed, 4°C), the pellet was washed for three times with 1 ml guanidine solution (0.3 M guanidine hydrochloride in 95% [v/v] ethanol and 2.5% [v/v] glycerol (1:1)). During every washing step, samples were mixed, incubated for 10 min at room temperature, and

centrifuged (5 min, 8,000 x g, 4°C). Another washing step with ethanol containing 2.5% glycerol [v/v] was performed, centrifuged, dried at room temperature, and dissolved in 1% SDS solution. All steps were carried out on ice unless otherwise noted.

- Cells were lysed with SB lysis buffer (50 mM tris-HCl, 1% [m/v] SDS, 10% [v/v] glycerol, 5% [v/v] β-mercaptoethanol, 0.004% [m/v] bromophenol blue), supplemented with a protease inhibitor mixture (Complete[®], Roche, Mannheim, Germany) according to the manufacturer's guidelines and frozen at -80°C. After thawing, samples were treated with ultrasound and centrifuged (10 min, 17,000 x g, 4°C).

2.11.2 Determination of protein concentration

The protein concentration was measured using the PierceTM BCA Protein Assay Kit (Thermo Fisher Scientific, Waltham, MA, USA) according to the manufacturer's instructions.

2.11.3 SDS-polyacrylamide gel electrophoresis (SDS-Page)

After thawing, equal amounts of samples were mixed 3:1 with loading dye (Roti[®] Load), denatured at 95°C for 5 min, and loaded onto the gel (Table 10). Proteins were separated in electrophoresis buffer (24.8 mM tris base, 1.92 mM glycine, 0.1% [w/v] SDS) at 80 V for 45 min, followed by 2 h at 120 V. To identify the proteins based on their molecular mass, a prestained protein marker was included.

Table 10: composition of the SDS gel

	resolving gel (12%)	stacking gel
H ₂ O	3.3 ml	3.4 ml
30% acrylamide / 0.8% bis-acrylamide solution	4 ml	0.83 ml
tris base (1.5 M pH 8.8)	2.5 ml	
tris base (1 M pH 6.8)		0.63 ml
SDS (10% [w/v])	100 µl	50 µl
APS (10% [w/v])	100 µl	50 µl
TEMED	10 µl	5 µl

2.11.4 Western Blot

After the separation of proteins with the gel, they were blotted onto a PVDF membrane (Immobilion-FL, Millipore, Schwalbach am Taunus, Germany) using the Mini-Transblot cell (Biorad, München, Germany). The membrane was activated by incubation with methanol for 30 s. Afterwards, the membrane, sponges, and blotting papers were preincubated in transfer buffer (24.8 mM tris base, 1.92 mM glycine, 20% [v/v] methanol, 0.05% [w/v] SDS), followed by a sandwich preparation with the gel. The blot was performed in transfer buffer overnight at 80 mA. On the following day, the membrane was incubated for 1 h at room temperature in rockland blocking buffer (RBB) (Rockland, Gilbertsville, PA, USA) in order to block unspecific binding sites.

2.11.5 Immunodetection

After blocking, membranes were incubated with diluted primary antibodies (see Table 11 for specific conditions). After primary antibody incubation, membranes were washed, each with the indicated buffer of the used primary antibody (see in Table 11) (2 x 5 min), and further washing steps were performed with PBST (2 x 5 min). Membranes were incubated with diluted secondary antibody as denoted and washed again with PBST (2 x 5 min) and PBS (2 x 5 min). The detection was carried out with the Odyssey Infrared Imaging System (LI-COR Biosciences, Lincoln, NE, USA). Relative signal intensities were determined by the Odyssey software or the ImageJ software.

Table 11: antibodies, dilution, and incubation conditions for immunodetection

primary antibody	dilution	incubation
Anti human tubulin, mouse IgG	1:1,000 in PBST + 5% [m/v] dried milk	3 h room temperature
Anti human GILZ, goat IgG	1:200 in gelatine buffer	3 h, 37 °C
Anti human GILZ, rabbit IgG	1:1,000 in RBB	over night, 4°C
Anti human DUSP1, rabbit gG	1:200 in PBST + 5% [m/v] dried milk	over night, 4°C
Anti human TLR2, rabbit IgG	vessels: 1:1,000, HUVEC: 1:500 in PBST + 5% [m/v] dried milk	3 h room temperature
Anti human ZFP36, rabbit IgG	1:1,000 in RBB	3 h room temperature
secondary antibody		
IRDye©800CW conjugated goat anti-mouse IgG	1 :5,000 in RBB	2 h, room temperature
IRDye©680 conjugated goat anti-mouse IgG	1 :10,000 in RBB	1.5 h, room temperature
IRDye©680 conjugated goat anti-rabbit IgG	1 :5,000 in RBB	2 h, room temperature
IRDye©800 conjugated donkey anti-goat IgG	1 :10,000 in RBB	2 h, room temperature

PBST: (0.1% [v/v] tween 20 in PBS (see 2.4.3))

RBB: rockland blocking buffer

gelatine buffer, pH 7.5: (gelatine A 0.75% [w/v], tween 20 0.1% [v/v], tris base 20 mM, NaCl 137 mM)

2.12 Statistics

Data are shown as mean +/- SEM using OriginPro9.1G (OriginLab Corporation, Northhampton, MA, USA). Statistical significance was determined by student's t-test (two samples) for cell culture experiments using Excel (Microsoft) and by Wilcoxon rank sum test for human samples using OriginPro9.1G unless otherwise noted.

* p<0.05; ** p<0.01; *** p<0.001

3 Results

3.1 Downregulation of glucocorticoid-induced leucine zipper (*GILZ*) promotes vascular inflammation

3.1.1 *GILZ* expression in degenerated vein bypasses

To identify degenerated vein bypasses as inflamed tissue, mRNA expression of the inflammatory markers *CCL2* (*MCP1*) and *TLR2* were measured and the expression levels were compared to healthy veins (Diesel *et al.*, 2012; Weber *et al.*, 2003). Both inflammatory markers were significantly increased (Figure 13 A, B). Additionally, inflamed veins revealed a significantly decreased *GILZ* mRNA expression (Figure 13 C). Similar results were observed analyzing *GILZ* and *TLR2* on protein level (Figure 14 A, B).

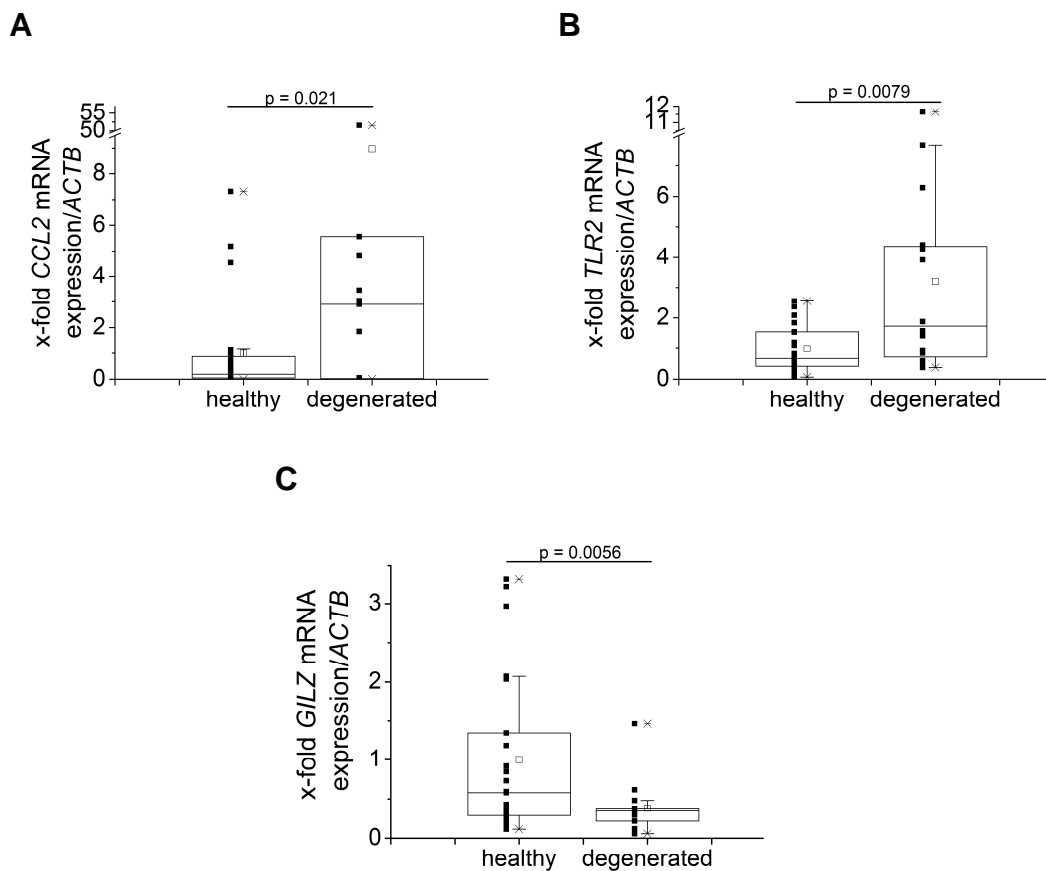


Figure 13: mRNA expression in human veins - *CCL2* (A), *TLR2* (B), and *GILZ* (C) mRNA expression in saphenous veins (n=23) and degenerated aortocoronary saphenous vein bypass grafts (n=15) were measured by real-time RT-PCR using *ACTB* (β -actin) for normalization. Data are presented as individual values (black squares) as well as 25th and 75th percentiles as boxes within geometric medians (line), arithmetic medians (square), 10th and 90th percentiles as whiskers, and ends of values (cross).

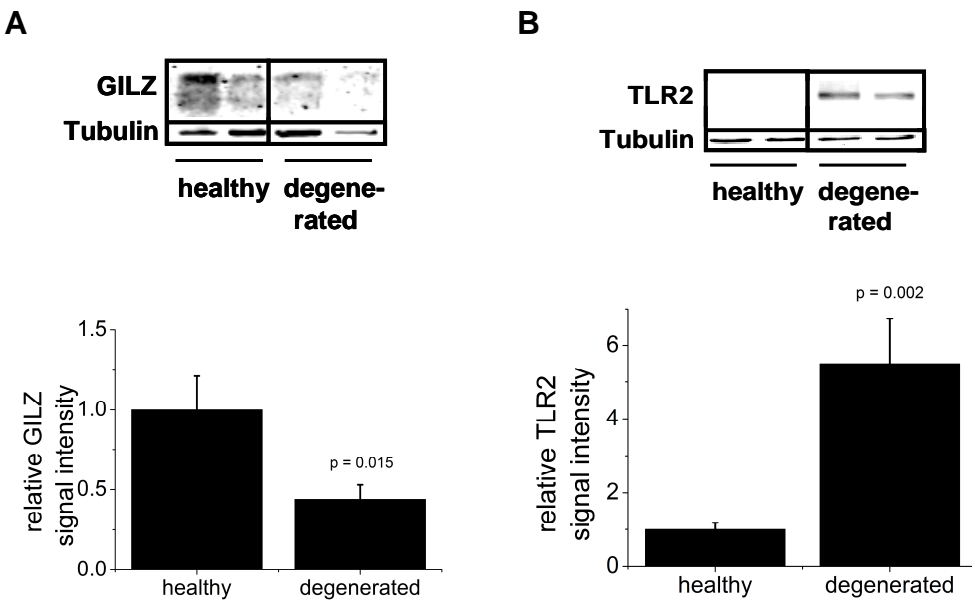


Figure 14: GILZ (A) and TLR2 (B) protein expression in human veins - Equal protein amounts were assessed by Western blot analysis using tubulin as loading control. One representative blot out of 4 independent experiments with 11 healthy and 12 degenerated samples is shown. Signal intensities are shown relative to the tubulin values, and values for healthy samples were set as one.

3.1.2 Localisation of GILZ in vessels

An antibody staining was performed in order to identify GILZ expressing cells. First, the specificity of the GILZ antibody was evaluated in THP-1 cells using a protocol for histological samples (Figure 15). As expected for GILZ expression, the treatment with the glucocorticoid receptor (GR) activator dexamethasone (Dex) resulted in a slightly stronger staining, while treatment with the TLR1/2 ligand Pam₃CSK₄ (Pam), which enhanced the inflammation *via* activation of TLR1/2, reduced the GILZ staining compared to control (Co).

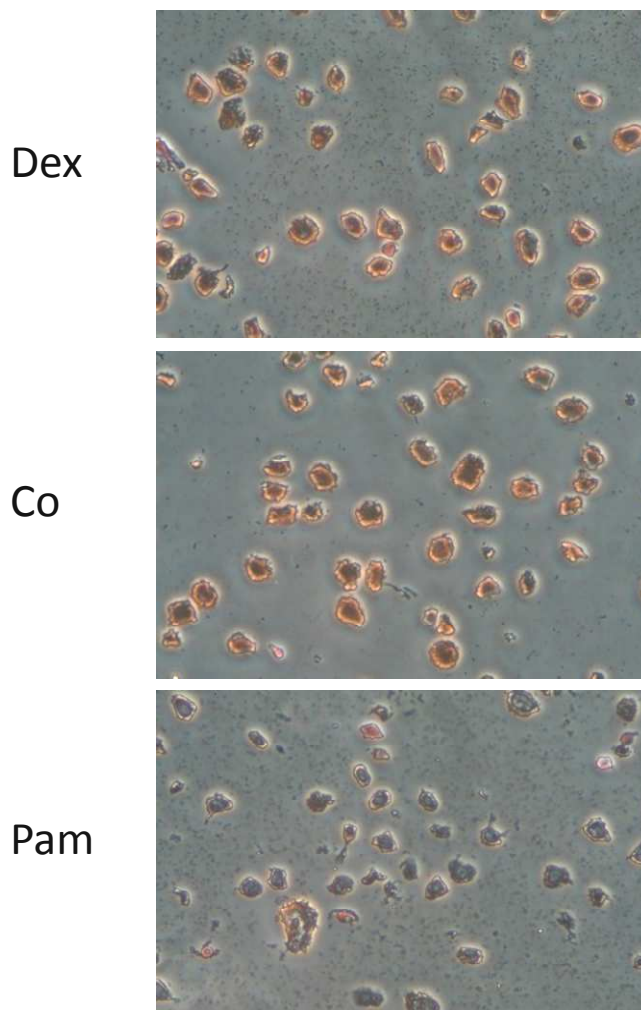


Figure 15: Specificity of the GILZ antibody - THP-1 cells were treated with 1 µM dexamethasone, 1 µg/ml Pam₃CSK₄ or left untreated for 8 h. Paraffin-embedding and cutting was kindly performed by Dr. Yvette Simon and staining by Dr. Sonja M. Kessler (Pharmaceutical Biology, Saarland University). The pictures were taken with a Zeiss Axiovert 40CFL phase contrast microscope (magnification 400x).

For the detection of GILZ localisation in vessels, murine and human histological samples were used (Figure 16). GILZ was clearly shown in the endothelial layer of both types of vessels and both species.

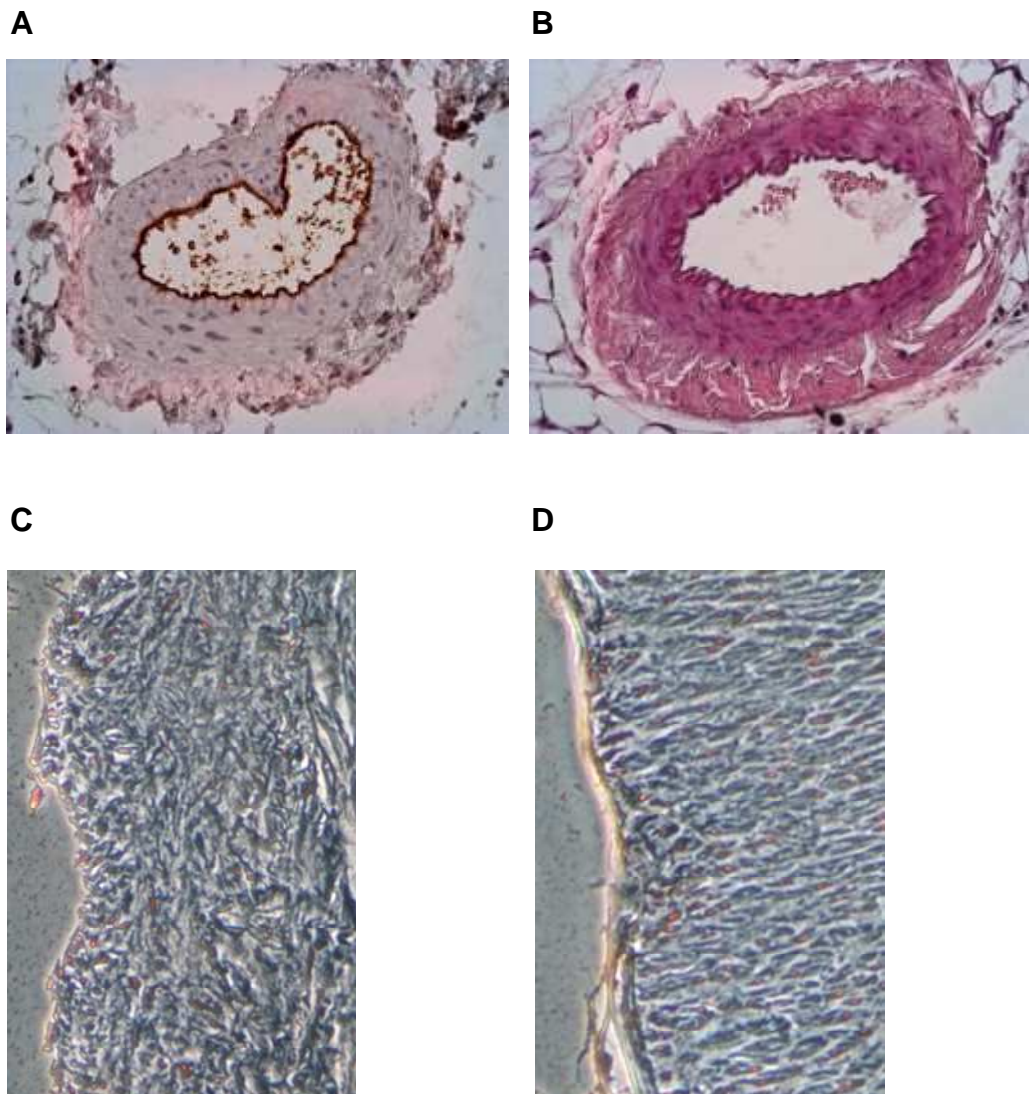


Figure 16: GILZ detection in histological samples of vessels - Localisation of GILZ expression (brown) is shown by GILZ immunostaining in a murine femoral artery (A) a human saphenous vein (C) and a human radial artery (D). Additionally, hematoxylin / eosin (HE) staining of a murine femoral artery (B) is shown. Paraffin-embedding and cutting was kindly performed by Dr. Yvette Simon and staining by Dr. Sonja M. Kessler (Pharmaceutical Biology, Saarland University). The pictures were taken with a Zeiss Axiovert 40CFL phase contrast microscope (magnification 50x (A, B) and 100x (C, D))

3.1.3 Inflammatory response in EC

Both, immunohistochemistry as well as data previously presented by ourselves and others suggested a distinct expression of GILZ in EC (Cheng *et al.*, 2013; Hahn *et al.*, 2014; Hoppstädter *et al.*, 2012). As shown in Figure 17 A, GILZ protein was down-regulated under inflammatory conditions, i.e. after TNF- α treatment.

Interestingly, the mRNA binding protein ZFP36, known to destabilize GILZ mRNA in M Φ (Hoppstädter *et al.*, 2012), was strongly induced by TNF- α (Figure 17 B).

Early after TNF- α treatment (1 h), ZFP36 was present in its low-phosphorylated, low molecular weight form, which is known to be the active, but instable variant. At later time points, the phosphorylated high-molecular weight isoform of ZFP36, which is inactive but stable (Brook *et al.*, 2006), predominated (Figure 17 B).

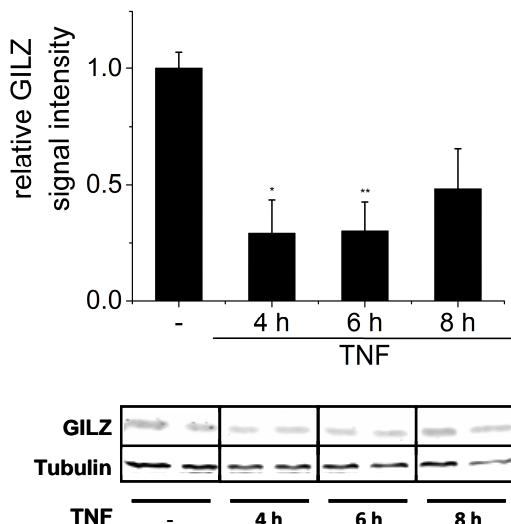
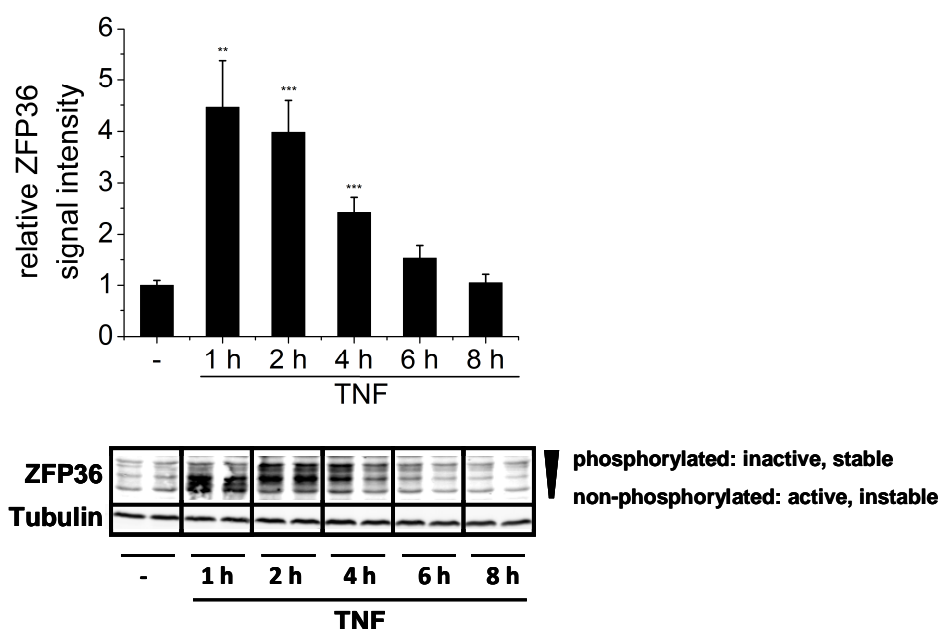
A**B**

Figure 17: Time-dependent GILZ and ZFP36 protein expression after TNF treatment - HUVEC were treated with 10 ng/ml TNF- α for the indicated time points. Protein levels were measured by Western blot analysis using tubulin as loading control. For GILZ (A) one blot of two, for ZFP36 (B) one blot of three independent experiments is shown with the respective quantification (duplicates).

In order to examine the functional link between GILZ and ZFP36 expression in HUVEC, a small hairpin RNA (shRNA)-mediated knockdown of ZFP36 was performed, which resulted in a diminished ZFP36 expression in contrast to the control lacZ plasmid transfected cells (co) (Figure 18 A). Simultaneously, this knockdown led to an enhanced GILZ protein expression (Figure 18 B). This suggested a key role for ZFP36 in the regulation of GILZ expression.

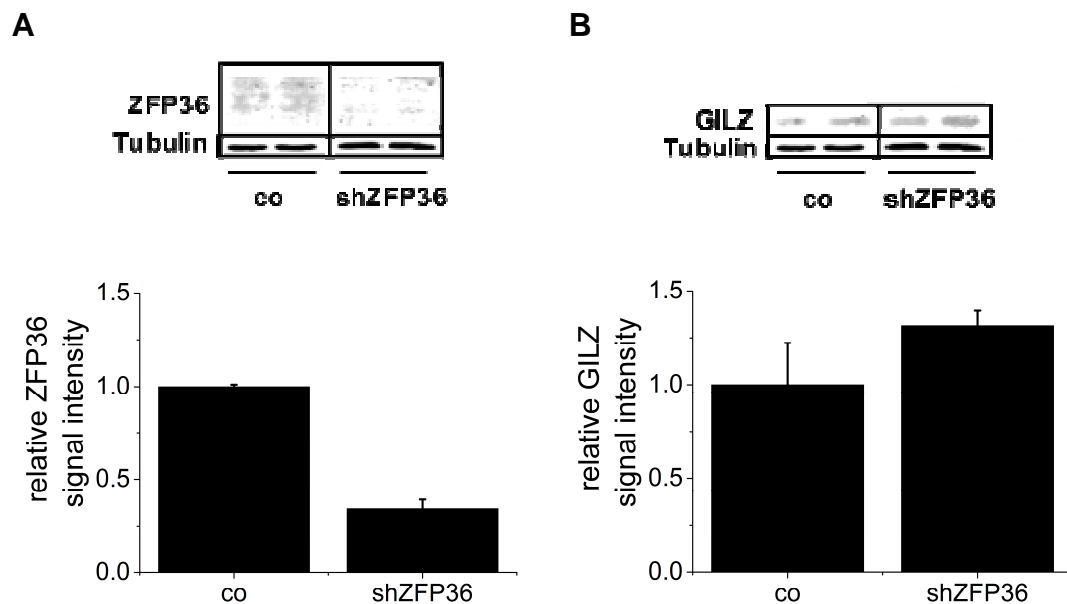


Figure 18: ZFP36 knockdown - HUVEC were transfected with 1 µg lacZ (co) or shZFP36 plasmid and cultivated for 24 h. Protein levels of ZFP36 (A) and GILZ (B) were measured by Western blot analysis using tubulin as loading control and quantified by ImageJ.

3.1.4 Regulation of GILZ and ZFP36 by anti-inflammatory laminar shear stress

Laminar shear stress is a physical force, which affects the mRNA and protein expression as well as the surface of EC in the vessel. Depending on this force, cells changed their shape and aligned in the direction of flow (Figure 19).

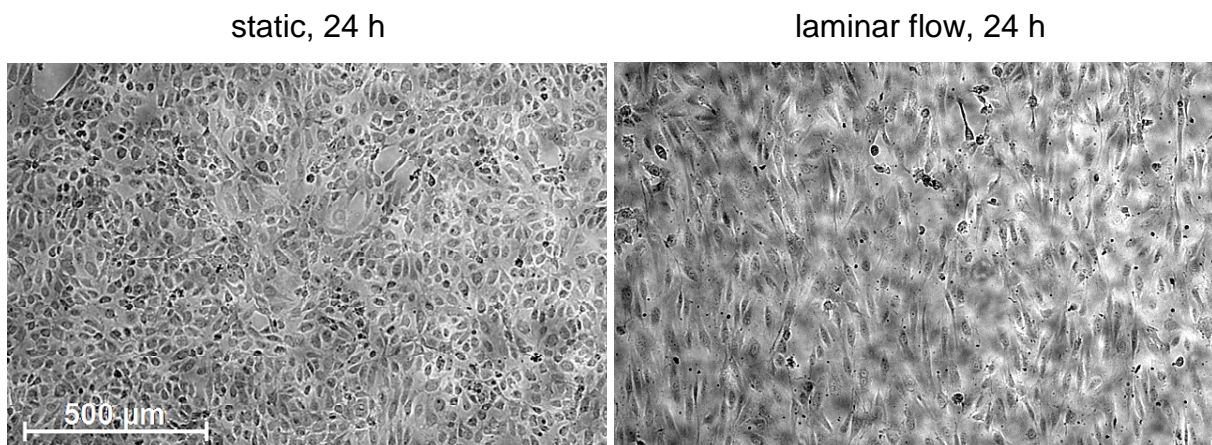


Figure 19: Alignment of HUVEC - Light microscopy showed HUVEC, either cultured statically or exposed to 24 h laminar flow (20 dynes/cm^2). The pictures were taken with a Zeiss LSM 510 confocal microscope (magnification 50x).

Laminar shear stress, generally seen as an anti-inflammatory and antiatherosclerotic stimulus, elevated *GILZ* mRNA levels in HUVEC (Figure 20 A), while inflammatory conditions, i.e. TNF- α treatment, downregulated GILZ. The same effect was observed on protein level (Figure 20 B). The anti-inflammatory activation state of HUVEC upon laminar shear stress was confirmed by elevated HO1 mRNA expression (Figure 20 C).

While ZFP36 was induced by TNF- α on the transcriptional level, its gene expression tended to decrease during laminar flow (Figure 20 D). A combination of laminar flow and TNF- α completely abrogated GILZ downregulation, which was typically observed upon TNF- α treatment in statically cultured HUVEC (Figure 20 E). Concordantly, ZFP36 induction by TNF- α was abrogated in cells exposed to laminar flow (Figure 20 F), suggesting that the lack of ZFP36 induction contributes to the elevated GILZ expression in TNF- α -treated shear stressed cells.

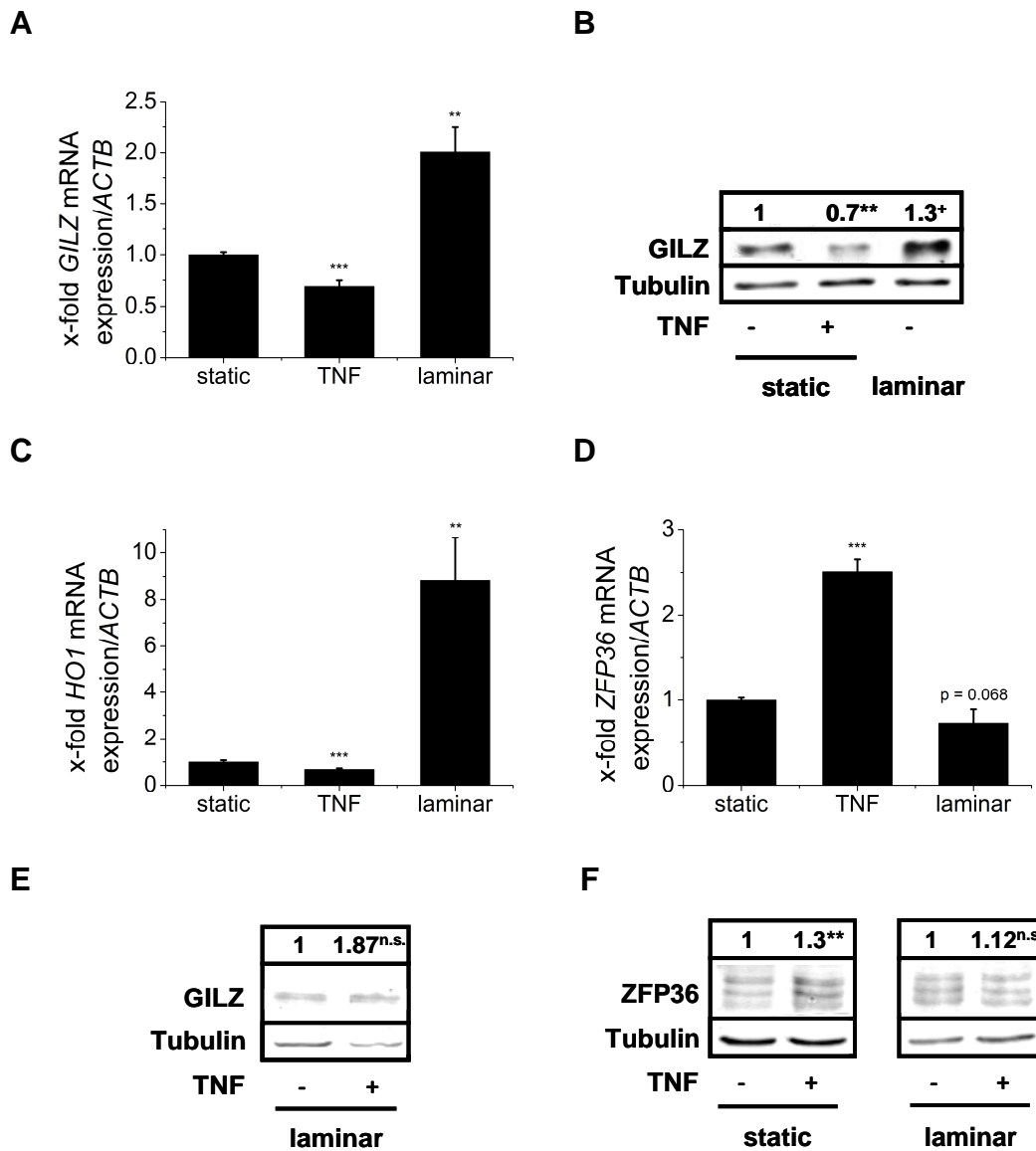


Figure 20: GILZ, HO1, and ZFP36 expression under inflammatory and anti-inflammatory conditions - HUVEC were treated with 10 ng/ml TNF- α under static conditions or exposed to 24 h laminar flow (20 dynes/cm 2) as indicated. *GILZ* (A), *HO1* (C), and *ZFP36* (D) mRNA levels were determined by real-time RT-PCR using *ACTB* for normalization. Values for untreated cells were set as one, **p<0.01, ***p<0.001 compared to untreated cells under static conditions. Data were obtained from four independent experiments performed in duplicate. *GILZ* (B, E) and *ZFP36* (F) protein levels were measured by Western blot analysis using tubulin as loading control and quantified by ImageJ ((B, F) n=6; (E) n=8 derived from 4 independent experiments). Values for untreated cells were set as one as indicated, **p<0.01, ***p<0.001, ⁺(B) p=0.051, ^{n.s.}(E) p=0.092, ^{n.s.}(F) p=0.187 compared to untreated cells.

These results were also confirmed analyzing human tissues. *ZFP36* protein levels were elevated in degenerated, inflamed venous bypasses compared to healthy veins (Figure 21).

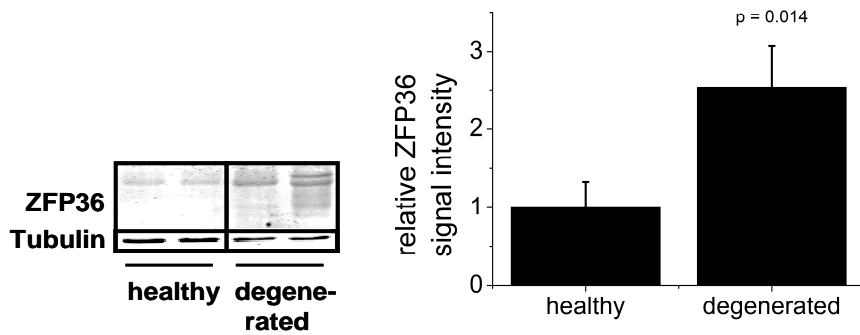


Figure 21: ZFP36 expression in human veins - Equal protein amounts were assessed by Western blot analysis using tubulin as loading control. One representative blot out of three independent experiments with 8 healthy veins and 10 degenerated, inflamed venous bypasses is shown. Signal intensities were measured relative to tubulin values, and values for healthy samples were set as one.

3.1.5 Mechanisms of GILZ downregulation in inflammation

Our data suggest an inverse regulation of ZFP36 and GILZ in inflammation and under anti-inflammatory conditions in HUVEC. In fact, ZFP36 has been reported to be a destabilizer of *GILZ* mRNA in MΦ (Hopftädter *et al.*, 2012) and to be regulated by DUSP1 (Huotari *et al.*, 2012), which inhibits MAPKs, most importantly p38 MAPK (Kiemer *et al.*, 2002a).

To assess the influence of p38 MAPK activation on ZFP36 and GILZ expression, HUVEC were transfected with a dominant negative mutant of p38 resulting in a significantly reduced ZFP36 mRNA expression, which was diminished in a greater extent by TNF- α treatment (Figure 22).

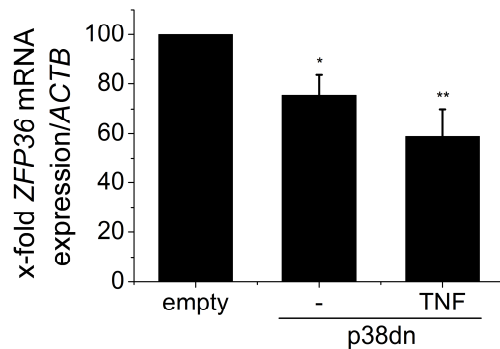


Figure 22: ZFP36 expression after overexpression of dominant negative (dn) p38 α MAPK - HUVEC were transfected with empty control vector (empty) or dn p38 α (p38dn) for 24 h and treated with 10 ng/ml TNF- α for another 4 h. Transfection was kindly performed by Dr. Kerstin Hirschfelder (Pharmaceutical Biology, Saarland University). mRNA levels were determined by real-time RT-PCR using *ACTB* for normalization. Values for cells transfected with control vector, untreated as well as TNF- α treated, were set as one hundred percent. Data show means +SEM of four independent experiments performed in duplicates, * $p < 0.05$, ** $p < 0.01$ compared to cells transfected with control vector.

As an additional approach, p38 phosphorylation in HUVEC was inhibited by pre-treatment with the p38 MAPK inhibitor SB203580 prior to TNF- α challenge. p38 inhibition antagonized TNF- α -mediated ZFP38 induction both on mRNA and protein level (Figure 23 A, B and E). Reduced ZFP36 expression was accompanied by an abrogation of GILZ downregulation (Figure 23 C, D and F). These results suggest that p38 inhibition enhances GILZ expression by reducing ZFP36 levels.

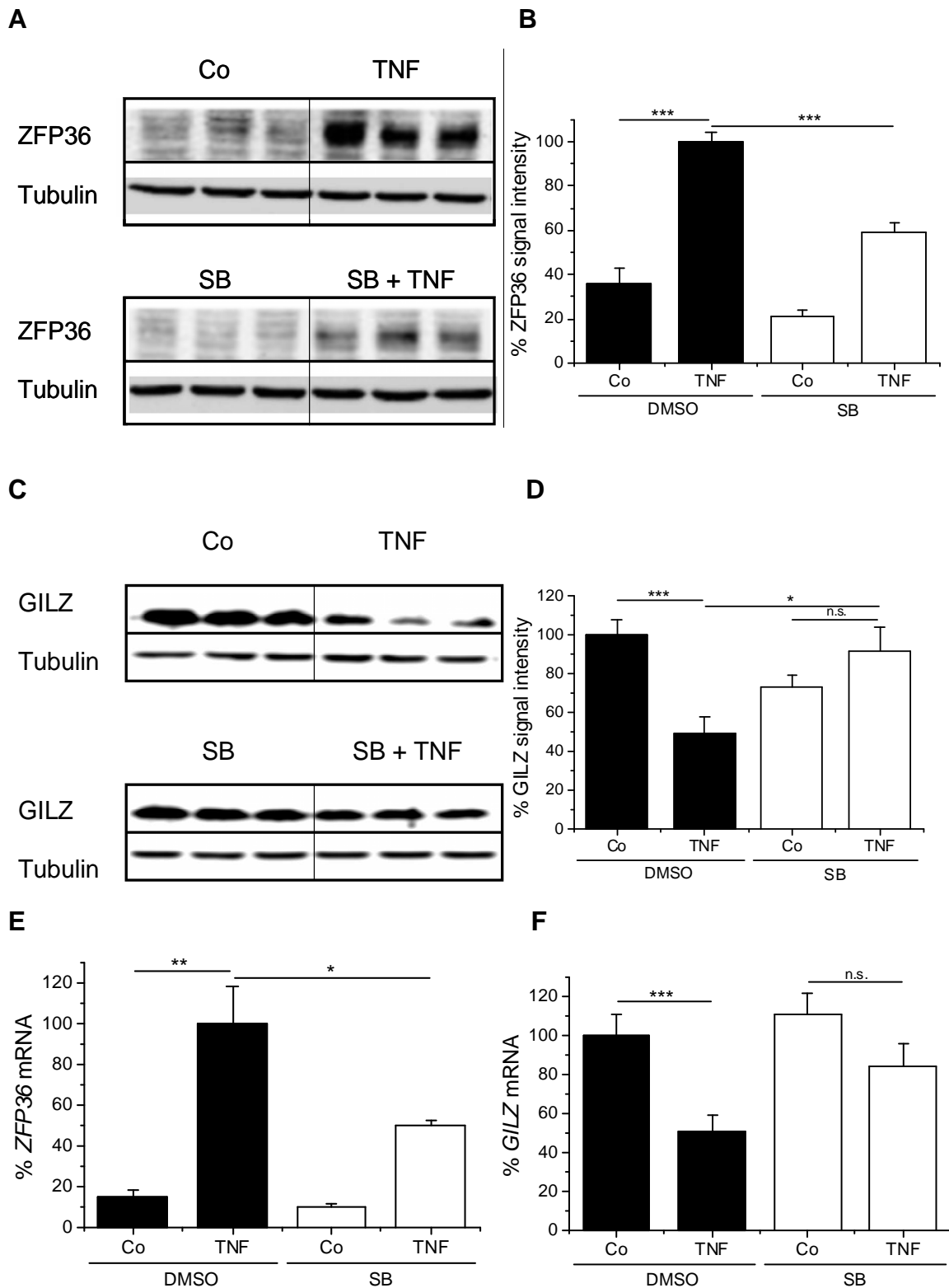


Figure 23: ZFP36 and GILZ expression after inhibition of p38 MAPK activity - HUVEC were pretreated with solvent control DMSO or SB203580 (10 μ M), followed by treatment with 10 ng/ml TNF- α for 2 h (A-B, E-F) or 4 h (C-D). Protein levels were measured by Western blot analysis using tubulin as loading control (A-D). mRNA levels were determined by real-time RT-PCR using ACTB for normalization (E-F). Values for cells pretreated with the solvent control DMSO, either in the presence (B, E) or absence (D, F) of TNF- α , were set as one hundred percent. Data show means of three (A-D) or two (E-F) independent experiments performed in triplicates, *p<0.05, **p<0.01, ***p<0.001, n.s.: not statistically significant. Experiments were kindly performed by Nina Hachenthal and Dr. Jessica Hoppestdäter (Pharmaceutical Biology, Saarland University).

Interestingly, a significant downregulation of *DUSP1* protein expression in degenerated vein bypasses was detected (Figure 24 A, B). In cultivated HUVEC, an upregulation of *DUSP1* mRNA levels by laminar shear stress and downregulation by TNF- α was observed (Figure 24 C).

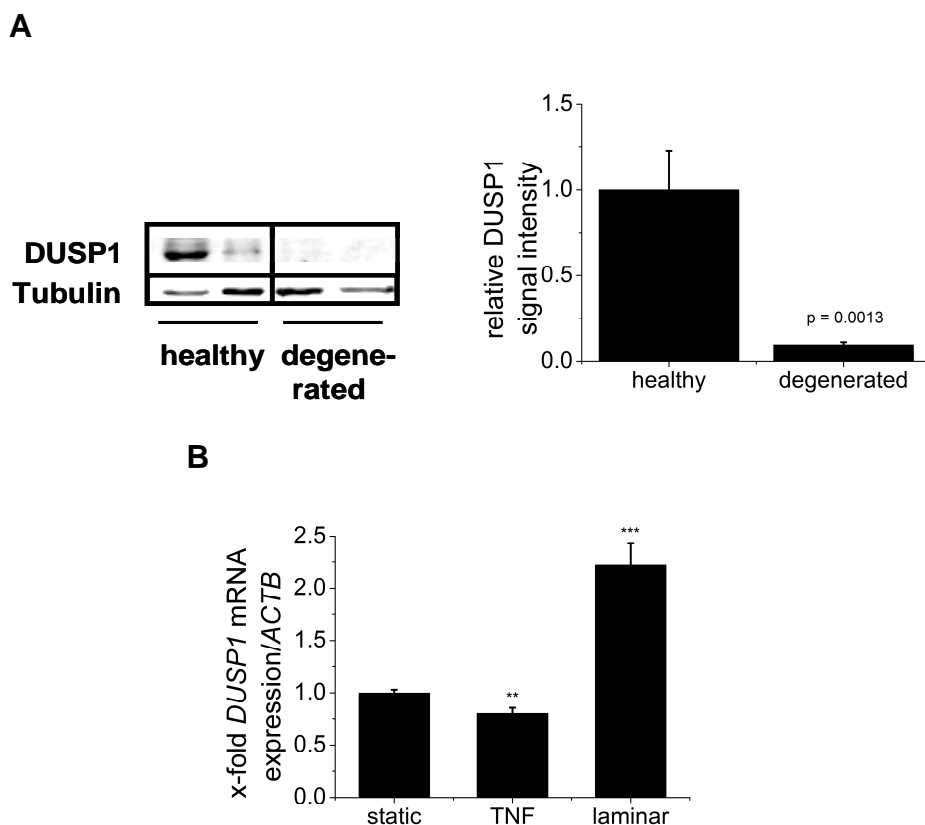


Figure 24: DUSP1 expression under inflammatory and anti-inflammatory conditions - (A) *DUSP1* protein expression in human veins. Equal protein amounts were assessed by Western blot analysis using tubulin as loading control. One representative blot out of four independent experiments with 11 healthy and 12 degenerated samples is shown. Signal intensities were measured relative to tubulin values, and values for samples from healthy tissues were set as one. (B) *DUSP1* mRNA expression under pro- and anti-inflammatory conditions. HUVEC were treated with 10 ng/ml TNF- α under static conditions or exposed to 24 h laminar flow (20 dynes/cm²) as indicated. mRNA levels were determined by real-time RT-PCR using *ACTB* for normalization. Values for untreated cells under static conditions were set as one, **p<0.01, ***p<0.001 compared to untreated cells. Data represent means of four independent experiments performed in duplicate.

3.1.6 Functional implications of GILZ downregulation

We aimed to determine whether GILZ downregulation has functional implications in inflammatory activation of HUVEC. We knocked down GILZ in HUVEC by siRNA resulting in reduced GILZ protein levels (Figure 25 A). Using a luciferase reporter gene under an NF- κ B promoter, we showed that GILZ knockdown significantly increased NF- κ B activity compared to control transfected cells (Figure 25 B); functionality of the luciferase assay was verified measuring TNF- α -induced NF- κ B activity (Figure 25 C).

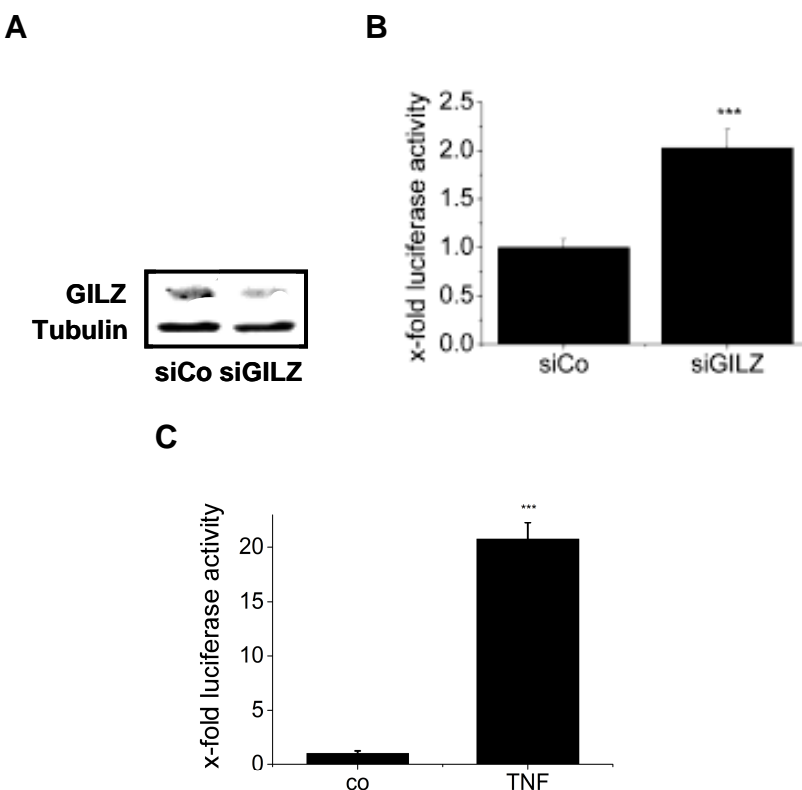


Figure 25: NF- κ B activation after GILZ knockdown - (A) HUVEC were transfected with GILZ siRNA (siGILZ) or control siRNA (siCo). Cells were harvested after 20 h. GILZ protein expression was analyzed by Western blot using tubulin as loading control. One representative blot out of four independent experiments is shown. (B) HUVEC were transfected with either siCo or siGILZ and an NF- κ B driven luciferase reporter construct. Cells were harvested 20 h post transfection. NF- κ B activity was determined by measuring luciferase activity. Data represent means of four independent experiments performed in quintuplicate. (Three of these experiments were performed by Dr. Kerstin Hirschfelder (Pharmaceutical Biology, Saarland University)). Values for siCo were set as one, *** $p<0.001$, compared to siCo transfected cells. (C) HUVEC were transfected with luciferase plasmid for 15 h and treated with 10 ng/ml TNF- α for 5 h or left untreated (co). NF- κ B activity was measured by luciferase assay. Data show one experiment each with 9 samples and data for co were set as one, *** $p<0.001$.

3.2 Lack of endothelial glucocorticoid-induced leucine zipper (GILZ) induction under atherogenic flow conditions

3.2.1 Inflammatory activation of HUVEC by low and oscillatory flow

Both, laminar shear stress at low flow rates as well as oscillatory shear stress, were previously reported to promote inflammatory activation of the endothelium (Hastings *et al.*, 2007). When we applied laminar flow of 2 dynes/cm² or oscillatory flow to primary HUVEC we in fact observed an elevated expression of a set of inflammatory mediators under both conditions (Figure 26). Oscillatory shear stress led to a significant upregulation of all inflammatory mediators with the exception of VCAM. Concordantly, VCAM is the only inflammatory marker, which was diminished by low shear stress. The other adhesion molecules and the cytokines CCL2 and IL-6 were slightly enhanced in response to low flow, while IL-8 and TLR2 were significantly upregulated.

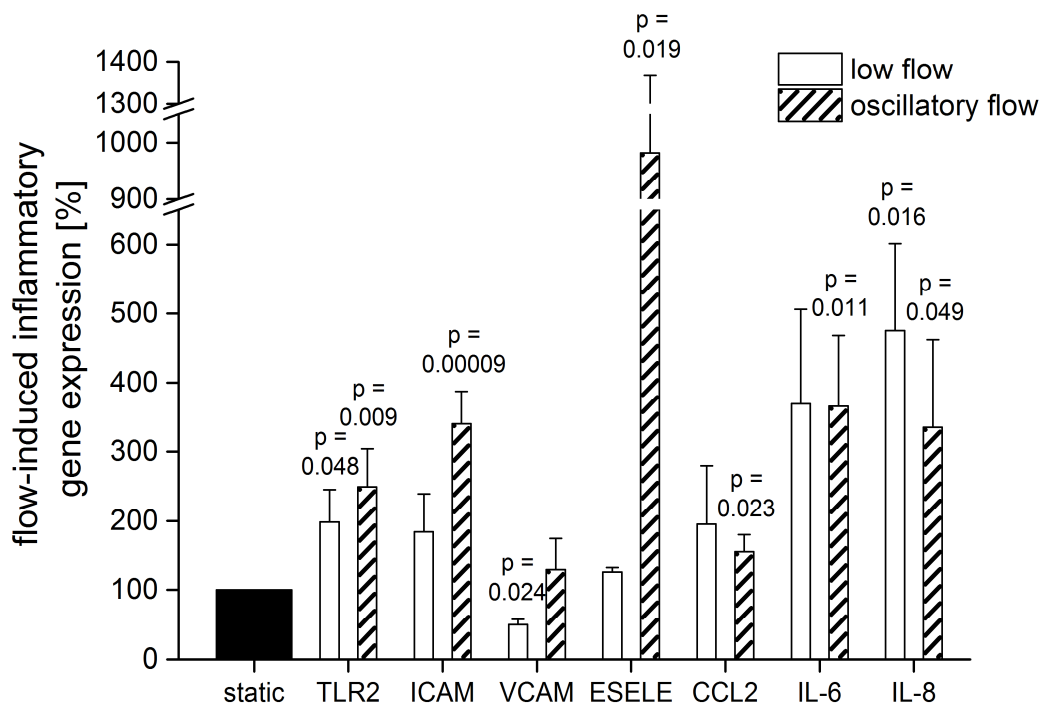


Figure 26: Expression of inflammatory mediators under inflammatory flow conditions - HUVEC were exposed to 24 h low (2 dynes/cm²) or oscillatory flow. mRNA levels were determined by real-time RT-PCR using ACTB for normalization. Values for untreated cells were set as one hundred percent. For low flow, data were obtained from three independent experiments, for oscillatory flow, from 8 independent experiments. All experiments were performed in duplicates.

Laminar shear stress of 20 dynes/cm² strongly induced the anti-inflammatory mediator HO1 (Blumenthal *et al.*, 2005; Hahn *et al.*, 2014; Kiemer *et al.*, 2003a), while oscillatory flow exhibited this effect to a much lower extent and low flow conditions even reduced *HO1* mRNA levels compared to static cultivation (Figure 27).

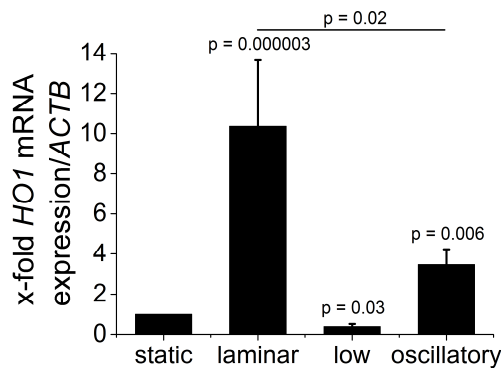


Figure 27: *HO1* mRNA expression under different flow conditions - HUVEC were exposed to 24 h laminar (20 dynes/cm²), low (2 dynes/cm²) or oscillatory flow. mRNA levels derived from four or three (low flow) independent experiments performed in duplicates were measured by real-time RT-PCR using *ACTB* for normalization. Values for untreated cells were set as one. Statistical differences were determined with Kruskal-Wallis-ANOVA followed by post-hoc-analysis with Mann-Whitney-U-test.

3.2.2 GILZ downregulation under inflammatory conditions

The results shown in chapter 3.1 demonstrate that the anti-inflammatory mediator GILZ is induced by laminar flow and downregulated under inflammatory conditions. We therefore hypothesized a lack of GILZ induction under atherogenic flow conditions. Low flow had in fact no effect on *GILZ* expression compared to static cultivation, while oscillatory flow even reduced *GILZ* mRNA levels (Figure 28 A). We therefore focussed the further work on oscillatory shear stress conditions.

GILZ has previously been shown to decrease during inflammatory cell activation, such as TLR activation of MΦ (Hoppstädter *et al.*, 2012) or TNF- α treatment of EC (chapter 3.1.3). We confirmed a respective downregulation of GILZ protein levels in HUVEC upon inflammatory oscillatory stress (Figure 28 B). Interestingly, TNF- α did not further reduce GILZ levels during oscillatory stress (Figure 28 B). These findings were confirmed on mRNA level (Figure 28 C).

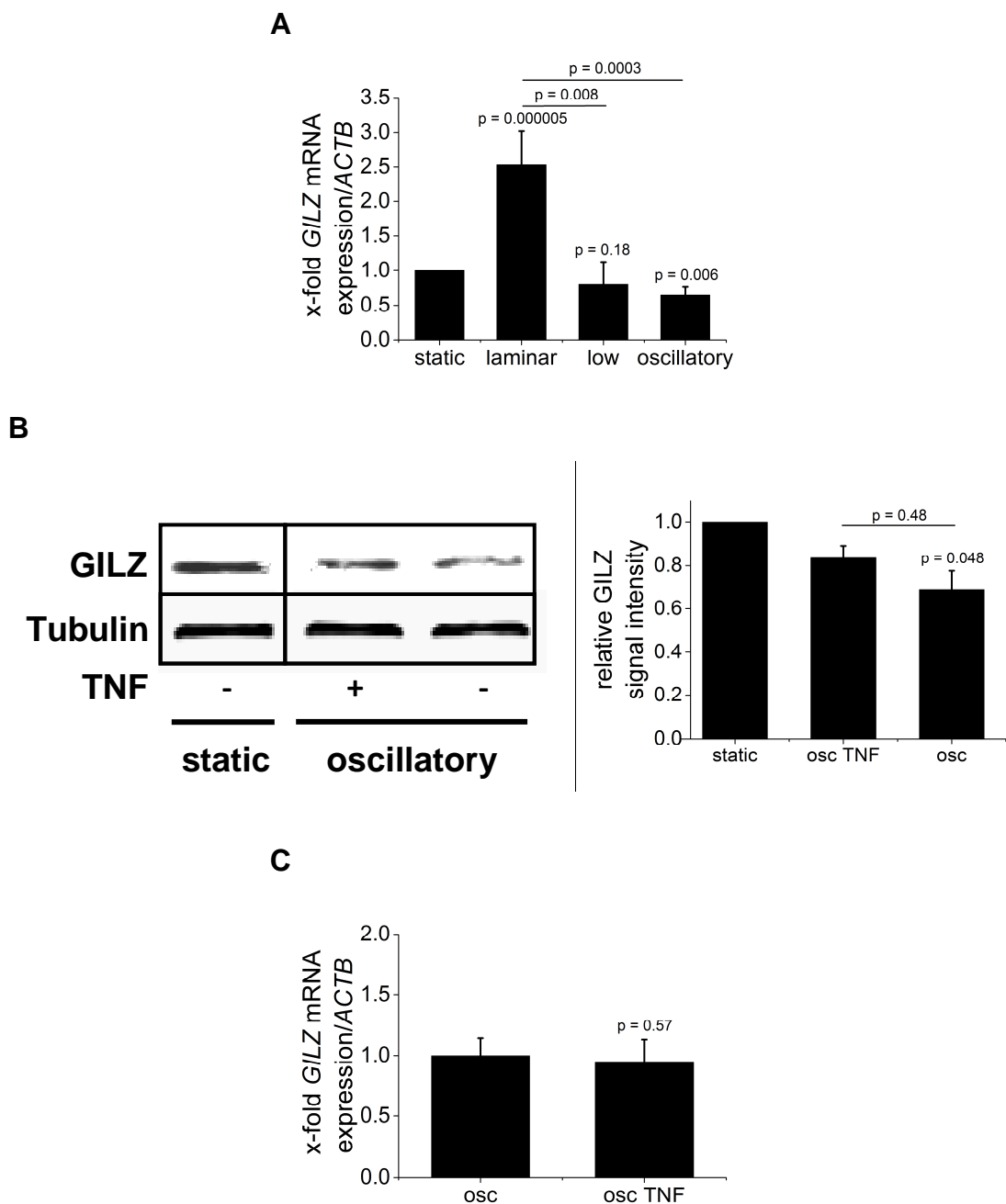


Figure 28: GILZ expression under inflammatory flow conditions - (A, C) *GILZ* mRNA expression under flow conditions. HUVEC were kept under static conditions or were exposed to 24 h laminar (20 dynes/cm^2), low (2 dynes/cm^2), or oscillatory flow. TNF- α treatment (10 ng/ml) was done for 2 h before the end of the experiment. mRNA levels were measured by real-time RT-PCR using *ACTB* for normalization and values for untreated cells were set as one. Data represent means of four or three (low flow) independent experiments performed in duplicate. (B) *GILZ* protein expression under oscillatory flow. HUVEC were set under oscillatory flow (osc) for 24 h without or with TNF- α treatment (10 ng/ml) for the last 3.5 h. Signal intensities of three independent experiments (duplicates) were measured relative to tubulin values. Values for statically cultivated cells were set as one. Statistical differences were determined with Kruskal-Wallis-ANOVA followed by post-hoc-analysis with Mann-Whitney-U-test.

3.2.3 Mechanism of GILZ downregulation under oscillatory flow

We previously showed that the mRNA binding protein ZFP36/TTP destabilizes *GILZ* mRNA and therefore is responsible for TNF-induced GILZ downregulation under inflammatory conditions (Hoppstädter *et al.*, 2012). Accordingly, we suggested that ZFP36 induction might be responsible for oscillatory flow-induced GILZ downregulation. In fact, oscillatory flow slightly induced *ZFP36* mRNA, although data did not reach statistical significance (Figure 29 A).

The results of chapter 3.1 demonstrate that laminar shear stress induced the phosphatase *DUSP1*, which counteracted ZFP36 induction. We hypothesized that oscillatory shear stress lacks this effect on *DUSP1*. However, we surprisingly observed that oscillatory shear stress had the same effect on *DUSP1* mRNA levels as laminar shear stress: both induced *DUSP1* mRNA expression (Figure 29 B). TNF downregulated the flow-induced *DUSP1* expression under both flow conditions, while laminar flow was only slightly decreased and oscillatory flow led to a significant reduction (Figure 29 B). These data suggest that lack of *DUSP1* induction is not the critical signalling factor distinguishing laminar and oscillatory flow-induced actions on GILZ expression in EC.

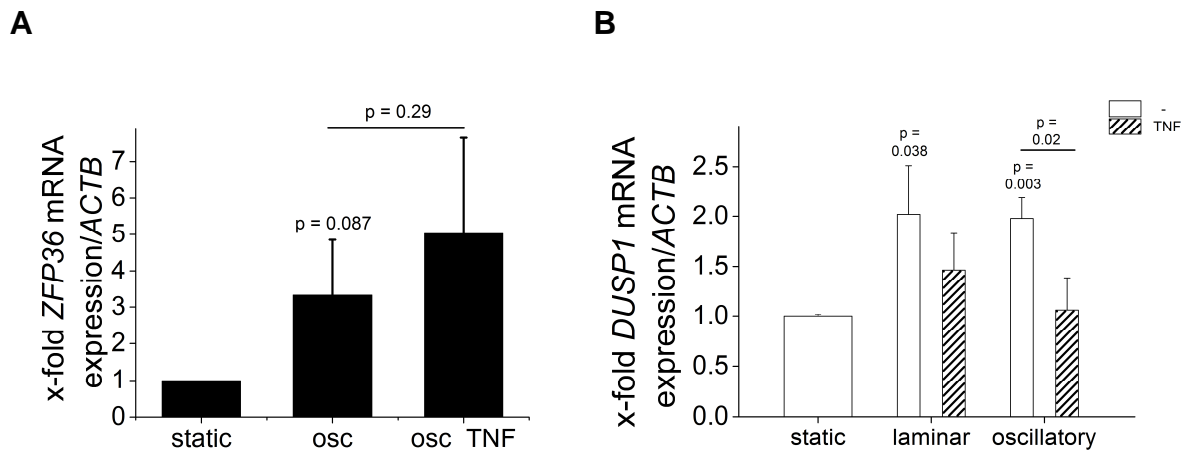


Figure 29: Mechanism of GILZ downregulation - *ZFP36* (A) and *DUSP1* (B) mRNA expression. HUVEC were exposed to laminar or oscillatory flow for 24 h without or with TNF treatment (10 ng/ml) for the last 2 h (A) or 3.5 h (B). mRNA levels derived from four independent experiments (duplicates) were determined by real-time RT-PCR using *ACTB* for normalization. Values for untreated cells were set as one.

3.2.4 Inflammatory activation in atherosclerotic clinical samples

We aimed to investigate the clinical relevance of our *in vitro* analyses in atherosclerotic vessels and observed that *GILZ* mRNA is downregulated in inflamed/atherosclerotic arteries compared to healthy arteries (Figure 30 A). Although mean and most samples were lower in atherosclerotic vessels, the data did not reach statistic significance. Concordantly, *ZFP36*, the regulator of *GILZ*, was significantly induced in atherosclerotic arteries (Figure 30 B). The mRNA of indicators for inflamed vessels, *TLR2* and *CCL2*, were significantly increased in atherosclerotic samples (Figure 30 C, D).

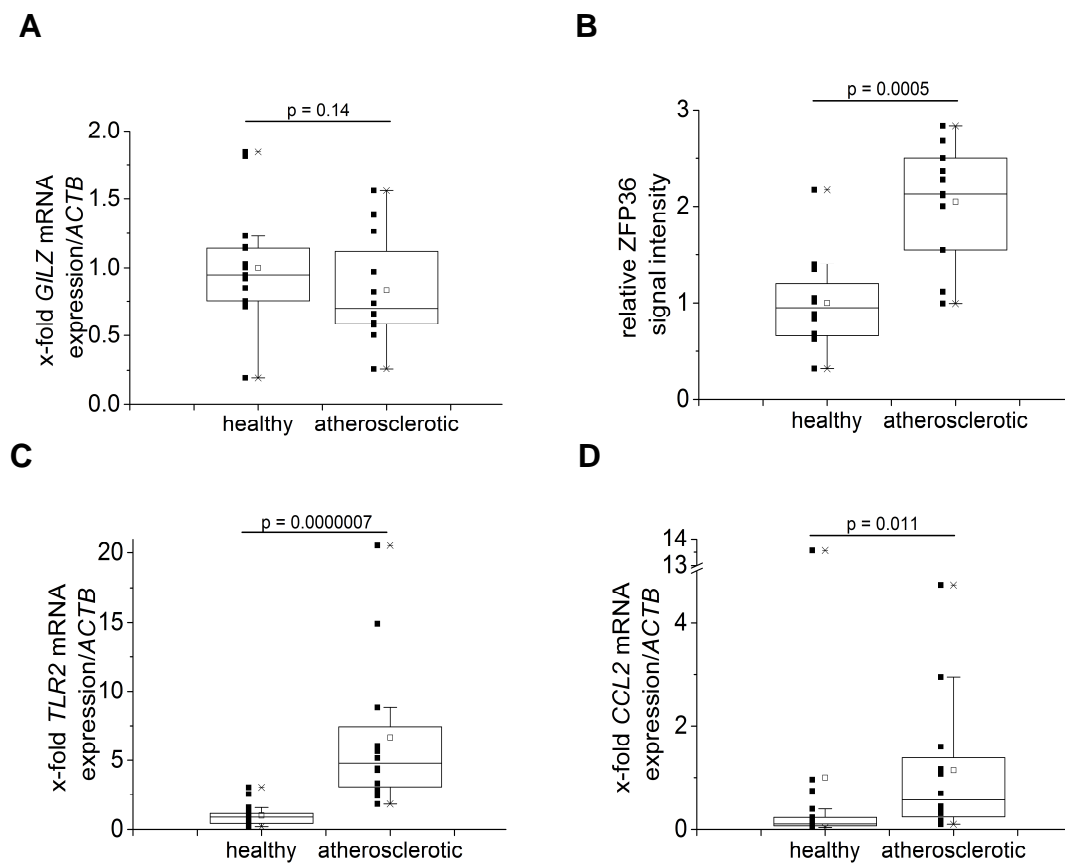


Figure 30: Inflammatory status in clinical samples - *GILZ* (A), *ZFP36* (B), *TLR2* (C), and *CCL2* (D) expression in human arteries. mRNA expression (A, C, D) in radial arteries ($n=17$) and atherosclerotic aorta ($n=12$) was quantified by real-time RT-PCR using *ACTB* for normalization. Equal protein amounts (B) were calculated by Western blot analysis compared to tubulin as loading control. Data show values of 12 healthy and 11 atherosclerotic samples. Signal intensities were determined relative to tubulin values. Data (A,B,C,D) are shown as individual values (black squares) as well as 25th and 75th percentiles as boxes within geometric medians (line), arithmetic medians (square), 10th and 90th percentiles as whiskers, and ends of values (cross). Values for healthy samples were set as one.

3.3 Epigenetic regulation by shear stress

3.3.1 IGF2 and H19 under flow conditions

Shear stress has been described to be a regulator of epigenetic events (Hastings *et al.*, 2007; Zhou *et al.*, 2011). *IGF2* and *H19* are well known epigenetically regulated genes and their products are known to play a role in atherosclerosis. In fact, they are important regulators of VSMC cell proliferation in atherosclerosis (Han *et al.*, 1996; Li *et al.*, 2009; Zaina & Nilsson, 2003; Zaina *et al.*, 2002). In this work, a significant regulation of both, *IGF2* and *H19*, was detected by different kinds of flow: while *IGF2* was upregulated by laminar and oscillatory flow (Figure 31 A), *H19* mRNA was significantly increased by laminar flow and decreased by oscillatory flow (Figure 31 B). Downregulation of *IGF2* by TNF- α after 3.5 h was abrogated with both kinds of flow (Figure 31 A). The downregulation of *H19* after TNF- α is abrogated by laminar flow and significantly increased by oscillatory flow after 2 h (Figure 31B).

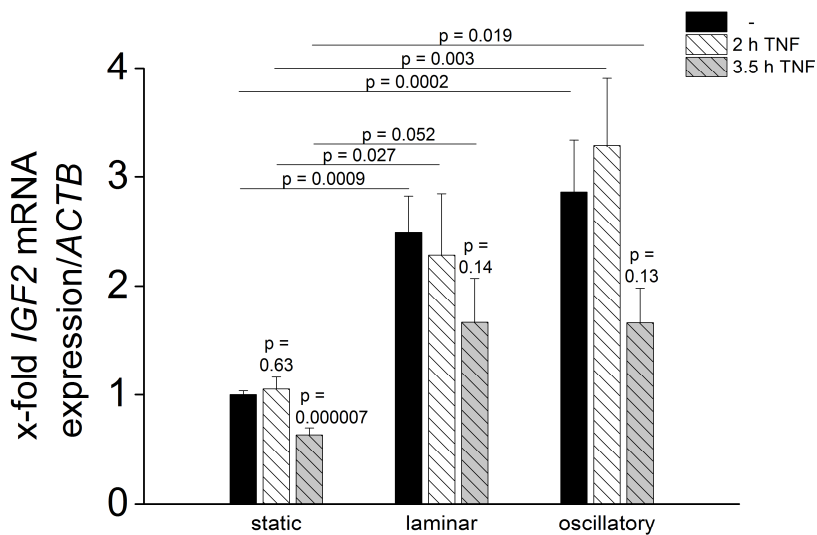
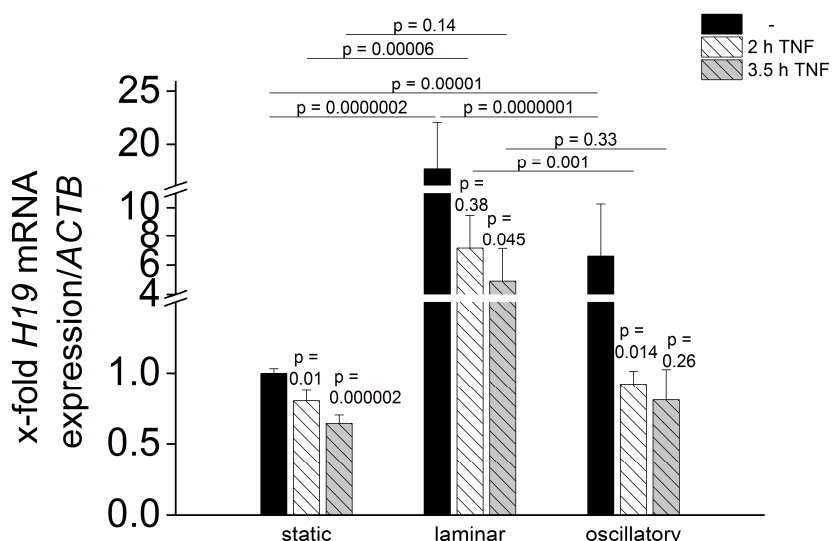
A**B**

Figure 31: *IGF2* (A) and *H19* (B) expression under oscillatory flow - HUVEC were exposed to laminar or oscillatory flow for 24 h without or with TNF- α treatment (10 ng/ml) for the last 2 h or 3.5 h as indicated. mRNA levels derived from four independent experiments (duplicates) were determined by real-time RT-PCR using *ACTB* (β -actin) for normalization and values for untreated cells were set as one. Significance is calculated between untreated and TNF- α treated cells of the same flow state except otherwise noted. Statistical differences were determined with Kruskal-Wallis-ANOVA followed by post-hoc-analysis with Mann-Whitney-U-test.

3.3.2 DNA Demethylation in HUVEC

To analyze if a demethylation of DNA methylation can alter the gene expression in HUVEC, we used 5-azacytidine (aza) as DNA demethylation reagent. *IGF2* (Figure 32 A), *H19* (Figure 32B) (Diesel et al., 2012) as well as *CTCF* (Figure 32 C) were

differently expressed after azacytidine treatment suggesting that DNA methylation is involved in the altered gene expression upon shear stress. Also *DUSP1* was significantly upregulated after azacytidine treatment (Figure 32 D). In contrast, azacytidine treatment did not lead to any significant alteration of *TLR2* (Diesel *et al.*, 2012) as well as *GILZ* mRNA expression in HUVEC (Figure 32 E, F).

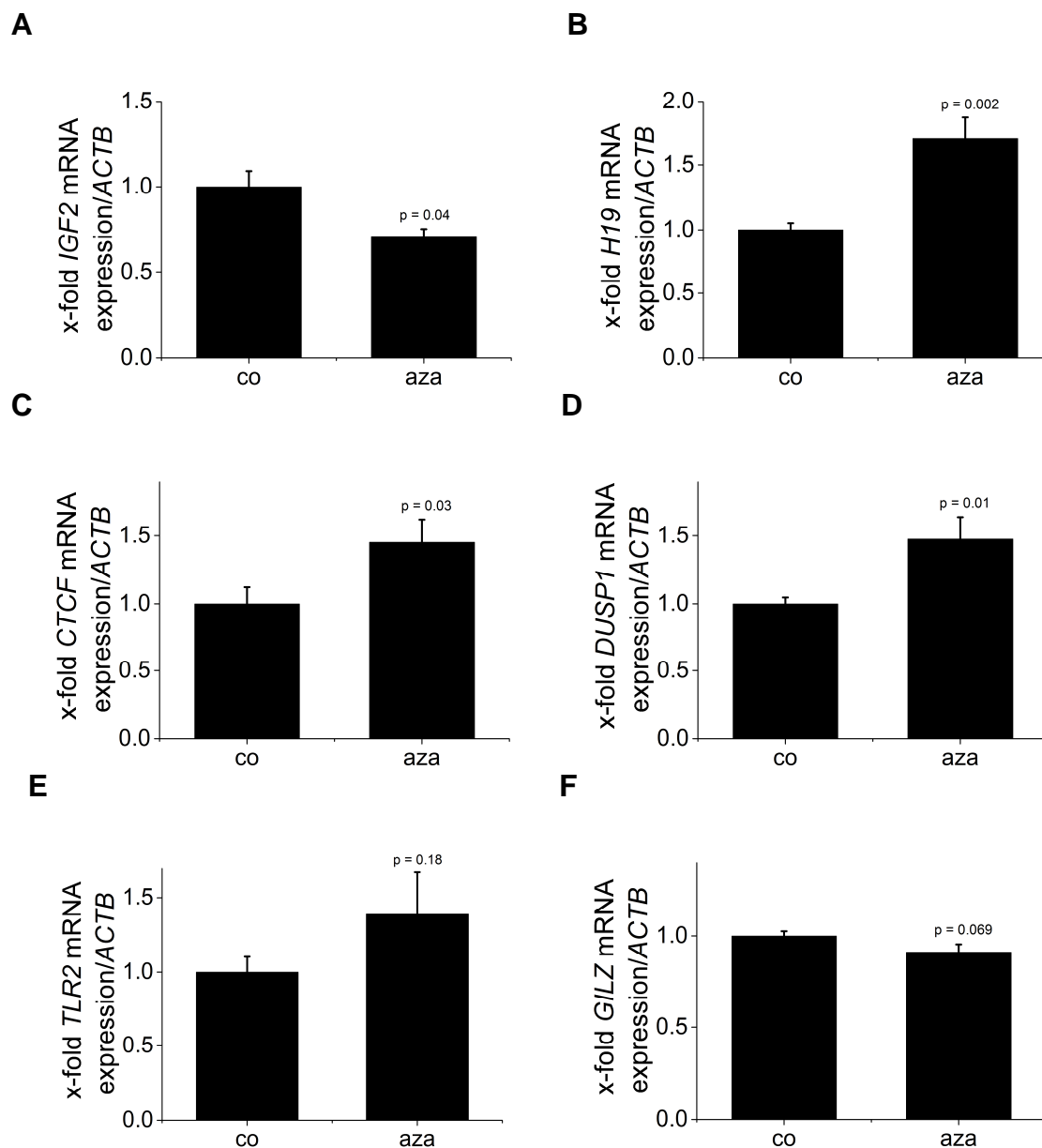


Figure 32: DNA demethylation - HUVEC were treated with 2 μ M 5-azacytidine (aza) for 48 h, whereby 5-azacytidine-containing medium was renewed after 24 h. mRNA levels derived from three (A, C, E, F), 5 (B) or 7 (D) experiments (duplicates) were determined by real-time RT-PCR using *ACTB* (β -actin) for normalization and values for untreated cells (co) were set as one. Experiments were performed in part by Nadège Ripoche and Dr. Britta Diesel (Pharmaceutical Biology, Saarland University).

3.3.2.1 DNA Demethylation under flow conditions

The results after azacytidine treatment suggest a possible regulation of mRNA expression under shear stress *via* DNA demethylation. Therefore, we analyzed the promoter methylation of different genes of interest under flow conditions with SNuPE. The mechanism of DUSP1 regulation under flow conditions was a matter of particular interest of this work. DUSP1 promoter was hypothesized to be demethylated by laminar and oscillatory flow as mechanism of its mRNA upregulation. For the SNuPE analysis, 6 CpG positions (Table 9) of bisulfite-DNA in three different regions were selected by Dr. Sascha Tierling (Genetics/Epigenetics, Prof. Dr. Walter, Saarland University) using UCSC Genome Browser, EMBOSS transeq, CBS.dtu, and VISTA Enhancer Browser. These regions had good expectations because of supposable enriched DNA methylations, enriched H3K4 methylations or binding sites of STAT. Two different positions in the promoter region were analyzed in the 5-aza-2-deoxycytidine (DAC) treatment sample set (one experiment, duplicates), whereby neither a methylation in the controls nor a demethylation by DAC was detected. Four further positions in two different predicted enhancer regions were investigated both in the DAC experiment and in one flow experiment (static, laminar and oscillatory flow, with and without TNF- α , duplicates). Still, none of these positions showed methylation of controls, nor demethylation in both experiments although the mRNA expression was enhanced by flow as well as by DAC (flow results are included in 3.2.3, DAC experiment in Figure 33 A). Upregulation of *H19* mRNA expression by demethylation was determined to validate the DAC experiment (Figure 33 B).

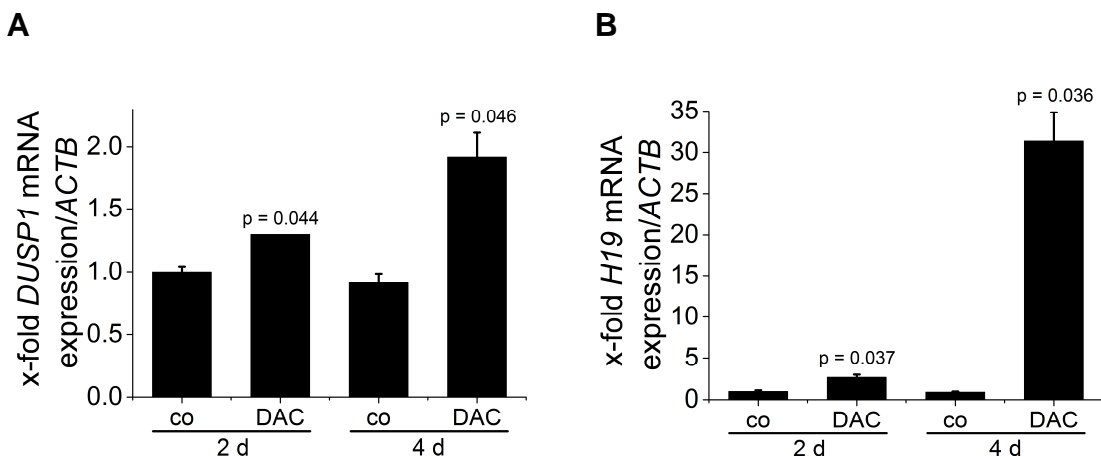


Figure 33: DNA demethylation - HUVEC were treated with 1 μ M 5-aza-2-deoxycytidine (DAC) for 2 d and 4 d, whereby 5-aza-2-deoxycytidine-containing medium was renewed each 24 h. mRNA levels derived from one experiment (duplicates) were determined by real-time RT-PCR using *ACTB* (β -actin) for normalization and values for untreated cells (co) of 2 d were set as one. Experiments were performed in part by Dr. Sonja M. Kessler (Pharmaceutical Biology, Saarland University). Significance is calculated between the respective untreated and treated cells of the same time point.

H19, which is well known as a demethylation-regulated gene, was also analyzed by SNuPE. We hypothesized DNA demethylation to occur during flow, because *H19* mRNA was strongly upregulated by laminar as well as oscillatory flow. Two CpG positions (Table 9) in the *H19* promoter region were used in the examination, which is known for the regulation of *H19* independent of *IGF2* (Diesel *et al.*, 2012; Gao *et al.*, 2002), because the expression of the two genes was not inversely regulated by flow. The SNuPE analysis showed a methylation of the promoter position in untreated cells, which was neither affected by flow nor by TNF- α .

Experimental procedures of bisulfite treatment and SNuPE analysis were in part kindly performed by Viktoria Weinhold, Beate Schmitt, Christina LO Porto and Dr. Sascha Tierling (Genetics/Epigenetics, Prof. Dr. Walter, Saarland University).

4 Discussion

4.1 Validation of the cell culture model for shear stress

4.1.1 Shear stress models

Two different methods to apply shear stress on cells are commonly accepted. One method is the production of flow with a cone and plate viscometer, which is turning above the cells (Dewey, Jr. *et al.*, 1981), another method is the use of a parallel plate flow chamber, wherein the cells are sitting and where the flow is produced by a pump (Frangos *et al.*, 1988). Both methods have been widely used for a long time and neither can be favoured, except perhaps because of planned downstream applications (i.e. direct microscopic visualization in a cone and plate viscometer vs. great amount of cells of the same flow for RNA analysis in a parallel plate flow chamber) (Brown, 2000). This work was generated with the second method and chambers were newly designed and constructed after Frangos *et al.* (1988).

4.1.2 Effects of shear stress

Shear stress is shown to be a regulator of gene expression *via* mechanotransduction (Davies, 2009). Furthermore, it is widely accepted that laminar flow is anti-inflammatory in contrast to disturbed as well as low flow, which are atheroprone (Cunningham & Gotlieb, 2005). The results of this work support these findings.

HO1 is known to have cell protective properties in various tissues and an anti-atherosclerotic potential as shown in different experimental settings (Immenschuh & Ramadori, 2000; Han *et al.*, 2009; Stocker & Perrella, 2006). Anti-inflammatory effects are achieved especially by the production of carbon monoxide and by the suppression of TLR4 signalling (Wang *et al.*, 2009; Chen *et al.*, 2014). Importantly, HO1 is induced by many stressors and counteracts their effects (Stocker & Perrella, 2006; Ryter *et al.*, 2006). An induction of HO1 by anti-inflammatory stimuli was also detected (e.g. ANP, IL-10) (Kiemer *et al.*, 2003a; Lee & Chau, 2002) as well as a significant induction by laminar flow in different systems: in HUVEC after 24 h and 12 dynes/cm² (Ali *et al.*, 2009; Zakkar *et al.*, 2008) or 25 dynes/cm² (McCormick *et al.*, 2001), in human aortic endothelial cells (HAEC) after 48 h at 20 dynes/cm² (Chen *et al.*, 2003), and in VSMC after 24 h at 20 dynes/cm² (Wagner *et al.*, 1997). Oscillatory flow led only to a slight HO1 induction compared to laminar flow of 12 dynes/cm² (Ali

et al., 2009; Zakkar *et al.*, 2008). These results, the increased expression by laminar flow and the lowered, slight induction by oscillatory flow, were confirmed by our data employing 20 dynes/cm² for 24 h. In the literature, HO1 upregulation was already seen after 4 h (15 dynes/cm²), whereby after this time no difference was detected compared to low flow (2 dynes/cm²) (Warabi *et al.*, 2007). Contrarily to these results, a significant decrease of HO1 expression under low flow compared to static conditions was detected by us after 24 h, indicating an inflammatory state of low flow after a longer time. The flow induced regulation of HO1 can be mediated by ARE in the HO1 promoter (Chen *et al.*, 2003).

For further confirmation of the inflammatory effect of low and oscillatory flow, 7 inflammatory mediators were analyzed and almost all of the analyzed genes were at least slightly enhanced, while IL-8 and TLR2 were significantly induced indicating an inflammatory activation of EC by low flow. For TLR2, no data under low shear stress are as yet available in literature. IL-8 is often analyzed as target under low flow and has been shown to be significantly enhanced by low flow (Hastings *et al.*, 2007; Yang *et al.*, 2005). In the endothelial cell line EA.Hy926, induction of IL-8 was shown to be triggered *via* NF-κB and AP-1 (Zhang *et al.*, 2012), whereas in HUVEC a MAPK dependent signalling was published (Cheng *et al.*, 2005; Cheng *et al.*, 2008). The slight induction of CCL2 under low flow in HUVEC and VSMC was previously shown by Hastings *et al.* (2007). CCL2 and IL-8 were also described to promote leukocyte adhesion under low flow inducing vascular inflammation (2 dynes/cm²) (Gerszten *et al.*, 1999). IL-6 has been described to be already upregulated after 8 h under low flow (4 dynes/cm²) (Shaik *et al.*, 2009). Whereas our data support a significant downregulation of VCAM under 24 h low shear stress compared to static cultivation, a significant upregulation has been described by several authors for HUVEC after 6 h (Zeng *et al.*, 2009), for HAEC (Zhu *et al.*, 2004), and for human retinal microvascular endothelial cells (HRMEC) (Ishibazawa *et al.*, 2013). This discrepancy may be explainable with an induction at an early time point with a subsequent counterregulation. The low upregulation of the adhesion molecule ICAM as observed in our hands has been described to be significantly increased in the literature in HUVEC (Yin *et al.*, 2011) (Zeng *et al.*, 2009), whereas for E-selectin, data exist only in HRMEC (Ishibazawa *et al.*, 2013).

Oscillatory flow has been identified as inducer of an inflammatory state in the literature (Davies, 2009; White & Frangos, 2007), and it seemed to have more inflammatory potential than low shear stress in our results. In fact, the inflammatory mediators mentioned above were all, except for VCAM, significantly upregulated at oscillatory conditions. An increased expression of VCAM as well as an upregulation of the other adhesion molecules ICAM and E-selectin at similar conditions has already been described for HUVEC (Chappell *et al.*, 1998) (Cicha *et al.*, 2008), in porcine aortic valve (Sucosky *et al.*, 2009), and in HAEC (Estrada *et al.*, 2011). The discrepancy of VCAM results in HUVEC might be explained with an induction of mRNA expression at an earlier time point (max. after 4 h), which is reduced after 24 h (Chappell *et al.*, 1998). TLR2 expression has been described to be enhanced by disturbed shear stress (Mullick *et al.*, 2008) and its induction by TNF- α treatment could be diminished by laminar, but not by disturbed flow (Dunzendorfer *et al.*, 2004). On the one hand, CCL2 was shown to be increased under oscillatory flow mediated by an increase in transglutaminase activity (Matlung *et al.*, 2012; Cheng *et al.*, 2007), while also no effect of oscillatory flow on CCL2 and IL-6 has been described (Urschel *et al.*, 2012).

4.2 GILZ downregulation at inflammatory conditions

GILZ is an anti-inflammatory mediator, which is inducible by anti-inflammatory stimuli such as glucocorticoids or IL-10 in different cell types (Berrebi *et al.*, 2003; Ayroldi & Riccardi, 2009; Godot *et al.*, 2006; Ayroldi *et al.*, 2014; Thiagarajah *et al.*, 2014). Its anti-inflammatory activity is mainly mediated *via* inhibition of NF- κ B and AP-1 by direct binding and preventing their nuclear translocation (Fan & Morand, 2012) or additional by inhibition of ERK (Hoppstädter *et al.*, 2015).

Stimulation with the inflammatory cytokines IL-1, TNF- α , and INF- γ leads to a GILZ decrease in epithelial cells (Eddleston *et al.*, 2007). These results are here confirmed by downregulation of GILZ protein expression after TNF- α treatment in HUVEC. Inflammatory stimuli, such as TLR ligands and TNF- α , also downregulate GILZ in MΦ (Hahn *et al.*, 2014; Hoppstädter *et al.*, 2012). Furthermore, we present evidence for a diminished GILZ expression in both degenerated vein bypasses and atherosclerotic arteries. Inflammation in the diseased vessels was confirmed by enhanced TLR2 and CCL2 expression. TLR2 upregulation was already shown in atherosclerotic plaques

of carotid arteries compared to internal mammary arteries (Edfeldt *et al.*, 2002) and CCL2 is a general marker for cardiovascular disease and inflammatory activation in EC (Niu & Kolattukudy, 2009; Szmitsko *et al.*, 2003; Tucci *et al.*, 2006).

A GILZ downregulation or even absence in other inflammatory diseases, such as chronic rhinosinusitis, Crohn's disease, or tuberculosis has been reported in the literature, indicating that the absence of GILZ is a general phenomenon in inflammation (Berrebi *et al.*, 2003; Zhang *et al.*, 2009).

Generally, atherosclerosis is known as a disease of arteries, while veins are not affected (Roy *et al.*, 2009). Still, vein graft remodelling, where pieces of veins after bypass surgeries are localized at atherosusceptible regions, is also characterized by inflammatory events, (Karper *et al.*, 2011; McPhee *et al.*, 2013) with only minor differences to the processes in arteries (Yazdani *et al.*, 2012). These differences are not based on the differences in the constitution of veins and arteries, but rather on the peripherals e.g. systemic hypertension, high plasma lipids, and altered local hemodynamics (Cox *et al.*, 1991; Hamby *et al.*, 1977; Hamby *et al.*, 1979). Interestingly, a significant GILZ downregulation was detected in degenerated veins contrarily to arteries. This fact may be explained by a basal inflammatory activation of healthy arteries of surgery patients in contrast to healthy veins, because atherosclerosis is characterized by a systemic infestation and various arteries of atherosclerotic patients might show signs of inflammation (Jashari *et al.*, 2013).

4.3 Mechanism of GILZ regulation under laminar flow

Blood flow influences atherosclerosis and the formation of atherosclerotic plaques by exerting shear stress on the vascular endothelium, which differs in magnitude and characteristics depending on the vascular anatomy and blood pressure (Frueh *et al.*, 2013). Shear stress alters the phenotype of EC, which respond to it *via* mechanosensory mediators that translate mechanical distortions into various molecular signals (Tzima *et al.*, 2005). A microarray study performed on 6 h and 24 h of laminar shear stress of 25 dynes/cm² on HUVEC already suggested an upregulation of GILZ by laminar flow (McCormick *et al.*, 2001). Still, the results were neither confirmed by realtime RT-PCR or on protein level, nor further mechanistic studies existed.

GILZ induction by laminar shear stress may be a result of GR activation, as described for bovine aortic endothelial cells (BAEC) (Ji *et al.*, 2003). Correspondingly, multiple GREs are present in the GILZ promoter (Ayroldi & Riccardi, 2009). Additionally, a regulation *via* SSREs in the promoter is possible. Two known SSREs, GA-GACC (Resnick *et al.*, 1993) (16x) and the more potent TGACTCC (Shyy *et al.*, 1995) (3x), can be found upstream of the GILZ transcription start site. Another possibility is the involvement of KLF2, which is known to cooperate with GRs resulting in anti-inflammatory answers (Chinenov *et al.*, 2014) and reduced by laminar flow (Wang *et al.*, 2006).

Furthermore, an epigenetic regulation is also conceivable, although as yet only little is known about epigenetic mechanisms in GILZ regulation. An indirect regulation was described, whereupon GR-dependent GILZ activation was inhibited by miR-124a and -18 overexpression by their binding to GR (Vreugdenhil *et al.*, 2009). So far, a direct regulation of GILZ by miRNA is not described. Recently, some first findings were kept in our laboratory (Hachenthal *et al.*, 2013): miRNA-21 has been shown to enhance GILZ expression. miRNA-21 is also known to be induced by 15 dynes/cm² laminar flow for 24 h (Weber *et al.*, 2010b), so it might be an appropriate candidate for further investigations. An additional candidate could be miRNA-18a, because it was kept as hit from in silico studies about miRNA dependent GILZ regulation (<http://ophid.utoronto.ca/mirDIP/>) and is induced by oscillatory flow compared to pulsatile flow at 12 dynes/cm² for 24 h (Wu *et al.*, 2011).

DNA methylation as a regulatory mechanism of gene expression was recently investigated and described to play a role in shear stress (Dunn *et al.*, 2014). We hypothesized it binding to regulate GILZ expression. Still, the treatment with the demethylation reagent 5-azacytidine did not result in a significant expression difference.

4.3.1 ZFP36 dependent GILZ downregulation

While TNF- α strongly downregulated GILZ in static HUVEC, a TNF- α challenge failed to diminish GILZ levels in HUVEC exposed to laminar shear stress. Accordingly, ZFP36 upregulation is missing in response to TNF- α treatment under laminar flow, whereas TNF- α strongly enhanced ZFP36 without flow in EC as well as in different other cell types i.e. in THP-1 (Tsai *et al.*, 2009) or in mouse fibroblasts (Chen *et al.*, 2012c). In a previous study, TLR activation was shown to induce GILZ downregula-

tion in primary human MΦ *via* the mRNA-binding protein ZFP36 (Hoppstädter *et al.*, 2012). Also in HUVEC, the TNF- α dependent GILZ downregulation was paralleled by an earlier, extensive induction of ZFP36, indicating a possible role of ZFP36 as a repressor of GILZ. This hypothesis was confirmed by knockdown of ZFP36, where TNF- α mediated GILZ downregulation was abrogated, as well as overexpression of ZFP36 in HUVEC resulting in reduced GILZ levels (Hahn *et al.*, 2014). We also showed an induction of ZFP36 in atherosclerotic arteries as well as in degenerated veins. These similar findings were reported for human and murine EC overlying atherosclerotic plaques (Zhang *et al.*, 2013). Interestingly, though, the authors suggested that ZFP36 upregulation was an atheroprotective process, since ZFP36 inhibits activation of NF- κ B and binds to cytokine mRNAs to reduce their transcript stability (Zhang *et al.*, 2013). These findings are conform with the general opinion of ZFP36 having anti-inflammatory properties, as a destabilizer of cytokine mRNAs, i.e. TNF- α , IL-8 and IL-6 (Aslam & Zaheer, 2011; Lai *et al.*, 1999; Lai *et al.*, 2006; Balakathiresan *et al.*, 2009; Zhao *et al.*, 2011; Sanduja *et al.*, 2011). Additionally, ZFP36 is a target of glucocorticoids, which are able to reduce mRNA stability of inflammatory mediators through elevation of ZFP36 protein expression (Smoak & Cidlowski, 2006; Anderson *et al.*, 2004).

In contrast, another group published a reduced ZFP36 expression by glucocorticoids in activated MΦ (Jalonen *et al.*, 2005), suggesting inflammatory properties for ZFP36. In addition, the anti-inflammatory mediator IL-10 was identified as a target of ZFP36, being elevated because of diminished decay in primary MΦ from ZFP36^(-/-) mice (Stoecklin *et al.*, 2008). These facts rather point to inflammatory actions of ZFP36. Taken together, ZFP36 might act either as an inflammatory or an anti-inflammatory mediator. Therefore, additional factors might be needed to orchestrate ZFP36 actions or a difference in the activation mechanism of ZFP36 may be responsible for inflammatory or anti-inflammatory transmission (Hammaker *et al.*, 2014). In this context, other mRNA-binding proteins might be involved, whose binding might be further modulated by miRNAs (George & Tenenbaum, 2006; Ciafre & Galardi, 2013). Furthermore, a direct regulation of ZFP36 by miRNA is proposable (Lu *et al.*, 2014; Rosenberger *et al.*, 2012; Zawada *et al.*, 2014).

4.3.2 DUSP1 in atherosclerosis

The p38 MAPK pathway is known to induce ZFP36 expression in MΦ and human pulmonary microvascular endothelial cells (Ronkina *et al.*, 2010; Stoecklin *et al.*, 2004; Shi *et al.*, 2012). In accordance with these results, a p38 inhibition *via* SB203580 also markedly reduced ZFP36 levels in HUVEC, whereas GILZ downregulation upon TNF- α -treatment was abrogated, indicating that p38 regulates GILZ expression *via* a mechanism involving ZFP36. SB203580 acts as a competitive inhibitor at the ATP binding site of p38 MAPK α and β (Kumar *et al.*, 1997; Young *et al.*, 1997). These two isoforms are mainly expressed in HUVEC compared to the other isoforms (Hale *et al.*, 1999). Additionally, ZFP36 downregulation was activated *via* isoform specific inhibition of p38 α by overexpression of dominant negative p38 α MAPK suggesting isoform p38 α to be responsible for this effect.

DUSP1 is a well known inhibitor of p38 MAPK (Kiemer *et al.*, 2002a) and therefore is considered to be an anti-inflammatory factor (Wancket *et al.*, 2012), which is also induced by glucocorticoids (Toh *et al.*, 2004). DUSP1 was also shown to be elevated by anti-inflammatory laminar flow, protecting arteries from inflammation. Dephosphorylation of p38 leads to decreased VCAM levels diminishing leukocyte adhesion (Zakkar *et al.*, 2008). Correspondingly, DUSP1 suppressed ZFP36 expression by abrogating p38 activity in different MΦ and epithelial cells (Huotari *et al.*, 2012). Our data suggest a similar mechanism, because DUSP1 induction by laminar shear stress was paralleled by moderately reduced ZFP36 levels and an enhanced GILZ expression. Additionally, DUSP1 was expressed in healthy, but not in degenerated veins.

Our results suggest an anti-atherosclerotic effect of DUSP1, a topic, which was discussed controversially in the literature. The results of Kim *et al.* (2012) and Zakkar *et al.* (2008) are in line with our findings, whereas Imaizumi *et al.* (2010) and Shen *et al.* (2010) showed the opposite, i. e. DUSP1 deficiency decreased atherosclerotic lesion development in mice as shown in apoE^(-/-) mice. The data supporting anti-atherosclerotic actions of DUSP1 were not only generated in DUSP1 deficient mice but also in human cells. These findings, that the use of apoE^(-/-) mice might have an impact on the DUSP1 effects. Therefore, the pro-atherosclerotic action of DUSP1 should be verified in another experimental setup. Importantly, atherosclerosis in mice is not absolutely comparable to the disease in humans (Libby *et al.*, 2011).

4.3.3 Regulation of DUSP1 by shear stress

Recently published results postulated a positive regulation of DUSP1 by GILZ in rheumatoid arthritis (Fan *et al.*, 2014), leading to a possible loop with self reinforcing anti-inflammatory effects, additionally to the GILZ regulation mechanisms discussed in chapter 4.3. Different mechanisms might be arguable for the induction of DUSP1 by laminar shear stress (Wancket *et al.*, 2012). These include regulation *via* SSREs or AREs, whereby as yet no SSREs or AREs have been identified in the DUSP1 promoter.

A further possibility is a regulation of DUSP1 expression *via* epigenetic mechanisms. Two miRNAs, which are known to be influenced by shear stress, regulate DUSP1 expression: miRNA-210 (Jin *et al.*, 2014), which was downregulated under laminar flow (Hergenreider *et al.*, 2012), and miRNA-101 (Gao *et al.*, 2014; Yang *et al.*, 2013), which was upregulated under laminar flow (Chen *et al.*, 2012b).

DNA methylation is also a possibility to modulate DUSP1 expression (Chen *et al.*, 2012a). In fact, treatment of HUVEC under static conditions with the demethylating reagent 5-azacytidine resulted in a significant DUSP1 upregulation. In this work, an epigenetic regulatory mechanism of DUSP1 expression by shear stress was not detected, although DNA methylations of six different positions (Table 9) in the DUSP1 promoter and two enhancer regions were investigated *via* SNuPE. In this process, the necessary negative controls of PCR and bisulfite treatment were always performed and examined with agarose gel electrophoresis. All steps were exactly performed and a demethylation mechanism by flow on the analyzed, well selected positions can be largely excluded, although normally, at least three experiments have to confirm a result. Still, DNA methylation processes can not be completely excluded, because the methylation might be located in different position.

Other epigenetic regulation, i.e. histone modification, remains to investigate. Furthermore, DUSP1 is acetylated and therefore deacetylated and regulated by HDAC-1, -2, and -3 by deacetylation (Jeong *et al.*, 2014), which all are shear stress responsive enzymes (Chen *et al.*, 2013). This post-translational modification do not change the DUSP1 expression itself, except *via* a self reinforcing loop, but it directly increased MAPK signaling downstream (Jeong *et al.*, 2014).

4.4 Mechanism of GILZ regulation under oscillatory flow

In contrast to atheroprotected regions under laminar flow in straight vessels, atherosclerotic plaques are localized in bifurcations or curvatures of vessels where disturbed and low shear stress develop, which exhibit inflammatory potential (Cunningham & Gotlieb, 2005; Wang *et al.*, 2013a). Inflammatory properties of low and oscillatory shear stress were confirmed *via* increased mRNA expression of different inflammatory mediators (see 4.1.2). It is known that oscillatory shear stress is able to alter gene expression into both, the same direction as laminar shear stress, but to a different extent, and the opposite direction (Rhee *et al.*, 2010). Even though in general the enhancement of inflammatory genes and proteins are detected under atheroprone flow conditions, the expression of anti-inflammatory mediators is rarely shown. Additionally, only few studies show the expression under all possible shear conditions. The gene expression of antioxidant NAD(P)H dehydrogenase, quinone 1 provided (NQO1) is generally enhanced under flow compared to static conditions, but the increase is higher under laminar flow compared to low as well as oscillatory flow (Chen *et al.*, 2003). Others revealed a decreased eNOS expression under oscillatory flow, while it is upregulated under laminar flow (Rhee *et al.*, 2010). Flow-mediated differences in HO1 expression were discussed in 4.1.2.

We showed that the expression of the anti-inflammatory mediator GILZ is not changed at low flow and diminished at oscillatory flow, in contrast to the increased levels under laminar flow. Suggesting a similar mechanism decreasing GILZ by oscillatory flow in contrast to laminar flow, we analyzed ZFP36 and DUSP1 levels. The enhancement of ZFP36 expression confirmed this hypothesis. However, DUSP1 was upregulated to the same extent as in laminar flow. Therefore, the mechanism of GILZ regulation by oscillatory flow has to be distinguished from general inflammatory cell activation and the activation under laminar flow. Other mechanisms of GILZ regulation are discussed in chapter 4.3.

Interestingly, TNF- α did not further reduce GILZ and enhance ZFP36 levels during oscillatory stress, which might suggest a slight protection against further inflammatory activation. This conclusion was recently drawn by Gauci *et al.* because disturbed flow enhances anti-inflammatory homeobox genes (Gauci *et al.*, 2014). Simultaneously, DUSP1 expression was reduced by TNF- α under oscillatory flow, which emphasizes

the existence of a different regulation. Mechanisms of DUSP1 regulation are discussed in chapter 4.3.3.

The upregulation of anti-inflammatory DUSP1 (Wancket *et al.*, 2012) by oscillatory shear stress is contrary to the concept of inflammatory oscillatory flow (Wang *et al.*, 2013a) as well as DUSP1 as anti-inflammatory mediator. Furthermore, it is in contrast to the other results of this work, i.e. its increase under laminar flow and its downregulation in degenerated veins. This effect of DUSP1 may be the reason for the downregulation of VCAM, because VCAM is a well known target downregulated by DUSP1 (Zakkar *et al.*, 2008).

4.5 Functional implications of GILZ downregulation

The anti-inflammatory properties of GILZ are postulated to play an important role in various inflammatory diseases (Berrebi *et al.*, 2003; Zhang *et al.*, 2009; Cannarile *et al.*, 2009). Furthermore, in EC overexpressing GILZ, it was recently shown to play a key role in vascular inflammation by inhibiting inflammatory leukocyte recruitment (Cheng *et al.*, 2013). So far, the functional activity of endogenous GILZ was not investigated in EC. The main anti-inflammatory properties of GILZ are mostly mediated *via* NF-κB inhibition (Ayroldi & Riccardi, 2009) but also by inhibition of ERK (Hoppstädter *et al.*, 2015).

NF-κB is an important pro-inflammatory transcription factor, which consists of five subunits (p65, RelB, c-Rel, p50, p52), forming homo- or heterodimers, predominantly the p65:p50 heterodimer (Hoffmann *et al.*, 2002). Activation is achieved by degradation of inhibitory protein kappa B (IκB), which binds NF-κB in the cytosol, followed by translocation into the nucleus and binding to NF-κB sensitive gene sequences (Hayden & Ghosh, 2004). Nuclear translocation of NF-κB results in the expression of mainly inflammatory modulators, such as cytokines, growth factors, and adhesion molecules (Kiemer *et al.*, 2002b; Hayden & Ghosh, 2008). GILZ has been shown to inhibit NF-κB by binding to the p65 subunit, leading to diminished cytokine transcription in various cell types, including EC (Ayroldi & Riccardi, 2009; Berrebi *et al.*, 2003; Cheng *et al.*, 2013; Di Marco *et al.*, 2007). Furthermore, GILZ knockdown was shown to activate cytokine expression in airway epithelial cells and to enhance NF-κB acti-

vation in LPS-treated MΦ (Eddleston *et al.*, 2007; Hoppstädter *et al.*, 2012). In accordance with these findings, the absence of GILZ resulted in an enhanced NF-κB activity in HUVEC, paralleled by nuclear translocation of p65 and p50 and NF-κB-dependent transcription of the inflammatory mediators TLR2, E-selectin and ICAM1 (Hahn *et al.*, 2014). Endothelial cell-specific NF-κB inhibition has been shown to protect mice from atherosclerosis and vascular remodelling. Therefore NF-κB might link reduced GILZ to the pathogenesis of atherosclerosis (Gareus *et al.*, 2008; Saito *et al.*, 2013). These findings show that the disappearance of GILZ liberates NF-κB and induces its activation suggesting that the absence of GILZ drives a proinflammatory response.

4.6 Regulation of *H19* and *IGF2* under shear stress

The imprinted genes *H19* and *IGF2* are mainly prenatally expressed and strongly downregulated after birth in most tissues (Weber *et al.*, 2001). Their expression is mainly described for various tumors suggesting a role in tumorigenesis (Kessler *et al.*, 2013; Taniguchi *et al.*, 1995; Matouk *et al.*, 2013). Additionally, IGF2 is known to be an important regulator in atherosclerosis and has been identified as atherogenic factor in human VSMC and in a mouse model (Zaina & Nilsson, 2003; Zaina *et al.*, 2002). *H19* has also been described to be expressed in VSMC of atherosclerotic lesions (Han *et al.*, 1996). Other investigations showed a function in cell proliferation of VSMC, with an increase in *H19* expression and a decrease of *IGF2* expression, which is mediated by enhanced CTCF expression and hypomethylation of an unmethylated imprinting control region (Li *et al.*, 2009). These findings are in contrast to our results, where *H19* is upregulated in EC by anti-inflammatory laminar flow and downregulated by oscillatory shear stress. Additionally, the regulatory mechanisms have to be different under laminar flow, because of an enhanced IGF2 expression. Under oscillatory flow, regulation *via* an imprinting control region is possible, because *H19* is decreased while *IGF2* is increased. According to this, two different mechanisms have to exist, probably including differently methylated sites in DNA. Gene expression data after treatment with 5-azacytidine indicate the relevance of this mechanism regulating the expression of these imprinted genes in HUVEC. Still, *via* SNuPE,

a differential DNA demethylation under flow was not detected, although atherosclerosis is known to be strongly regulated by DNA methylation (Zaina *et al.*, 2014).

In the SNuPE experiment, the necessary negative controls of PCR and bisulfite treatment were always performed and examined with agarose gel electrophoresis. All steps were exactly performed and demethylation mechanism by flow on the analyzed, well selected positions in the promoter of *H19* (Table 9) (Diesel *et al.*, 2012; Gao *et al.*, 2002) can be largely excluded, although normally, at least three experiments have to confirm a result. Furthermore, a demethylation mechanism is not totally impossible for the regulation of *H19*, the methylation can also be at another position. Other epigenetic regulation, i.e. histone modification, remains to investigate.

Due to their strong regulation in EC by different types of flow, *IGF2* and *H19* might still play a role in the formation of atherosclerosis. Whereas *H19* is differently regulated at different flow types, *IGF2* is generally upregulated. Furthermore, they are regulators of obesity and overweight (Perkins *et al.*, 2012; Morita *et al.*, 2014), which are risk factors for the development of atherosclerosis. Upregulation of *H19* was also reported for the inflammatory disease rheumatoid arthritis (Stuhlmuller *et al.*, 2003). In contrast, in EC, *H19* expression is diminished at inflammatory conditions such as oscillatory flow or TNF- α treatment. In chondrocytes, TNF- α also leads to a decrease of *H19* (Steck *et al.*, 2012). Interestingly, the downregulation of both, *IGF2* and *H19*, upon TNF- α is abrogated under laminar and oscillatory flow.

Data in the literature on the role of *H19* and *IGF2* in the development of atherosclerosis were obtained from VSMC, where they are potent regulators of cell proliferation, a key event in the development of atherosclerosis (Han *et al.*, 1996; Li *et al.*, 2009; Zaina *et al.*, 2002; Zaina & Nilsson, 2003). Similar to EC, the gene expression of VSMC is also modulated by shear forces of blood flow, therefore this effect might be flow-induced.

The functions and regulatory mechanisms of *H19* and *IGF2* in EC have to be elucidated in further experiments.

5 Summary

5.1 Summary

Atherosclerosis is a chronic inflammatory cardiovascular disease with high prevalence and a major cause of morbidity and mortality. High risk factors for development and progression of atherosclerotic plaques are low and disturbed shear stress, while laminar flow is important for physiological functions of the endothelium. Endothelial dysfunction is involved in the pathological processes of atherosclerosis, which is characterized by an inflammatory activation of the endothelium.

The anti-inflammatory factor glucocorticoid-induced leucine zipper (GILZ), which mediates the anti-inflammatory actions of glucocorticoids, was a matter of particular interest of this work. A downregulation and following NF- κ B activation under inflammatory conditions was indicated for several cells and diseases. As regulation mechanism, ZFP36 was already shown to be a destabilizer of GILZ in macrophages and to be regulated by DUSP1 in lung epithelial cells. However in EC, GILZ was only known to be constitutively expressed as well as upregulated under laminar flow without any further mechanistic studies.

Enhanced NF- κ B activation, caused by GILZ knockdown, was also confirmed for EC, suggesting the promotion of vascular inflammation by GILZ absence. Further, a downregulation of GILZ was shown in EC under inflammatory conditions: (I) upon treatment with the inflammatory cytokine TNF- α , (II) upon oscillatory flow and (III) in human inflamed vessels. In contrast, anti-inflammatory laminar flow increased GILZ expression. The TNF-induced downregulation of GILZ was facilitated by induction of the mRNA binding protein ZFP36, which was also elevated in human inflamed vessels. In contrast, the downregulation of GILZ by inflammatory oscillatory flow had to be independent of ZFP36 (Figure 34).

As an anti-inflammatory stimulus, laminar flow was used, whereby the GILZ expression was upregulated, while a diminished ZFP36 and an enhanced DUSP1 expression was detected. Mechanistic examinations showed a dependency of GILZ upregulation by ZFP36, which itself was downregulated *via* inhibition of p38 MAPK (Figure 35 A). Additionally, laminar flow is able to enhance the TNF- α mediated GILZ downregulation by suppressing ZFP36 induction (Figure 35 B).

Although DUSP1 expression was independently upregulated under oscillatory flow, GILZ downregulation was also paralleled by diminished DUSP1 levels in human inflamed vessels.

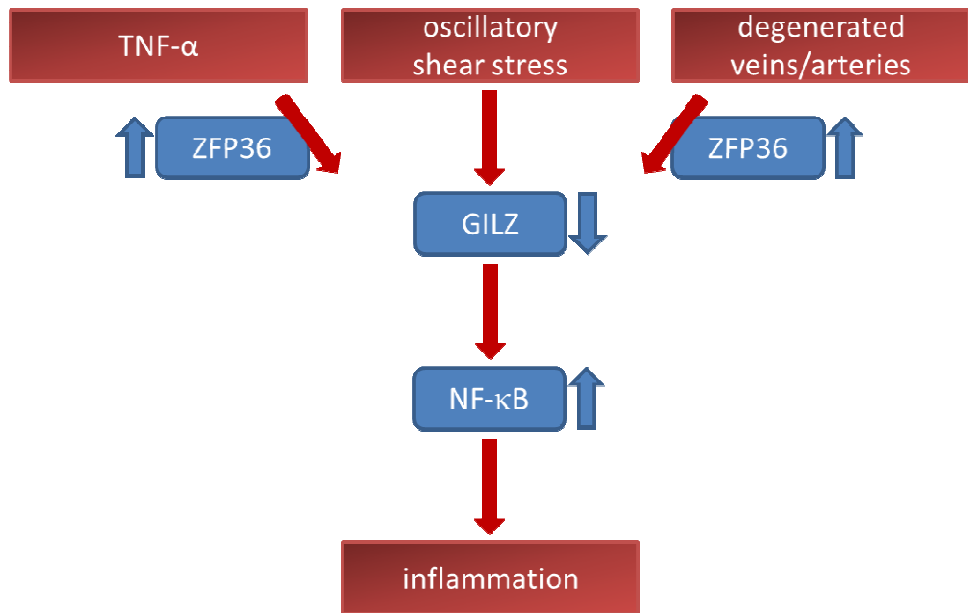


Figure 34: Inflammatory activation of GILZ

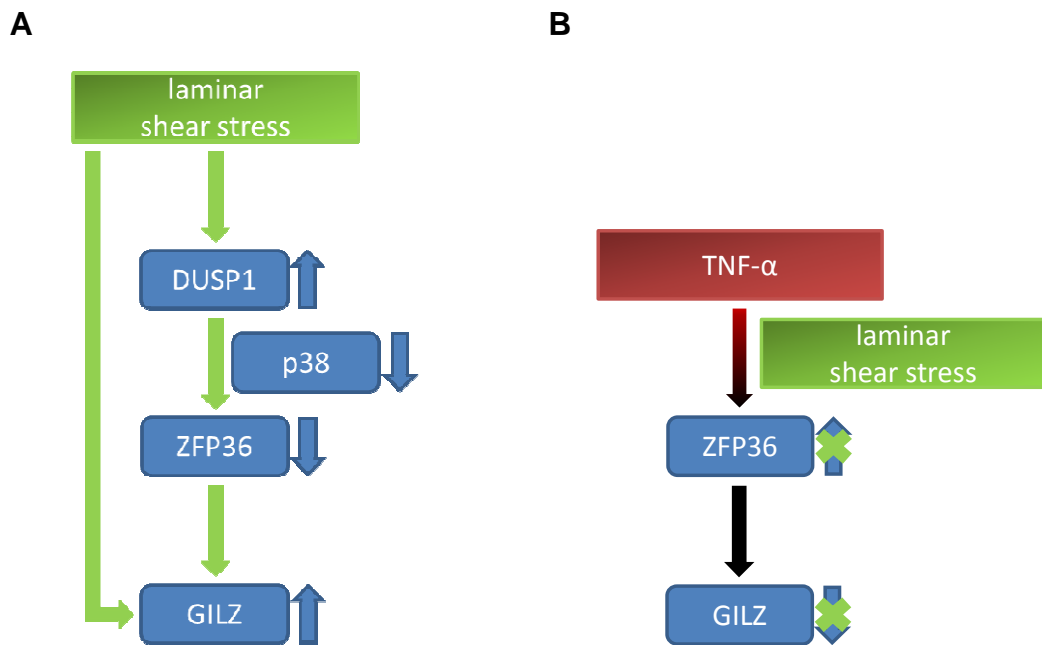
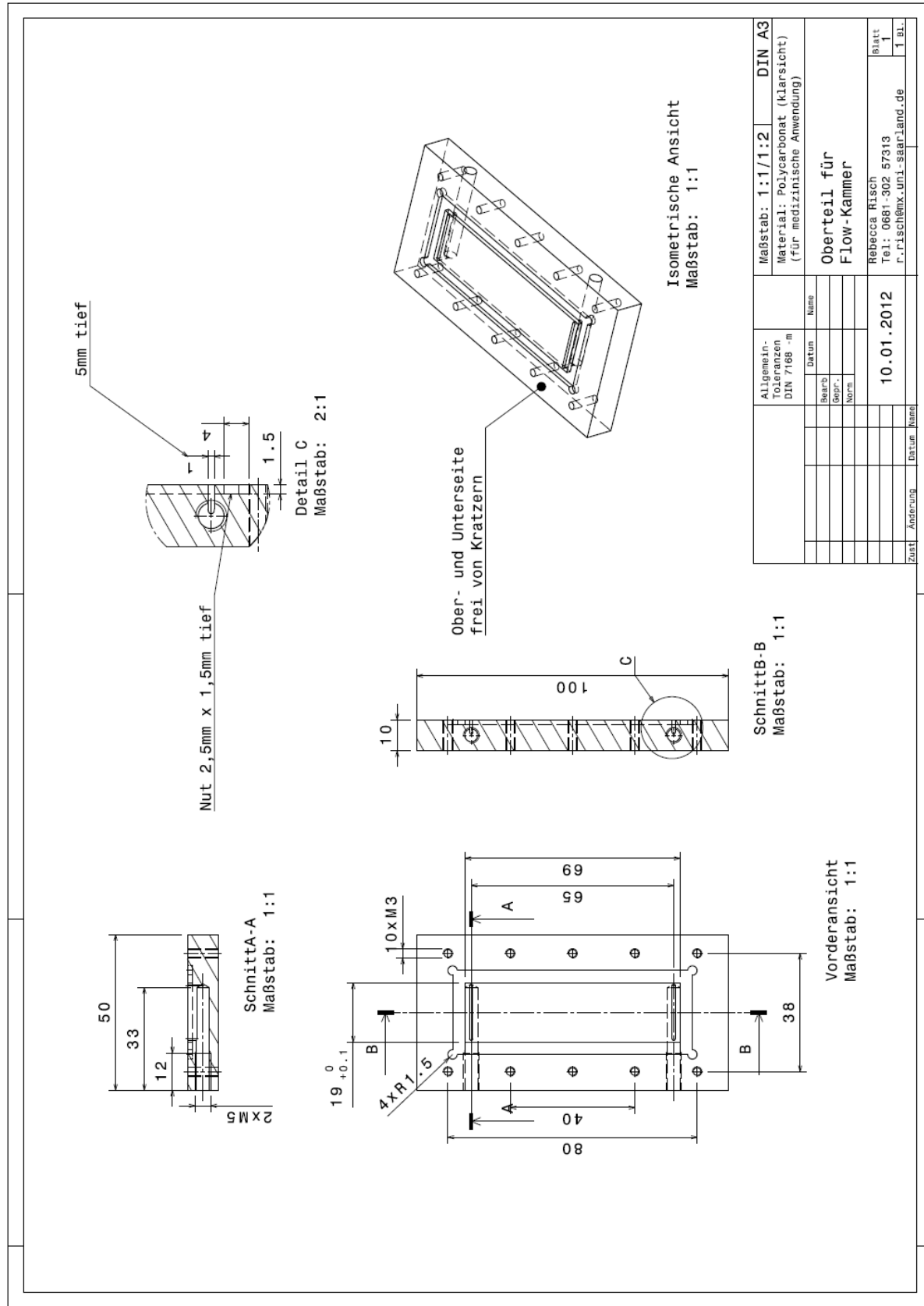


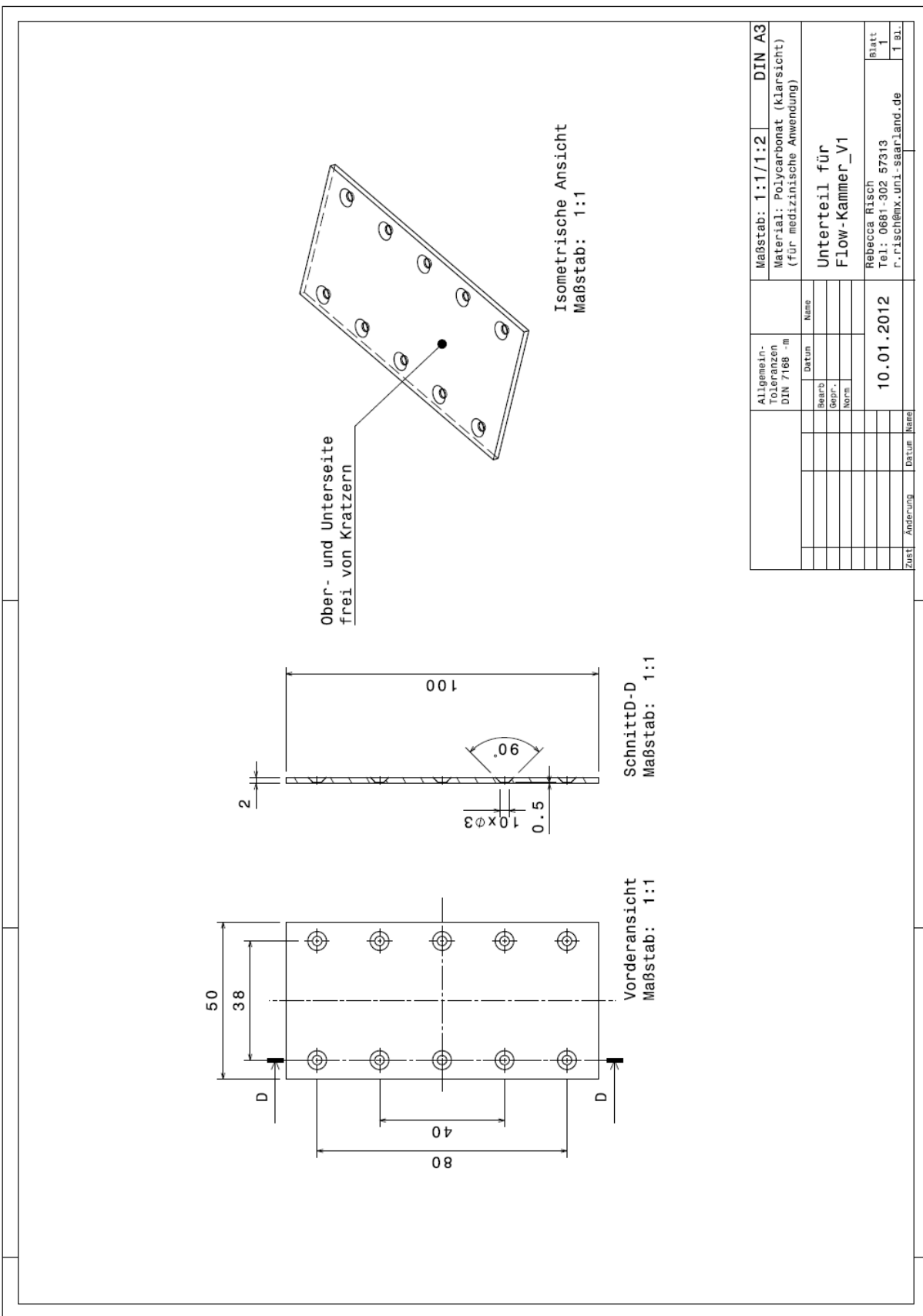
Figure 35: Mechanism of GILZ upregulation by laminar flow (A) and abrogation of TNF-α-induced inflammatory activation by laminar shear stress (B)

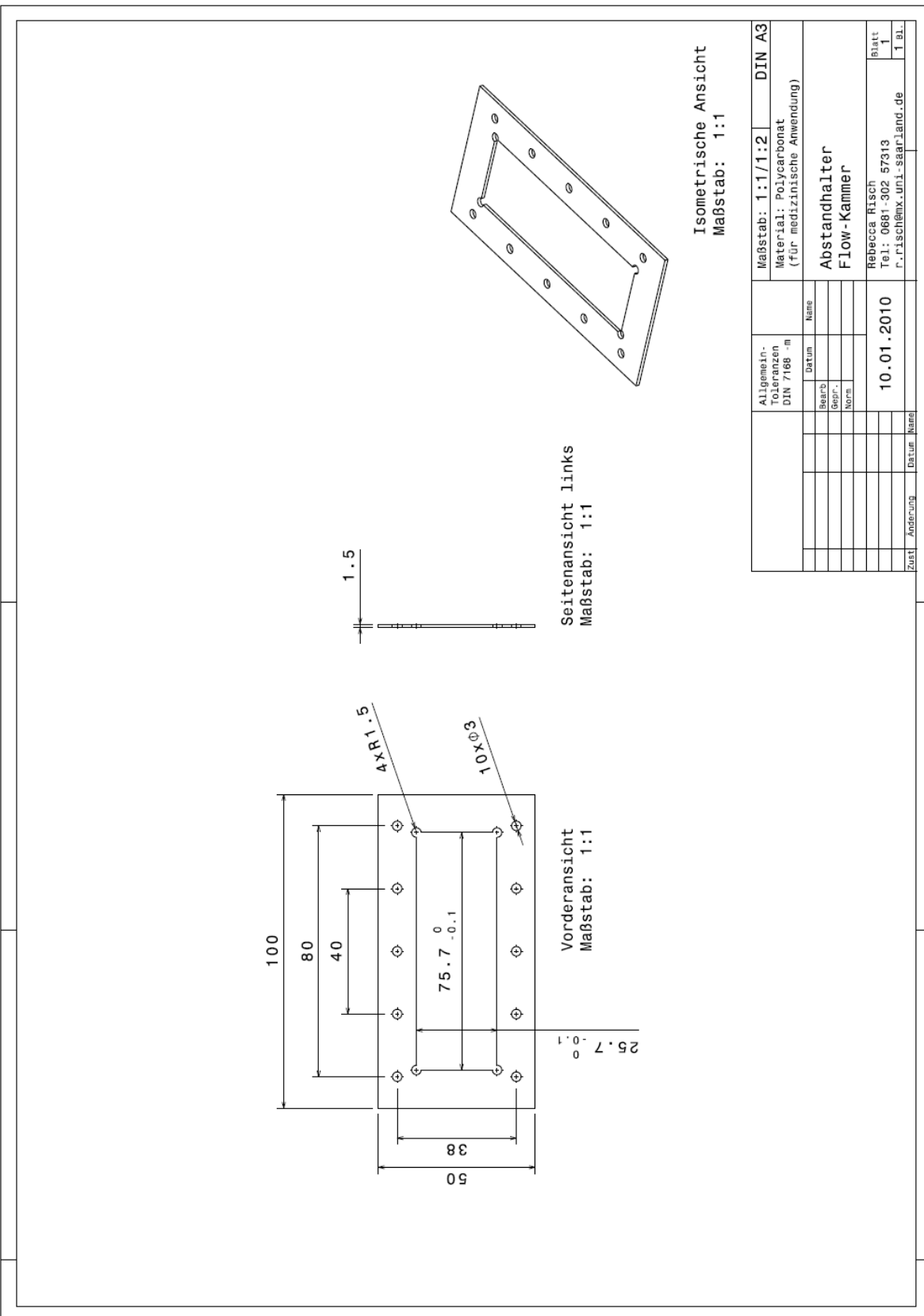
Taken together, our data show that the downregulation of GILZ in human EC promotes vascular inflammation by suppressing NF-κB activation. This assumption is supported by decreased GILZ levels found in atherosclerotic vessels and by oscillatory flow, while laminar flow leads to GILZ enhancement, suggesting GILZ as a key factor in the pathogenesis of atherosclerosis and the upregulation of GILZ as a potential target for the treatment of the inflamed endothelium.

6 Supplement

6.1 Plans of parallel plate flow chambers







References

References

- Alessi DR, Smythe C, Keyse SM. 1993.** The human CL100 gene encodes a Tyr/Thr-protein phosphatase which potently and specifically inactivates MAP kinase and suppresses its activation by oncogenic ras in Xenopus oocyte extracts. *Oncogene* **8:** 2015-2020.
- Ali F, Zakkar M, Karu K, Lidington EA, Hamdulay SS, Boyle JJ, Zloh M, Bauer A, Haskard DO, Evans PC, Mason JC. 2009.** Induction of the cytoprotective enzyme heme oxygenase-1 by statins is enhanced in vascular endothelium exposed to laminar shear stress and impaired by disturbed flow. *J.Biol.Chem.* **284:** 18882-18892.
- Anderson P, Phillips K, Stoecklin G, Kedersha N. 2004.** Post-transcriptional regulation of proinflammatory proteins. *J.Leukoc.Biol.* **76:** 42-47.
- Aslam N, Zaheer I. 2011.** The biosynthesis characteristics of TTP and TNF can be regulated through a posttranscriptional molecular loop. *J.Biol.Chem.* **286:** 3767-3776.
- Asselin-Labat ML, David M, Biola-Vidamment A, Lecoeuche D, Zennaro MC, Bertoglio J, Pallardy M. 2004.** GILZ, a new target for the transcription factor FoxO3, protects T lymphocytes from interleukin-2 withdrawal-induced apoptosis. *Blood* **104:** 215-223.
- Ayroldi E, Macchiarulo A, Riccardi C. 2014.** Targeting glucocorticoid side effects: selective glucocorticoid receptor modulator or glucocorticoid-induced leucine zipper? A perspective. *FASEB J.*
- Ayroldi E, Migliorati G, Bruscoli S, Marchetti C, Zollo O, Cannarile L, D'Adamio F, Riccardi C. 2001.** Modulation of T-cell activation by the glucocorticoid-induced leucine zipper factor via inhibition of nuclear factor kappaB. *Blood* **98:** 743-753.
- Ayroldi E, Riccardi C. 2009.** Glucocorticoid-induced leucine zipper (GILZ): a new important mediator of glucocorticoid action. *FASEB J.* **23:** 3649-3658.
- Ayroldi E, Zollo O, Macchiarulo A, Di MB, Marchetti C, Riccardi C. 2002.** Glucocorticoid-induced leucine zipper inhibits the Raf-extracellular signal-regulated kinase pathway by binding to Raf-1. *Mol.Cell Biol.* **22:** 7929-7941.
- Balakathiresan NS, Bhattacharyya S, Gutti U, Long RP, Jozwik C, Huang W, Srivastava M, Pollard HB, Biswas R. 2009a.** Tristetraprolin regulates IL-8 mRNA stability in cystic fibrosis lung epithelial cells. *Am.J.Physiol Lung Cell Mol.Physiol* **296:** L1012-L1018.
- Beaulieu E, Ngo D, Santos L, Yang YH, Smith M, Jorgensen C, Escriou V, Scherman D, Courties G, Apparailly F, Morand EF. 2010.** Glucocorticoid-induced leucine zipper is an endogenous antiinflammatory mediator in arthritis. *Arthritis Rheum.* **62:** 2651-2661.
- Bergman D, Halje M, Nordin M, Engstrom W. 2013.** Insulin-like growth factor 2 in development and disease: a mini-review. *Gerontology* **59:** 240-249.

- Berrebi D, Bruscoli S, Cohen N, Foussat A, Migliorati G, Bouchet-Delbos L, Maillot MC, Portier A, Couderc J, Galanaud P, Peuchmaur M, Riccardi C, Emilie D. 2003.** Synthesis of glucocorticoid-induced leucine zipper (GILZ) by macrophages: an anti-inflammatory and immunosuppressive mechanism shared by glucocorticoids and IL-10. *Blood* **101**: 729-738.
- Blackshear PJ. 2002.** Tristetraprolin and other CCCH tandem zinc-finger proteins in the regulation of mRNA turnover. *Biochem.Soc.Trans.* **30**: 945-952.
- Blumenthal SB, Kiemer AK, Tiegs G, Seyfried S, Holtje M, Brandt B, Holtje HD, Zahler S, Vollmar AM. 2005.** Metalloporphyrins inactivate caspase-3 and -8. *FASEB J.* **19**: 1272-1279.
- Boon RA, Horrevoets AJ. 2009b.** Key transcriptional regulators of the vasoprotective effects of shear stress. *Hamostaseologie*. **29**: 39-3.
- Bordenave L. 2014.** The Gene Expression of Human Endothelial Cells Is Modulated by Subendothelial Extracellular Matrix Proteins: Short-Term Response to Laminar Shear Stress. *Tissue Eng Part A*.
- Brook M, Tchen CR, Santalucia T, McIlrath J, Arthur JS, Saklatvala J, Clark AR. 2006.** Posttranslational regulation of tristetraprolin subcellular localization and protein stability by p38 mitogen-activated protein kinase and extracellular signal-regulated kinase pathways. *Mol.Cell Biol.* **26**: 2408-2418.
- Brown TD. 2000.** Techniques for mechanical stimulation of cells in vitro: a review. *J.Biomech.* **33**: 3-14.
- Cannarile L, Cuzzocrea S, Santucci L, Agostini M, Mazzon E, Esposito E, Muia C, Coppo M, Di PR, Riccardi C. 2009.** Glucocorticoid-induced leucine zipper is protective in Th1-mediated models of colitis. *Gastroenterology* **136**: 530-541.
- Cannarile L, Zollo O, D'Adamio F, Ayroldi E, Marchetti C, Tabilio A, Bruscoli S, Riccardi C. 2001.** Cloning, chromosomal assignment and tissue distribution of human GILZ, a glucocorticoid hormone-induced gene. *Cell Death.Differ.* **8**: 201-203.
- Cao W, Bao C, Padalko E, Lowenstein CJ. 2008.** Acetylation of mitogen-activated protein kinase phosphatase-1 inhibits Toll-like receptor signaling. *J.Exp.Med.* **205**: 1491-1503.
- Carballo E, Lai WS, Blackshear PJ. 1998.** Feedback inhibition of macrophage tumor necrosis factor-alpha production by tristetraprolin. *Science* **281**: 1001-1005.
- Chappell DC, Varner SE, Nerem RM, Medford RM, Alexander RW. 1998b.** Oscillatory shear stress stimulates adhesion molecule expression in cultured human endothelium. *Circ.Res.* **82**: 532-539.
- Charles CH, Abler AS, Lau LF. 1992.** cDNA sequence of a growth factor-inducible immediate early gene and characterization of its encoded protein. *Oncogene* **7**: 187-190.

- Chen FM, Chang HW, Yang SF, Huang YF, Nien PY, Yeh YT, Hou MF.** 2012a. The mitogen-activated protein kinase phosphatase-1 (MKP-1) gene is a potential methylation biomarker for malignancy of breast cancer. *Exp.Mol.Med.* **44:** 356-362.
- Chen K, Fan W, Wang X, Ke X, Wu G, Hu C.** 2012b. MicroRNA-101 mediates the suppressive effect of laminar shear stress on mTOR expression in vascular endothelial cells. *Biochem.Biophys.Res.Commun.* **427:** 138-142.
- Chen LJ, Wei SY, Chiu JJ.** 2013. Mechanical regulation of epigenetics in vascular biology and pathobiology. *J.Cell Mol.Med.* **17:** 437-448.
- Chen RJ, Yuan HH, Zhang TY, Wang ZZ, Hu AK, Wu LL, Yang ZP, Mao YJ, Ji DJ, Zhu XR.** 2014. Heme Oxygenase-2 Suppress TNF-alpha and IL6 Expression via TLR4/MyD88-Dependent Signaling Pathway in Mouse Cerebral Vascular Endothelial Cells. *Mol.Neurobiol.*
- Chen X, Wei Z, Wang W, Yan R, Xu X, Cai Q.** 2012c. Role of RNA-binding protein tristetraprolin in tumor necrosis factor-alpha mediated gene expression. *Biochem.Biophys.Res.Commun.* **428:** 327-332.
- Chen XL, Varner SE, Rao AS, Grey JY, Thomas S, Cook CK, Wasserman MA, Medford RM, Jaiswal AK, Kunsch C.** 2003. Laminar flow induction of antioxidant response element-mediated genes in endothelial cells. A novel anti-inflammatory mechanism. *J.Biol.Chem.* **278:** 703-711.
- Chen Z, Gibson TB, Robinson F, Silvestro L, Pearson G, Xu B, Wright A, Vandebilt C, Cobb MH.** 2001. MAP kinases. *Chem.Rev.* **101:** 2449-2476.
- Cheng C, Tempel D, van HR, de Boer HC, Segers D, Huisman M, van Zonneveld AJ, Leenen PJ, van der SA, Serruys PW, de CR, Krams R.** 2007. Shear stress-induced changes in atherosclerotic plaque composition are modulated by chemokines. *J.Clin.Invest* **117:** 616-626.
- Cheng M, Li Y, Chen H, Nie Y, Zhang Y, Liu X.** 2005. [Effect of ERK1/2 on low shear stress-induced expression of IL-8 mRNA in human endothelial cells]. *Sheng Wu Yi.Xue.Gong Xue.Za Zhi.* **22:** 230-234.
- Cheng M, Wu J, Li Y, Nie Y, Chen H.** 2008. Activation of MAPK participates in low shear stress-induced IL-8 gene expression in endothelial cells. *Clin.Biomech.(Bristol., Avon.)* **23 Suppl 1:** S96-S103.
- Cheng Q, Fan H, Ngo D, Beaulieu E, Leung P, Lo CY, Burgess R, van der Zwan YG, White SJ, Khachigian LM, Hickey MJ, Morand EF.** 2013. GILZ Overexpression Inhibits Endothelial Cell Adhesive Function through Regulation of NF-kappaB and MAPK Activity. *J.Immunol.* **191:** 424-433.
- Chinenov Y, Coppo M, Gupte R, Sacta MA, Rogatsky I.** 2014. Glucocorticoid receptor coordinates transcription factor-dominated regulatory network in macrophages. *BMC.Genomics* **15:** 656.
- Chiu JJ, Lee PL, Chen CN, Lee CI, Chang SF, Chen LJ, Lien SC, Ko YC, Usami S, Chien S.** 2004. Shear stress increases ICAM-1 and decreases VCAM-1 and E-

- selectin expressions induced by tumor necrosis factor-[alpha] in endothelial cells. *Arterioscler.Thromb.Vasc.Biol.* **24**: 73-79.
- Chlupac J, Filova E, Havlikova J, Matejka R, Riedel T, Houska M, Brynda E, Pamula E, Remy M, Bareille R, Fernandez P, Daculsi R, Bourget C, Bacakova L,**
- Cho IJ, Woo NR, Kim SG. 2008.** The identification of C/EBPbeta as a transcription factor necessary for the induction of MAPK phosphatase-1 by toll-like receptor-4 ligand. *Arch.Biochem.Biophys.* **479**: 88-96.
- Chomczynski P, Sacchi N. 1987.** Single-step method of RNA isolation by acid guanidinium thiocyanate-phenol-chloroform extraction. *Anal.Biochem.* **162**: 156-159.
- Chyu KY, Shah PK. 2014.** Can we vaccinate against atherosclerosis? *J.Cardiovasc.Pharmacol.Ther.* **19**: 77-82.
- Ciafre SA, Galardi S. 2013.** microRNAs and RNA-binding proteins: a complex network of interactions and reciprocal regulations in cancer. *RNA.Biol.* **10**: 935-942.
- Cicha I, Beronov K, Ramirez EL, Osterode K, Goppelt-Struebe M, Raaz D, Yilmaz A, Daniel WG, Garlichs CD. 2009.** Shear stress preconditioning modulates endothelial susceptibility to circulating TNF-alpha and monocytic cell recruitment in a simplified model of arterial bifurcations. *Atherosclerosis* **207**: 93-102.
- Cicha I, Goppelt-Struebe M, Yilmaz A, Daniel WG, Garlichs CD. 2008.** Endothelial dysfunction and monocyte recruitment in cells exposed to non-uniform shear stress. *Clin.Hemorheol.Microcirc.* **39**: 113-119.
- Clark AR, Dean JL, Saklatvala J. 2003.** Post-transcriptional regulation of gene expression by mitogen-activated protein kinase p38. *FEBS Lett.* **546**: 37-44.
- Cohen N, Mouly E, Hamdi H, Maillot MC, Pallardy M, Godot V, Capel F, Balian A, Naveau S, Galanaud P, Lemoine FM, Emilie D. 2006.** GILZ expression in human dendritic cells redirects their maturation and prevents antigen-specific T lymphocyte response. *Blood* **107**: 2037-2044.
- Cox JL, Chiasson DA, Gotlieb AI. 1991.** Stranger in a strange land: the pathogenesis of saphenous vein graft stenosis with emphasis on structural and functional differences between veins and arteries. *Prog.Cardiovasc.Dis.* **34**: 45-68.
- Cuadrado A, Nebreda AR. 2010.** Mechanisms and functions of p38 MAPK signalling. *Biochem.J.* **429**: 403-417.
- Cunningham KS, Gotlieb AI. 2005.** The role of shear stress in the pathogenesis of atherosclerosis. *Lab Invest* **85**: 9-23.
- D'Adamio F, Zollo O, Moraca R, Ayroldi E, Bruscoli S, Bartoli A, Cannarile L, Migliorati G, Riccardi C. 1997.** A new dexamethasone-induced gene of the leucine zipper family protects T lymphocytes from TCR/CD3-activated cell death. *Immunity* **7**: 803-812.
- Dai G, Vaughn S, Zhang Y, Wang ET, Garcia-Cardena G, Gimbrone MA, Jr. 2007.** Biomechanical forces in atherosclerosis-resistant vascular regions regulate

endothelial redox balance via phosphoinositol 3-kinase/Akt-dependent activation of Nrf2. *Circ.Res.* **101**: 723-733.

Davies PF. 1995. Flow-mediated endothelial mechanotransduction. *Physiol Rev.* **75**: 519-560.

Davies PF. 2009. Hemodynamic shear stress and the endothelium in cardiovascular pathophysiology. *Nat.Clin Pract Cardiovasc Med.* **6**: 16-26.

Davies PF, Barbee KA, Volin MV, Robotewskyj A, Chen J, Joseph L, Griem ML, Wernick MN, Jacobs E, Polacek DC, DePaola N, Barakat AI. 1997. Spatial relationships in early signaling events of flow-mediated endothelial mechanotransduction. *Annu.Rev.Physiol* **59**: 527-549.

Davis ME, Grumbach IM, Fukai T, Cutchins A, Harrison DG. 2004. Shear stress regulates endothelial nitric-oxide synthase promoter activity through nuclear factor kappaB binding. *J.Biol.Chem.* **279**: 163-168.

De Keulenaer GW, Chappell DC, Ishizaka N, Nerem RM, Alexander RW, Griendling KK. 1998. Oscillatory and steady laminar shear stress differentially affect human endothelial redox state: role of a superoxide-producing NADH oxidase. *Circ.Res.* **82**: 1094-1101.

Delfino DV, Agostini M, Spinicelli S, Vito P, Riccardi C. 2004. Decrease of Bcl-xL and augmentation of thymocyte apoptosis in GILZ overexpressing transgenic mice. *Blood* **104**: 4134-4141.

Dewey CF, Jr., Bussolari SR, Gimbrone MA, Jr., Davies PF. 1981. The dynamic response of vascular endothelial cells to fluid shear stress. *J.Bioeng.* **103**: 177-185.

Di Marco B, Massetti M, Bruscoli S, Macchiarulo A, Di VR, Velardi E, Donato V, Migliorati G, Riccardi C. 2007. Glucocorticoid-induced leucine zipper (GILZ)/NF-kappaB interaction: role of GILZ homo-dimerization and C-terminal domain. *Nucleic Acids Res.* **35**: 517-528.

Diesel B, Ripoche N, Risch RT, Tierling S, Walter J, Kiemer AK. 2012. Inflammation-induced up-regulation of TLR2 expression in human endothelial cells is independent of differential methylation in the TLR2 promoter CpG island. *Innate Immun.* **18**: 112-123.

Dimmeler S, Fleming I, Fisslthaler B, Hermann C, Busse R, Zeiher AM. 1999. Activation of nitric oxide synthase in endothelial cells by Akt-dependent phosphorylation. *Nature* **399**: 601-605.

Dolan JM, Kolega J, Meng H. 2013. High wall shear stress and spatial gradients in vascular pathology: a review. *Ann.Bioeng.* **41**: 1411-1427.

Dunn J, Qiu H, Kim S, Jjingo D, Hoffman R, Kim CW, Jang I, Son DJ, Kim D, Pan C, Fan Y, Jordan IK, Jo H. 2014. Flow-dependent epigenetic DNA methylation regulates endothelial gene expression and atherosclerosis. *J.Clin.Invest* **124**: 3187-3199.

- Dunzendorfer S, Lee HK, Tobias PS.** 2004. Flow-dependent regulation of endothelial Toll-like receptor 2 expression through inhibition of SP1 activity. *Circ.Res.* **95:** 684-691.
- Eades LE, Thiagarajah AS, Harris J, Jones SA, Morand EF, Leech M.** 2014. GILZ: a new link between the hypothalamic pituitary adrenal axis and rheumatoid arthritis? *Immunol.Cell Biol.*
- Eddleston J, Herschbach J, Wagelie-Steffen AL, Christiansen SC, Zuraw BL.** 2007a. The anti-inflammatory effect of glucocorticoids is mediated by glucocorticoid-induced leucine zipper in epithelial cells. *J.Allergy Clin.Immunol.* **119:** 115-122.
- Edfeldt K, Swedenborg J, Hansson GK, Yan ZQ.** 2002. Expression of toll-like receptors in human atherosclerotic lesions: a possible pathway for plaque activation. *Circulation* **105:** 1158-1161.
- Emmons J, Townley-Tilson WH, Deleault KM, Skinner SJ, Gross RH, Whitfield ML, Brooks SA.** 2008. Identification of TTP mRNA targets in human dendritic cells reveals TTP as a critical regulator of dendritic cell maturation. *RNA* **14:** 888-902.
- Engstrom W, Shokrai A, Otte K, Granerus M, Gessbo A, Bierke P, Madej A, Sjolund M, Ward A.** 1998. Transcriptional regulation and biological significance of the insulin like growth factor II gene. *Cell Prolif.* **31:** 173-189.
- Estrada R, Giridharan GA, Nguyen MD, Prabhu SD, Sethu P.** 2011. Microfluidic endothelial cell culture model to replicate disturbed flow conditions seen in atherosclerosis susceptible regions. *Biomicrofluidics* **5:** 32006-3200611.
- Fan H, Kao W, Yang YH, Gu R, Harris J, Fingerle-Rowson G, Bucala R, Ngo D, Beaulieu E, Morand EF.** 2014. Macrophage Migration Inhibitory Factor Inhibits the Antiinflammatory Effects of Glucocorticoids via Glucocorticoid-Induced Leucine Zipper. *Arthritis Rheumatol.* **66:** 2059-2070.
- Fan H, Morand EF.** 2012. Targeting the side effects of steroid therapy in autoimmune diseases: the role of GILZ. *Discov.Med.* **13:** 123-133.
- Fang Y, Shi C, Manduchi E, Civelek M, Davies PF.** 2010. MicroRNA-10a regulation of proinflammatory phenotype in athero-susceptible endothelium in vivo and in vitro. *Proc.Natl.Acad.Sci.U.S.A* **107:** 13450-13455.
- Fechir M, Linker K, Pautz A, Hubrich T, Forstermann U, Rodriguez-Pascual F, Kleinert H.** 2005. Tristetraprolin regulates the expression of the human inducible nitric-oxide synthase gene. *Mol.Pharmacol.* **67:** 2148-2161.
- Feil R, Khosla S.** 1999. Genomic imprinting in mammals: an interplay between chromatin and DNA methylation? *Trends Genet.* **15:** 431-435.
- Frangos JA, McIntire LV, Eskin SG.** 1988. Shear stress induced stimulation of mammalian cell metabolism. *Biotechnol.Bioeng.* **32:** 1053-1060.
- Frohlich J, Al-Sarraf A.** 2013. Cardiovascular risk and atherosclerosis prevention. *Cardiovasc.Pathol.* **22:** 16-18.

- Frueh J, Maimari N, Homma T, Bovens SM, Pedrigi RM, Towhidi L, Krams R.** 2013. Systems biology of the functional and dysfunctional endothelium. *Cardiovasc.Res.* **99:** 334-341.
- Fürst R, Brueckl C, Kuebler WM, Zahler S, Krotz F, Gorlach A, Vollmar AM, Kiemer AK.** 2005. Atrial natriuretic peptide induces mitogen-activated protein kinase phosphatase-1 in human endothelial cells via Rac1 and NAD(P)H oxidase/Nox2-activation. *Circ.Res.* **96:** 43-53.
- Fürst R, Schroeder T, Eilken HM, Bubik MF, Kiemer AK, Zahler S, Vollmar AM.** 2007. MAPK phosphatase-1 represents a novel anti-inflammatory target of glucocorticoids in the human endothelium. *FASEB J.* **21:** 74-80.
- Gabory A, Ripoche MA, Yoshimizu T, Dandolo L.** 2006. The H19 gene: regulation and function of a non-coding RNA. *Cytogenet.Genome Res.* **113:** 188-193.
- Gao Y, Liu F, Fang L, Cai R, Zong C, Qi Y.** 2014. Genkwanin inhibits proinflammatory mediators mainly through the regulation of miR-101/MKP-1/MAPK pathway in LPS-activated macrophages. *PLoS.One.* **9:** e96741.
- Gao ZH, Suppola S, Liu J, Heikkila P, Janne J, Voutilainen R.** 2002. Association of H19 promoter methylation with the expression of H19 and IGF-II genes in adrenocortical tumors. *J.Clin.Endocrinol.Metab* **87:** 1170-1176.
- Gareus R, Kotsaki E, Xanthoulea S, van dM, I, Gijbels MJ, Kardakaris R, Polykratis A, Kollias G, de Winther MP, Pasparakis M.** 2008. Endothelial cell-specific NF-kappaB inhibition protects mice from atherosclerosis. *Cell Metab* **8:** 372-383.
- Gauci I, Luong L, Mahmoud M, Duckles H, Hsiao S, DeLuca A, Evans P.** 2014. 192 The induction of homeobox genes by disturbed flow limits inflammation at atherosusceptible sites. *Heart* **100 Suppl 3:** A106-A107.
- George AD, Tenenbaum SA.** 2006. MicroRNA modulation of RNA-binding protein regulatory elements. *RNA.Biol.* **3:** 57-59.
- Gerszten RE, Garcia-Zepeda EA, Lim YC, Yoshida M, Ding HA, Gimbrone MA, Jr., Luster AD, Luscinskas FW, Rosenzweig A.** 1999. MCP-1 and IL-8 trigger firm adhesion of monocytes to vascular endothelium under flow conditions. *Nature* **398:** 718-723.
- Giannoukakis N, Deal C, Paquette J, Goodyer CG, Polychronakos C.** 1993. Parental genomic imprinting of the human IGF2 gene. *Nat.Genet.* **4:** 98-101.
- Gimbrone MA, Jr., Garcia-Cardena G.** 2013. Vascular endothelium, hemodynamics, and the pathobiology of atherosclerosis. *Cardiovasc.Pathol.* **22:** 9-15.
- Glynne R, Ghandour G, Rayner J, Mack DH, Goodnow CC.** 2000. B-lymphocyte quiescence, tolerance and activation as viewed by global gene expression profiling on microarrays. *Immunol.Rev.* **176:** 216-246.
- Go AS, Mozaffarian D, Roger VL, Benjamin EJ, Berry JD, Blaha MJ, Dai S, Ford ES, Fox CS, Franco S, Fullerton HJ, Gillespie C, Hailpern SM, Heit JA, Howard VJ, Huffman MD, Judd SE, Kissela BM, Kittner SJ, Lackland DT, Lichtman JH,**

- Lisabeth LD, Mackey RH, Magid DJ, Marcus GM, Marelli A, Matchar DB, McGuire DK, Mohler ER, III, Moy CS, Mussolino ME, Neumar RW, Nichol G, Pandey DK, Paynter NP, Reeves MJ, Sorlie PD, Stein J, Towfighi A, Turan TN, Virani SS, Wong ND, Woo D, Turner MB.** 2013. Heart Disease and Stroke Statistics--2014 Update: A Report From the American Heart Association. *Circulation*.
- Godot V, Garcia G, Capel F, Arock M, Durand-Gasselin I, sselin-Labat ML, Emiliie D, Humbert M.** 2006. Dexamethasone and IL-10 stimulate glucocorticoid-induced leucine zipper synthesis by human mast cells. *Allergy* **61**: 886-890.
- Hachenthal N, Stadter T, Leidinger P, Grässer F, Meese E, Bruscoli S, Riccardi C, Kiemer AK, and Hoppstädter J.** (2013). Mechanisms of MyD88- and TRIF-dependent downregulation of the glucocorticoid induced leucine zipper (GILZ) in macrophages – mRNA destabilization vs. microRNAs. *Front. Immunol.* Conference Abstract: 15th International Congress of Immunology (ICI)
- Hahn RT, Hoppstadter J, Hirschfelder K, Hachenthal N, Diesel B, Kessler SM, Huwer H, Kiemer AK.** 2014. Downregulation of the glucocorticoid-induced leucine zipper (GILZ) promotes vascular inflammation. *Atherosclerosis* **234**: 391-400.
- Hale KK, Trollinger D, Rihanek M, Manthey CL.** 1999. Differential expression and activation of p38 mitogen-activated protein kinase alpha, beta, gamma, and delta in inflammatory cell lineages. *J.Immunol.* **162**: 4246-4252.
- Hamby RI, Aintablian A, Handler M, Voleti C, Weisz D, Garvey JW, Wisoff G.** 1979. Aortocoronary saphenous vein bypass grafts. Long-term patency, morphology and blood flow in patients with patent grafts early after surgery. *Circulation* **60**: 901-909.
- Hamby RI, Aintablian A, Wisoff BG, Hartstein ML.** 1977. Comparative study of the postoperative flow in the saphenous vein and internal mammary artery bypass grafts. *Am.Heart J.* **93**: 306-315.
- Hammaker D, Boyle DL, Topolewski K, Firestein GS.** 2014. Differential regulation of anti-inflammatory genes by p38 MAP kinase and MAP kinase kinase 6. *J.Inflamm.(Lond)* **11**: 14.
- Han DK, Khaing ZZ, Pollock RA, Haudenschild CC, Liau G.** 1996. H19, a marker of developmental transition, is reexpressed in human atherosclerotic plaques and is regulated by the insulin family of growth factors in cultured rabbit smooth muscle cells. *J.Clin.Invest* **97**: 1276-1285.
- Han Z, Varadharaj S, Giedt RJ, Zweier JL, Szeto HH, Alevriadou BR.** 2009. Mitochondria-derived reactive oxygen species mediate heme oxygenase-1 expression in sheared endothelial cells. *J.Pharmacol.Exp.Ther.* **329**: 94-101.
- Hansson GK, Nilsson J.** 2009. Vaccination against atherosclerosis? Induction of atheroprotective immunity. *Semin.Immunopathol.* **31**: 95-101.
- Harris TA, Yamakuchi M, Ferlito M, Mendell JT, Lowenstein CJ.** 2008. MicroRNA-126 regulates endothelial expression of vascular cell adhesion molecule 1. *Proc.Natl.Acad.Sci.U.S.A* **105**: 1516-1521.

- Hastings NE, Simmers MB, McDonald OG, Wamhoff BR, Blackman BR.** 2007. Atherosclerosis-prone hemodynamics differentially regulates endothelial and smooth muscle cell phenotypes and promotes pro-inflammatory priming. *Am.J.Physiol Cell Physiol* **293**: C1824-C1833.
- Hayden MS, Ghosh S.** 2004. Signaling to NF-kappaB. *Genes Dev.* **18**: 2195-2224.
- Hayden MS, Ghosh S.** 2008. Shared principles in NF-kappaB signaling. *Cell* **132**: 344-362.
- Hergenreider E, Heydt S, Treguer K, Boettger T, Horrevoets AJ, Zeiher AM, Scheffer MP, Frangakis AS, Yin X, Mayr M, Braun T, Urbich C, Boon RA, Dommeler S.** 2012. Atheroprotective communication between endothelial cells and smooth muscle cells through miRNAs. *Nat.Cell Biol.* **14**: 249-256.
- Herlaar E, Brown Z.** 1999. p38 MAPK signalling cascades in inflammatory disease. *Mol.Med.Today* **5**: 439-447.
- Hierck BP, Van der HK, Alkemade FE, Van de PS, Van Thienen JV, Groenendijk BC, Bax WH, Van der LA, Deruiter MC, Horrevoets AJ, Poelmann RE.** 2008. Primary cilia sensitize endothelial cells for fluid shear stress. *Dev.Dyn.* **237**: 725-735.
- Himburg HA, Grzybowski DM, Hazel AL, LaMack JA, Li XM, Friedman MH.** 2004. Spatial comparison between wall shear stress measures and porcine arterial endothelial permeability. *Am.J.Physiol Heart Circ.Physiol* **286**: H1916-H1922.
- Hoffmann A, Levchenko A, Scott ML, Baltimore D.** 2002. The IkappaB-NF-kappaB signaling module: temporal control and selective gene activation. *Science* **298**: 1241-1245.
- Holliday CJ, Ankeny RF, Jo H, Nerem RM.** 2011. Discovery of shear- and side-specific mRNAs and miRNAs in human aortic valvular endothelial cells. *Am.J.Physiol Heart Circ.Physiol* **301**: H856-H867.
- Hoppstädter J, Diesel B, Eifler LK, Schmidt T, Brüne B, Kiemer AK.** 2012. Glucocorticoid-Induced Leucine Zipper is downregulated in human alveolar macrophages upon Toll-like receptor activation. *Eur.J.Immunol.* **42**: 1-13.
- Hoppstädter J, Kessler SM, Bruscoli S, Huwer H, Riccardi C, Kiemer AK.** 2015, Glucocorticoid-induced leucine zipper (GILZ): a critical factor in macrophage endotoxin tolerance, *in press*
- Houston P, White BP, Campbell CJ, Braddock M.** 1999. Delivery and expression of fluid shear stress-inducible promoters to the vessel wall: applications for cardiovascular gene therapy. *Hum.Gene Ther.* **10**: 3031-3044.
- Huotari N, Hommo T, Taimi V, Nieminen R, Moilanen E, Korhonen R.** 2012. Regulation of tristetraprolin expression by mitogen-activated protein kinase phosphatase-1. *APMIS* **120**: 988-999.
- Imaizumi S, Grijalva V, Priceman S, Wu L, Su F, Farias-Eisner R, Hama S, Navab M, Fogelman AM, Reddy ST.** 2010. Mitogen-activated protein kinase phosphatase-1

deficiency decreases atherosclerosis in apolipoprotein E null mice by reducing monocyte chemoattractant protein-1 levels. *Mol.Genet.Metab* **101**: 66-75.

Immenschuh S, Ramadori G. 2000. Gene regulation of heme oxygenase-1 as a therapeutic target. *Biochem.Pharmacol.* **60**: 1121-1128.

Ishibazawa A, Nagaoka T, Yokota H, Ono S, Yoshida A. 2013. Low shear stress up-regulation of proinflammatory gene expression in human retinal microvascular endothelial cells. *Exp.Eye Res.* **116**: 308-311.

Jaffe EA, Nachman RL, Becker CG, Minick CR. 1973. Culture of human endothelial cells derived from umbilical veins. Identification by morphologic and immunologic criteria. *J.Clin.Invest* **52**: 2745-2756.

Jalonen U, Lahti A, Korhonen R, Kankaanranta H, Moilanen E. 2005. Inhibition of tristetraprolin expression by dexamethasone in activated macrophages. *Biochem.Pharmacol.* **69**: 733-740.

Jashari F, Ibrahimi P, Nicoll R, Bajraktari G, Wester P, Henein MY. 2013. Coronary and carotid atherosclerosis: similarities and differences. *Atherosclerosis* **227**: 193-200.

Jeong Y, Du R, Zhu X, Yin S, Wang J, Cui H, Cao W, Lowenstein CJ. 2014. Histone deacetylase isoforms regulate innate immune responses by deacetylating mitogen-activated protein kinase phosphatase-1. *J.Leukoc.Biol.* **95**: 651-659.

Ji JY, Jing H, Diamond SL. 2003. Shear stress causes nuclear localization of endothelial glucocorticoid receptor and expression from the GRE promoter. *Circ.Res.* **92**: 279-285.

Jin Y, Pang T, Nelin LD, Wang W, Wang Y, Yan J, Zhao C. 2014. MKP-1 is a target of miR-210 and mediate the negative regulation of miR-210 inhibitor on hypoxic hPASMC proliferation. *Cell Biol.Int.*

Jirik FR, Podor TJ, Hirano T, Kishimoto T, Loskutoff DJ, Carson DA, Lotz M. 1989. Bacterial lipopolysaccharide and inflammatory mediators augment IL-6 secretion by human endothelial cells. *J.Immunol.* **142**: 144-147.

Karaki S, Garcia G, Tcherakian C, Capel F, Tran T, Pallardy M, Humbert M, Emilie D, Godot V. 2014. Enhanced glucocorticoid-induced leucine zipper in dendritic cells induces allergen-specific regulatory CD4(+) T-cells in respiratory allergies. *Allergy* **69**: 624-631.

Karper JC, de Vries MR, van den Brand BT, Hoefer IE, Fischer JW, Jukema JW, Niessen HW, Quax PH. 2011. Toll-like receptor 4 is involved in human and mouse vein graft remodeling, and local gene silencing reduces vein graft disease in hypercholesterolemic APOE*3Leiden mice. *Arterioscler.Thromb.Vasc.Biol.* **31**: 1033-1040.

Kessler SM, Pokorny J, Zimmer V, Laggai S, Lammert F, Bohle RM, Kiemer AK. 2013. IGF2 mRNA binding protein p62/IMP2-2 in hepatocellular carcinoma: antiapoptotic action is independent of IGF2/PI3K signaling. *Am.J.Physiol Gastrointest.Liver Physiol* **304**: G328-G336.

- Kester HA, Blanchetot C, den HJ, van der Saag PT, van der BB. 1999.** Transforming growth factor-beta-stimulated clone-22 is a member of a family of leucine zipper proteins that can homo- and heterodimerize and has transcriptional repressor activity. *J.Biol.Chem.* **274:** 27439-27447.
- Keyse SM. 2000.** Protein phosphatases and the regulation of mitogen-activated protein kinase signalling. *Curr.Opin.Cell Biol.* **12:** 186-192.
- Kiemer AK, Bildner N, Weber NC, Vollmar AM. 2003a.** Characterization of heme oxygenase 1 (heat shock protein 32) induction by atrial natriuretic peptide in human endothelial cells. *Endocrinology* **144:** 802-812.
- Kiemer AK, Gerwig T, Gerbes AL, Meissner H, Bilzer M, Vollmar AM. 2003b.** Kupffer-cell specific induction of heme oxygenase 1 (hsp32) by the atrial natriuretic peptide--role of cGMP. *J.Hepatol.* **38:** 490-498.
- Kiemer AK, Weber NC, Furst R, Bildner N, Kulhanek-Heinze S, Vollmar AM. 2002a.** Inhibition of p38 MAPK activation via induction of MKP-1: atrial natriuretic peptide reduces TNF-alpha-induced actin polymerization and endothelial permeability. *Circ.Res.* **90:** 874-881.
- Kiemer AK, Weber NC, Vollmar AM. 2002b.** Induction of IkappaB: atrial natriuretic peptide as a regulator of the NF-kappaB pathway. *Biochem.Biophys.Res.Commun.* **295:** 1068-1076.
- Kim HS, Ullevig SL, Zamora D, Lee CF, Asmis R. 2012.** Redox regulation of MAPK phosphatase 1 controls monocyte migration and macrophage recruitment. *Proc.Natl.Acad.Sci.U.S.A* **109:** E2803-E2812.
- Kolbus A, Blazquez-Domingo M, Carotta S, Bakker W, Luedemann S, von LM, Steinlein P, Beug H. 2003.** Cooperative signaling between cytokine receptors and the glucocorticoid receptor in the expansion of erythroid progenitors: molecular analysis by expression profiling. *Blood* **102:** 3136-3146.
- Kouzarides T. 2007.** Chromatin modifications and their function. *Cell* **128:** 693-705.
- Kubista M, Andrade JM, Bengtsson M, Forootan A, Jonak J, Lind K, Sindelka R, Sjöback R, Sjogreen B, Strombom L, Stahlberg A, Zoric N. 2006.** The real-time polymerase chain reaction. *Mol.Aspects Med.* **27:** 95-125.
- Kumar S, McDonnell PC, Gum RJ, Hand AT, Lee JC, Young PR. 1997.** Novel homologues of CSBP/p38 MAP kinase: activation, substrate specificity and sensitivity to inhibition by pyridinyl imidazoles. *Biochem.Biophys.Res.Commun.* **235:** 533-538.
- Kutty RS, Nair SK. 2008,** Surgery for coronary artery disease, *Surgery*, **26**, 501-509
- Kuwano Y, Kim HH, Abdelmohsen K, Pullmann R, Jr., Martindale JL, Yang X, Gorospe M. 2008.** MKP-1 mRNA stabilization and translational control by RNA-binding proteins HuR and NF90. *Mol.Cell Biol.* **28:** 4562-4575.
- Lai WS, Carballo E, Strum JR, Kennington EA, Phillips RS, Blackshear PJ. 1999.** Evidence that tristetraprolin binds to AU-rich elements and promotes the

- deadenylation and destabilization of tumor necrosis factor alpha mRNA. *Mol.Cell Biol.* **19**: 4311-4323.
- Lai WS, Parker JS, Grissom SF, Stumpo DJ, Blackshear PJ. 2006.** Novel mRNA targets for tristetraprolin (TTP) identified by global analysis of stabilized transcripts in TTP-deficient fibroblasts. *Mol.Cell Biol.* **26**: 9196-9208.
- LaMack JA, Himborg HA, Li XM, Friedman MH. 2005.** Interaction of wall shear stress magnitude and gradient in the prediction of arterial macromolecular permeability. *Ann.Biomed.Eng* **33**: 457-464.
- Lawan A, Shi H, Gatzke F, Bennett AM. 2013.** Diversity and specificity of the mitogen-activated protein kinase phosphatase-1 functions. *Cell Mol.Life Sci.* **70**: 223-237.
- Lee TS, Chau LY. 2002.** Heme oxygenase-1 mediates the anti-inflammatory effect of interleukin-10 in mice. *Nat.Med.* **8**: 240-246.
- Leighton PA, Saam JR, Ingram RS, Stewart CL, Tilghman SM. 1995.** An enhancer deletion affects both H19 and Igf2 expression. *Genes Dev.* **9**: 2079-2089.
- Li L, Xie J, Zhang M, Wang S. 2009.** Homocysteine harasses the imprinting expression of IGF2 and H19 by demethylation of differentially methylated region between IGF2/H19 genes. *Acta Biochim.Biophys.Sin.(Shanghai)* **41**: 464-471.
- Libby P, Ridker PM, Hansson GK. 2011.** Progress and challenges in translating the biology of atherosclerosis. *Nature* **473**: 317-325.
- Libert C, Dejager L. 2014.** How steroids steer T cells. *Cell Rep.* **7**: 938-939.
- Lin WL, He XB, Svensson K, Adam G, Li YM, Tang TW, Paldi A, Pfeifer S, Ohlsson R. 1999.** The genotype and epigenotype synergize to diversify the spatial pattern of expression of the imprinted H19 gene. *Mech.Dev.* **82**: 195-197.
- Lin YW, Chuang SM, Yang JL. 2003.** ERK1/2 achieves sustained activation by stimulating MAPK phosphatase-1 degradation via the ubiquitin-proteasome pathway. *J.Biol.Chem.* **278**: 21534-21541.
- Liu Y, Gorospe M, Yang C, Holbrook NJ. 1995.** Role of mitogen-activated protein kinase phosphatase during the cellular response to genotoxic stress. Inhibition of c-Jun N-terminal kinase activity and AP-1-dependent gene activation. *J.Biol.Chem.* **270**: 8377-8380.
- Liu Y, Zhang Y, Schmelzer K, Lee TS, Fang X, Zhu Y, Spector AA, Gill S, Morisseau C, Hammock BD, Shyy JY. 2005.** The antiinflammatory effect of laminar flow: the role of PPARgamma, epoxyeicosatrienoic acids, and soluble epoxide hydrolase. *Proc.Natl.Acad.Sci.U.S.A* **102**: 16747-16752.
- Liu Y, Zhu Y, Rannou F, Lee TS, Formentin K, Zeng L, Yuan X, Wang N, Chien S, Forman BM, Shyy JY. 2004.** Laminar flow activates peroxisome proliferator-activated receptor-gamma in vascular endothelial cells. *Circulation* **110**: 1128-1133.

- Livak KJ, Schmittgen TD.** 2001. Analysis of relative gene expression data using real-time quantitative PCR and the 2(-Delta Delta C(T)) Method. *Methods* **25:** 402-408.
- Lu YC, Chang SH, Hafner M, Li X, Tuschi T, Elemento O, Hla T.** 2014. ELAVL1 modulates transcriptome-wide miRNA binding in murine macrophages. *Cell Rep.* **9:** 2330-2343.
- Makinen PI, Yla-Herttuala S.** 2013. Therapeutic gene targeting approaches for the treatment of dyslipidemias and atherosclerosis. *Curr.Opin.Lipidol.* **24:** 116-122.
- Malek AM, Izumo S.** 1995. Control of endothelial cell gene expression by flow. *J.Biomech.* **28:** 1515-1528.
- Marin T, Gongol B, Chen Z, Woo B, Subramaniam S, Chien S, Shyy JY.** 2013. Mechanosensitive microRNAs-role in endothelial responses to shear stress and redox state. *Free Radic.Biol.Med.* **64:** 61-68.
- Matlung HL, Neele AE, Groen HC, van GK, Tuna BG, van WA, de VJ, Wentzel JJ, Hoogenboezem M, van Buul JD, VanBavel E, Bakker EN.** 2012. Transglutaminase activity regulates atherosclerotic plaque composition at locations exposed to oscillatory shear stress. *Atherosclerosis* **224:** 355-362.
- Matouk I, Raveh E, Ohana P, Lail RA, Gershtain E, Gilon M, de GN, Czerniak A, Hochberg A.** 2013. The increasing complexity of the oncofetal h19 gene locus: functional dissection and therapeutic intervention. *Int.J.Mol.Sci.* **14:** 4298-4316.
- Mattick JS.** 2009. The genetic signatures of noncoding RNAs. *PLoS.Genet.* **5:** e1000459.
- McCormick SM, Eskin SG, McIntire LV, Teng CL, Lu CM, Russell CG, Chittur KK.** 2001. DNA microarray reveals changes in gene expression of shear stressed human umbilical vein endothelial cells. *Proc.Natl.Acad.Sci.U.S.A* **98:** 8955-8960.
- McPhee JT, Nguyen LL, Ho KJ, Ozaki CK, Conte MS, Belkin M.** 2013. Risk prediction of 30-day readmission after infringuinal bypass for critical limb ischemia. *J.Vasc.Surg.* **57:** 1481-1488.
- Mittelstadt PR, Ashwell JD.** 2001. Inhibition of AP-1 by the glucocorticoid-inducible protein GILZ. *J.Biol.Chem.* **276:** 29603-29610.
- Miyakawa AA, de Lourdes JM, Krieger JE.** 2004. Identification of two novel shear stress responsive elements in rat angiotensin I converting enzyme promoter. *Physiol Genomics* **17:** 107-113.
- Moore LD, Le T, Fan G.** 2013. DNA methylation and its basic function. *Neuropsychopharmacology* **38:** 23-38.
- Morita S, Horii T, Kimura M, Arai Y, Kamei Y, Ogawa Y, Hatada I.** 2014. Paternal allele influences high fat diet-induced obesity. *PLoS.One.* **9:** e85477.

- Mukherjee N, Jacobs NC, Hafner M, Kennington EA, Nusbaum JD, Tuschl T, Blackshear PJ, Ohler U.** 2014. Global target mRNA specification and regulation by the RNA-binding protein ZFP36. *Genome Biol.* **15:** R12.
- Mullick AE, Soldau K, Kiosses WB, Bell TA, III, Tobias PS, Curtiss LK.** 2008. Increased endothelial expression of Toll-like receptor 2 at sites of disturbed blood flow exacerbates early atherogenic events. *J.Exp.Med.* **205:** 373-383.
- Mullis K, Falloona F, Scharf S, Saiki R, Horn G, Erlich H.** 1986. Specific enzymatic amplification of DNA in vitro: the polymerase chain reaction. *Cold Spring Harb.Symp.Quant.Biol.* **51 Pt 1:** 263-273.
- Mullis KB, Falloona FA.** 1987. Specific synthesis of DNA in vitro via a polymerase-catalyzed chain reaction. *Methods Enzymol.* **155:** 335-350.
- Nagel T, Resnick N, Dewey CF, Jr., Gimbrone MA, Jr.** 1999. Vascular endothelial cells respond to spatial gradients in fluid shear stress by enhanced activation of transcription factors. *Arterioscler.Thromb.Vasc.Biol.* **19:** 1825-1834.
- Ni CW, Hsieh HJ, Chao YJ, Wang DL.** 2003. Shear flow attenuates serum-induced STAT3 activation in endothelial cells. *J.Biol.Chem.* **278:** 19702-19708.
- Ni CW, Qiu H, Jo H.** 2011. MicroRNA-663 upregulated by oscillatory shear stress plays a role in inflammatory response of endothelial cells. *Am.J.Physiol Heart Circ.Physiol* **300:** H1762-H1769.
- Niu J, Kolattukudy PE.** 2009. Role of MCP-1 in cardiovascular disease: molecular mechanisms and clinical implications. *Clin.Sci.(Lond)* **117:** 95-109.
- Patel MJ, Blazing MA.** 2013. Inflammation and atherosclerosis: disease modulating therapies. *Curr.Treat.Options.Cardiovasc.Med.* **15:** 681-695.
- Perez SA, Mahaira LG, Demirtzoglou FJ, Sotiropoulou PA, Ioannidis P, Iliopoulos EG, Gritzapis AD, Sotiriadou NN, Baxevanis CN, Papamichail M.** 2005. A potential role for hydrocortisone in the positive regulation of IL-15-activated NK-cell proliferation and survival. *Blood* **106:** 158-166.
- Perkins E, Murphy SK, Murtha AP, Schildkraut J, Jirtle RL, mark-Wahnefried W, Forman MR, Kurtzberg J, Overcash F, Huang Z, Hoyo C.** 2012. Insulin-like growth factor 2/H19 methylation at birth and risk of overweight and obesity in children. *J.Pediatr.* **161:** 31-39.
- Pinheiro I, Dejager L, Petta I, Vandevyver S, Puimege L, Mahieu T, Ballegeer M, Van HF, Riccardi C, Vuylsteke M, Libert C.** 2013. LPS resistance of SPRET/Ei mice is mediated by Gilz, encoded by the Tsc22d3 gene on the X chromosome. *EMBO Mol.Med.* **5:** 456-470.
- Post WS, Goldschmidt-Clermont PJ, Wilhite CC, Heldman AW, Sussman MS, Ouyang P, Milliken EE, Issa JP.** 1999. Methylation of the estrogen receptor gene is associated with aging and atherosclerosis in the cardiovascular system. *Cardiovasc.Res.* **43:** 985-991.

- Qin X, Wang X, Wang Y, Tang Z, Cui Q, Xi J, Li YS, Chien S, Wang N.** 2010. MicroRNA-19a mediates the suppressive effect of laminar flow on cyclin D1 expression in human umbilical vein endothelial cells. *Proc.Natl.Acad.Sci.U.S.A* **107**: 3240-3244.
- Rachmilewitz J, Goshen R, Ariel I, Schneider T, de GN, Hochberg A.** 1992. Parental imprinting of the human H19 gene. *FEBS Lett.* **309**: 25-28.
- Raingeaud J, Gupta S, Rogers JS, Dickens M, Han J, Ulevitch RJ, Davis RJ.** 1995. Pro-inflammatory cytokines and environmental stress cause p38 mitogen-activated protein kinase activation by dual phosphorylation on tyrosine and threonine. *J.Biol.Chem.* **270**: 7420-7426.
- Rao X, Zhong J, Zhang S, Zhang Y, Yu Q, Yang P, Wang MH, Fulton DJ, Shi H, Dong Z, Wang D, Wang CY.** 2011. Loss of methyl-CpG-binding domain protein 2 enhances endothelial angiogenesis and protects mice against hind-limb ischemic injury. *Circulation* **123**: 2964-2974.
- Resnick N, Collins T, Atkinson W, Bonthron DT, Dewey CF, Jr., Gimbron MA, Jr.** 1993. Platelet-derived growth factor B chain promoter contains a cis-acting fluid shear-stress-responsive element. *Proc.Natl.Acad.Sci.U.S.A* **90**: 7908.
- Resnick N, Yahav H, Shay-Salit A, Shushy M, Schubert S, Zilberman LC, Woffovitz E.** 2003c. Fluid shear stress and the vascular endothelium: for better and for worse. *Prog.Biophys.Mol.Biol.* **81**: 177-199.
- Rhee WJ, Ni CW, Zheng Z, Chang K, Jo H, Bao G.** 2010. HuR regulates the expression of stress-sensitive genes and mediates inflammatory response in human umbilical vein endothelial cells. *Proc.Natl.Acad.Sci.U.S.A* **107**: 6858-6863.
- Ronkina N, Menon MB, Schwermann J, Tiedje C, Hitti E, Kotlyarov A, Gaestel M.** 2010. MAPKAP kinases MK2 and MK3 in inflammation: complex regulation of TNF biosynthesis via expression and phosphorylation of tristetraprolin. *Biochem.Pharmacol.* **80**: 1915-1920.
- Rosenberger CM, Podymyminogin RL, Navarro G, Zhao GW, Askovich PS, Weiss MJ, Aderem A.** 2012. miR-451 regulates dendritic cell cytokine responses to influenza infection. *J.Immunol.* **189**: 5965-5975.
- Roy H, Bhardwaj S, Yla-Herttuala S.** 2009. Molecular genetics of atherosclerosis. *Hum.Genet.* **125**: 467-491.
- Rubanyi GM, Romero JC, Vanhoutte PM.** 1986. Flow-induced release of endothelium-derived relaxing factor. *Am.J.Physiol* **250**: H1145-H1149.
- Ryter SW, Alam J, Choi AM.** 2006. Heme oxygenase-1/carbon monoxide: from basic science to therapeutic applications. *Physiol Rev.* **86**: 583-650.
- Saito T, Hasegawa Y, Ishigaki Y, Yamada T, Gao J, Imai J, Uno K, Kaneko K, Ogihara T, Shimosawa T, Asano T, Fujita T, Oka Y, Katagiri H.** 2013. Importance of endothelial NF-kappaB signalling in vascular remodelling and aortic aneurysm formation. *Cardiovasc.Res.* **97**: 106-114.

- Sanduja S, Blanco FF, Dixon DA.** 2011. The roles of TTP and BRF proteins in regulated mRNA decay. *Wiley Interdiscip Rev RNA*. **2**: 42-57.
- Schichl YM, Resch U, Hofer-Warbinek R, de MR.** 2009. Tristetraprolin impairs NF-kappaB/p65 nuclear translocation. *J Biol Chem*. **284**: 29571-29581.
- Schoneveld AH, Hoefer I, Sluijter JP, Laman JD, de Kleijn DP, Pasterkamp G.** 2008. Atherosclerotic lesion development and Toll like receptor 2 and 4 responsiveness. *Atherosclerosis* **197**: 95-104.
- Shaik SS, Soltau TD, Chaturvedi G, Totapally B, Hagood JS, Andrews WW, Athar M, Voitenok NN, Killingsworth CR, Patel RP, Fallon MB, Maheshwari A.** 2009b. Low intensity shear stress increases endothelial ELR+ CXC chemokine production via a focal adhesion kinase-p38 β MAPK-NF- κ B pathway. *J Biol Chem*. **284**: 5945-5955.
- Shen J, Chandrasekharan UM, Ashraf MZ, Long E, Morton RE, Liu Y, Smith JD, DiCorleto PE.** 2010. Lack of mitogen-activated protein kinase phosphatase-1 protects ApoE-null mice against atherosclerosis. *Circ Res*. **106**: 902-910.
- Shi JX, Su X, Xu J, Zhang WY, Shi Y.** 2012. MK2 posttranscriptionally regulates TNF-alpha-induced expression of ICAM-1 and IL-8 via tristetraprolin in human pulmonary microvascular endothelial cells. *Am J Physiol Lung Cell Mol Physiol* **302**: L793-L799.
- Shi X, Shi W, Li Q, Song B, Wan M, Bai S, Cao X.** 2003. A glucocorticoid-induced leucine-zipper protein, GILZ, inhibits adipogenesis of mesenchymal cells. *EMBO Rep*. **4**: 374-380.
- Shuto T, Xu H, Wang B, Han J, Kai H, Gu XX, Murphy TF, Lim DJ, Li JD.** 2001. Activation of NF- κ B by nontypeable *Hemophilus influenzae* is mediated by toll-like receptor 2-TAK1-dependent NIK-IKK alpha/beta- κ B alpha and MKK3/6-p38 MAP kinase signaling pathways in epithelial cells. *Proc Natl Acad Sci U S A* **98**: 8774-8779.
- Shyy JY, Li YS, Lin MC, Chen W, Yuan S, Usami S, Chien S.** 1995. Multiple cis-elements mediate shear stress-induced gene expression. *J Biomech*. **28**: 1451-1457.
- Silberman M, Barac YD, Yahav H, Wolfowitz E, Einav S, Resnick N, Binah O.** 2009. Shear stress-induced transcriptional regulation via hybrid promoters as a potential tool for promoting angiogenesis. *Angiogenesis*. **12**: 231-242.
- Siow RC, Sato H, Mann GE.** 1999. Heme oxygenase-carbon monoxide signalling pathway in atherosclerosis: anti-atherogenic actions of bilirubin and carbon monoxide? *Cardiovasc Res*. **41**: 385-394.
- Smoak K, Cidlowski JA.** 2006. Glucocorticoids regulate tristetraprolin synthesis and posttranscriptionally regulate tumor necrosis factor alpha inflammatory signaling. *Mol Cell Biol*. **26**: 9126-9135.
- Son DJ, Kumar S, Takabe W, Kim CW, Ni CW, berts-Grill N, Jang IH, Kim S, Kim W, Won KS, Baker AH, Woong SJ, Ferrara KW, Jo H.** 2013. The atypical mech-

anosensitive microRNA-712 derived from pre-ribosomal RNA induces endothelial inflammation and atherosclerosis. *Nat.Commun.* **4**: 3000.

Soundararajan R, Zhang TT, Wang J, Vandewalle A, Pearce D. 2005. A novel role for glucocorticoid-induced leucine zipper protein in epithelial sodium channel-mediated sodium transport. *J.Biol.Chem.* **280**: 39970-39981.

Srinivasan M, Blackburn C, Lahiri DK. 2014. Functional characterization of a competitive peptide antagonist of p65 in human macrophage-like cells suggests therapeutic potential for chronic inflammation. *Drug Des Devel.Ther.* **8**: 2409-2421.

Srinivasan M, Janardhanam S. 2011. Novel p65 Binding Glucocorticoid-induced Leucine Zipper Peptide Suppresses Experimental Autoimmune Encephalomyelitis. *J.Biol.Chem.* **286**: 44799-44810.

Steck E, Boeuf S, Gabler J, Werth N, Schnatzer P, Diederichs S, Richter W. 2012b. Regulation of H19 and its encoded microRNA-675 in osteoarthritis and under anabolic and catabolic in vitro conditions. *J.Mol.Med.(Berl)* **90**: 1185-1195.

Stefani G, Slack FJ. 2008. Small non-coding RNAs in animal development. *Nat.Rev.Mol.Cell Biol.* **9**: 219-230.

Stocker R, Perrella MA. 2006. Heme oxygenase-1: a novel drug target for atherosclerotic diseases? *Circulation* **114**: 2178-2189.

Stoecklin G, Stubbs T, Kedersha N, Wax S, Rigby WF, Blackwell TK, Anderson P. 2004. MK2-induced tristetraprolin:14-3-3 complexes prevent stress granule association and ARE-mRNA decay. *EMBO J.* **23**: 1313-1324.

Stoecklin G, Tenenbaum SA, Mayo T, Chittur SV, George AD, Baroni TE, Blackshear PJ, Anderson P. 2008. Genome-wide analysis identifies interleukin-10 mRNA as target of tristetraprolin. *J.Biol.Chem.* **283**: 11689-11699.

Stuhlmuller B, Kunisch E, Franz J, Martinez-Gamboa L, Hernandez MM, Pruss A, Ulbrich N, Erdmann VA, Burmester GR, Kinne RW. 2003. Detection of oncofetal h19 RNA in rheumatoid arthritis synovial tissue. *Am.J.Pathol.* **163**: 901-911.

Su B, Karin M. 1996. Mitogen-activated protein kinase cascades and regulation of gene expression. *Curr.Opin.Immunol.* **8**: 402-411.

Sucosky P, Balachandran K, Elhammali A, Jo H, Yoganathan AP. 2009. Altered shear stress stimulates upregulation of endothelial VCAM-1 and ICAM-1 in a BMP-4- and TGF-beta1-dependent pathway. *Arterioscler.Thromb.Vasc.Biol.* **29**: 254-260.

Szmitko PE, Wang CH, Weisel RD, de Almeida Jr, Anderson TJ, Verma S. 2003. New markers of inflammation and endothelial cell activation: Part I. *Circulation* **108**: 1917-1923.

Takada Y, Shinkai F, Kondo S, Yamamoto S, Tsuboi H, Korenaga R, Ando J. 1994. Fluid shear stress increases the expression of thrombomodulin by cultured human endothelial cells. *Biochem.Biophys.Res.Commun.* **205**: 1345-1352.

- Taniguchi T, Sullivan MJ, Ogawa O, Reeve AE. 1995.** Epigenetic changes encompassing the IGF2/H19 locus associated with relaxation of IGF2 imprinting and silencing of H19 in Wilms tumor. *Proc.Natl.Acad.Sci.U.S.A* **92:** 2159-2163.
- Tenhuinen R, Marver HS, Schmid R. 1968.** The enzymatic conversion of heme to bilirubin by microsomal heme oxygenase. *Proc.Natl.Acad.Sci.U.S.A* **61:** 748-755.
- Thiagarajah AS, Eades LE, Thomas PR, Guymer EK, Morand EF, Clarke DM, Leech M. 2014.** GILZ: Glitzing up our understanding of the glucocorticoid receptor in psychopathology. *Brain Res.* **1574:** 60-69.
- Thompson RC, Allam AH, Lombardi GP, Wann LS, Sutherland ML, Sutherland JD, Soliman MA, Frohlich B, Mininberg DT, Monge JM, Vallodolid CM, Cox SL, bd el-Maksoud G, Badr I, Miyamoto MI, el-Halim Nur el-Din, Narula J, Finch CE, Thomas GS. 2013.** Atherosclerosis across 4000 years of human history: the Horus study of four ancient populations. *Lancet* **381:** 1211-1222.
- Toh ML, Yang Y, Leech M, Santos L, Morand EF. 2004.** Expression of mitogen-activated protein kinase phosphatase 1, a negative regulator of the mitogen-activated protein kinases, in rheumatoid arthritis: up-regulation by interleukin-1beta and glucocorticoids. *Arthritis Rheum.* **50:** 3118-3128.
- Torzewski M, Bhakdi S. 2013.** Complement and atherosclerosis-united to the point of no return? *Clin.Biochem.* **46:** 20-25.
- Tsai CS, Chen DL, Lin SJ, Tsai JC, Lin TC, Lin CY, Chen YH, Huang GS, Tsai HY, Lin FY, Li CY. 2009.** TNF-alpha inhibits toll-like receptor 4 expression on monocytic cells via tristetraprolin during cardiopulmonary bypass. *Shock* **32:** 40-48.
- Tucci M, Quatraro C, Frassanito MA, Silvestris F. 2006.** Deregulated expression of monocyte chemoattractant protein-1 (MCP-1) in arterial hypertension: role in endothelial inflammation and atheromasia. *J.Hypertens.* **24:** 1307-1318.
- Tybl E, Shi FD, Kessler SM, Tierling S, Walter J, Bohle RM, Wieland S, Zhang J, Tan EM, Kiemer AK. 2011.** Overexpression of the IGF2-mRNA binding protein p62 in transgenic mice induces a steatotic phenotype. *J.Hepatol.* **54:** 994-1001.
- Tynan SH, Lundein SG, Allan GF. 2004.** Cell type-specific bidirectional regulation of the glucocorticoid-induced leucine zipper (GILZ) gene by estrogen. *J.Steroid Biochem.Mol.Biol.* **91:** 225-239.
- Tzima E. 2006.** Role of small GTPases in endothelial cytoskeletal dynamics and the shear stress response. *Circ.Res.* **98:** 176-185.
- Tzima E, Irani-Tehrani M, Kiosses WB, Dejana E, Schultz DA, Engelhardt B, Cao G, DeLisser H, Schwartz MA. 2005.** A mechanosensory complex that mediates the endothelial cell response to fluid shear stress. *Nature* **437:** 426-431.
- Urschel K, Cicha I, Daniel WG, Garlichs CD. 2012.** Shear stress patterns affect the secreted chemokine profile in endothelial cells. *Clin.Hemorheol.Microcirc.* **50:** 143-152.

- Uyttenhove C, Van SJ.** 2012. Anti-cytokine auto-vaccinations as tools for the analysis of cytokine function in vivo. *Cytokine Growth Factor Rev.* **23:** 1-6.
- van Diepen JA, Berbee JF, Havekes LM, Rensen PC.** 2013. Interactions between inflammation and lipid metabolism: relevance for efficacy of anti-inflammatory drugs in the treatment of atherosclerosis. *Atherosclerosis* **228:** 306-315.
- Vreugdenhil E, Verissimo CS, Mariman R, Kamphorst JT, Barbosa JS, Zweers T, Champagne DL, Schouten T, Meijer OC, de Kloet ER, Fitzsimons CP.** 2009. MicroRNA 18 and 124a down-regulate the glucocorticoid receptor: implications for glucocorticoid responsiveness in the brain. *Endocrinology* **150:** 2220-2228.
- Wagner CT, Durante W, Christodoulides N, Hellums JD, Schafer AI.** 1997. Hemodynamic forces induce the expression of heme oxygenase in cultured vascular smooth muscle cells. *J.Clin.Invest* **100:** 589-596.
- Walpolo PL, Gotlieb AI, Cybulsky MI, Langille BL.** 1995. Expression of ICAM-1 and VCAM-1 and monocyte adherence in arteries exposed to altered shear stress. *Arterioscler.Thromb.Vasc.Biol.* **15:** 2-10.
- Walpolo PL, Gotlieb AI, Langille BL.** 1993. Monocyte adhesion and changes in endothelial cell number, morphology, and F-actin distribution elicited by low shear stress in vivo. *Am.J.Pathol.* **142:** 1392-1400.
- Wancket LM, Frazier WJ, Liu Y.** 2012. Mitogen-activated protein kinase phosphatase (MKP)-1 in immunology, physiology, and disease. *Life Sci.* **90:** 237-248.
- Wang C, Baker BM, Chen CS, Schwartz MA.** 2013a. Endothelial cell sensing of flow direction. *Arterioscler.Thromb.Vasc.Biol.* **33:** 2130-2136.
- Wang N, Butler JP, Ingber DE.** 1993. Mechanotransduction across the cell surface and through the cytoskeleton. *Science* **260:** 1124-1127.
- Wang N, Miao H, Li YS, Zhang P, Haga JH, Hu Y, Young A, Yuan S, Nguyen P, Wu CC, Chien S.** 2006. Shear stress regulation of Kruppel-like factor 2 expression is flow pattern-specific. *Biochem.Biophys.Res.Commun.* **341:** 1244-1251.
- Wang W, Lee Y, Lee CH.** 2013c. Review: The physiological and computational approaches for atherosclerosis treatment. *Int.J.Cardiol.* **167:** 1664-1676.
- Wang XM, Kim HP, Nakahira K, Ryter SW, Choi AM.** 2009. The heme oxygenase-1/carbon monoxide pathway suppresses TLR4 signaling by regulating the interaction of TLR4 with caveolin-1. *J.Immunol.* **182:** 3809-3818.
- Wang Y, Miao X, Liu Y, Li F, Liu Q, Sun J, Cai L.** 2014. Dysregulation of histone acetyltransferases and deacetylases in cardiovascular diseases. *Oxid.Med.Cell Longev.* **2014:** 641979.
- Warabi E, Takabe W, Minami T, Inoue K, Itoh K, Yamamoto M, Ishii T, Kodama T, Noguchi N.** 2007. Shear stress stabilizes NF-E2-related factor 2 and induces anti-oxidant genes in endothelial cells: role of reactive oxygen/nitrogen species. *Free Radic.Biol.Med.* **42:** 260-269.

- Weber C, Schober A, Zernecke A.** 2010a. MicroRNAs in arterial remodelling, inflammation and atherosclerosis. *Curr.Drug Targets.* **11:** 950-956.
- Weber M, Baker MB, Moore JP, Searles CD.** 2010b. MiR-21 is induced in endothelial cells by shear stress and modulates apoptosis and eNOS activity. *Biochem.Biophys.Res.Commun.* **393:** 643-648.
- Weber M, Milligan L, Delalbre A, Antoine E, Brunel C, Cathala G, Forne T.** 2001. Extensive tissue-specific variation of allelic methylation in the Igf2 gene during mouse fetal development: relation to expression and imprinting. *Mech.Dev.* **101:** 133-141.
- Weber NC, Blumenthal SB, Hartung T, Vollmar AM, Kiemer AK.** 2003. ANP inhibits TNF-alpha-induced endothelial MCP-1 expression--involvement of p38 MAPK and MKP-1. *J.Leukoc.Biol.* **74:** 932-941.
- Wei Y, Nazari-Jahantigh M, Neth P, Weber C, Schober A.** 2013. MicroRNA-126, -145, and -155: a therapeutic triad in atherosclerosis? *Arterioscler.Thromb.Vasc.Biol.* **33:** 449-454.
- White CR, Frangos JA.** 2007. The shear stress of it all: the cell membrane and mechanochemical transduction. *Philos.Trans.R.Soc.Lond B Biol.Sci.* **362:** 1459-1467.
- Whitmarsh AJ, Davis RJ.** 1996. Transcription factor AP-1 regulation by mitogen-activated protein kinase signal transduction pathways. *J.Mol.Med.(Berl)* **74:** 589-607.
- Williams KJ, Tabas I.** 1998. The response-to-retention hypothesis of atherogenesis reinforced. *Curr.Opin.Lipidol.* **9:** 471-474.
- Winter J, Jung S, Keller S, Gregory RI, Diederichs S.** 2009. Many roads to maturity: microRNA biogenesis pathways and their regulation. *Nat.Cell Biol.* **11:** 228-234.
- Wu W, Xiao H, Laguna-Fernandez A, Villarreal G, Jr., Wang KC, Geary GG, Zhang Y, Wang WC, Huang HD, Zhou J, Li YS, Chien S, Garcia-Cardenas G, Shyy JY.** 2011. Flow-Dependent Regulation of Kruppel-Like Factor 2 Is Mediated by MicroRNA-92a. *Circulation* **124:** 633-641.
- Xing F, Jiang Y, Liu J, Zhao K, Mo Y, Qin Q, Wang J, Ouyang J, Zeng Y.** 2006. Role of AP1 element in the activation of human eNOS promoter by lysophosphatidyl-choline. *J.Cell Biochem.* **98:** 872-884.
- Yan MS, Matouk CC, Marsden PA.** 2010. Epigenetics of the vascular endothelium. *J.Appl.Physiol (1985.)* **109:** 916-926.
- Yang J, Lu YW, Lu MM, Leng RX, Pan HF, Ye DQ.** 2013. MicroRNA-101, mitogen-activated protein kinases and mitogen-activated protein kinases phosphatase-1 in systemic lupus erythematosus. *Lupus* **22:** 115-120.
- Yang QW, Mou L, Lv FL, Wang JZ, Wang L, Zhou HJ, Gao D.** 2005. Role of Toll-like receptor 4/NF-kappaB pathway in monocyte-endothelial adhesion induced by low shear stress and ox-LDL. *Biorheology* **42:** 225-236.

- Yao Y, Rabodzey A, Dewey CF, Jr. 2007.** Glycocalyx modulates the motility and proliferative response of vascular endothelium to fluid shear stress. *Am.J.Physiol Heart Circ.Physiol* **293:** H1023-H1030.
- Yazdani SK, Otsuka F, Nakano M, Finn AV, Virmani R. 2012.** Do animal models of vein graft atherosclerosis predict outcomes in man? *Atherosclerosis* **223:** 102-105.
- Yin W, Shanmugavelayudam SK, Rubenstein DA. 2011.** The effect of physiologically relevant dynamic shear stress on platelet and endothelial cell activation. *Thromb.Res.* **127:** 235-241.
- Young PR, McLaughlin MM, Kumar S, Kassis S, Doyle ML, McNulty D, Gallagher TF, Fisher S, McDonnell PC, Carr SA, Huddleston MJ, Seibel G, Porter TG, Livi GP, Adams JL, Lee JC. 1997.** Pyridinyl imidazole inhibitors of p38 mitogen-activated protein kinase bind in the ATP site. *J.Biol.Chem.* **272:** 12116-12121.
- Zaina S, Heyn H, Carmona FJ, Varol N, Sayols S, Condom E, Ramirez-Ruz J, Gomez A, Goncalves I, Moran S, Esteller M. 2014.** A DNA Methylation Map of Human Atherosclerosis. *Circ.Cardiovasc.Genet.*
- Zaina S, Nilsson J. 2003.** Insulin-like growth factor II and its receptors in atherosclerosis and in conditions predisposing to atherosclerosis. *Curr.Opin.Lipidol.* **14:** 483-489.
- Zaina S, Pettersson L, Ahren B, Branen L, Hassan AB, Lindholm M, Mattsson R, Thyberg J, Nilsson J. 2002.** Insulin-like growth factor II plays a central role in atherosclerosis in a mouse model. *J.Biol.Chem.* **277:** 4505-4511.
- Zakkar M, Chaudhury H, Sandvik G, Enesa K, Luong IA, Cuhlmann S, Mason JC, Krams R, Clark AR, Haskard DO, Evans PC. 2008.** Increased endothelial mitogen-activated protein kinase phosphatase-1 expression suppresses proinflammatory activation at sites that are resistant to atherosclerosis. *Circ.Res.* **103:** 726-732.
- Zawada AM, Rogacev KS, Muller S, Rotter B, Winter P, Fliser D, Heine GH. 2014.** Massive analysis of cDNA Ends (MACE) and miRNA expression profiling identifies proatherogenic pathways in chronic kidney disease. *Epigenetics.* **9:** 161-172.
- Zeng W, Li L, Yuan W, Wei Y, Mi J, Sun J, Wen C, Zhang W, Ying D, Zhu C. 2009.** A20 overexpression inhibits low shear flow-induced CD14-positive monocyte recruitment to endothelial cells. *Biorheology* **46:** 21-30.
- Zhang H, Taylor WR, Joseph G, Caracciolo V, Gonzales DM, Sidell N, Seli E, Blackshear PJ, Kallen CB. 2013.** mRNA-binding protein ZFP36 is expressed in atherosclerotic lesions and reduces inflammation in aortic endothelial cells. *Arterioscler.Thromb.Vasc.Biol.* **33:** 1212-1220.
- Zhang XH, Lu X, Long XB, You XJ, Gao QX, Cui YH, Liu Z. 2009.** Chronic rhinosinusitis with and without nasal polyps is associated with decreased expression of glucocorticoid-induced leucine zipper. *Clin.Exp.Allergy* **39:** 647-654.
- Zhang Y, Lai Y, Chen HQ, Liu YF. 2012.** AP-1 and NF-kappaB transcriptionally regulate interleukin-8 in EA.Hy926 cells under shear stress. *Cell Biol.Int.* **36:** 251-254.

Zhao W, Liu M, D'Silva NJ, Kirkwood KL. 2011. Tristetraprolin regulates interleukin-6 expression through p38 MAPK-dependent affinity changes with mRNA 3' untranslated region. *J.Interferon Cytokine Res.* **31:** 629-637.

Zhou J, Li YS, Wang KC, Chien S. 2014. Epigenetic Mechanism in Regulation of Endothelial Function by Disturbed Flow: Induction of DNA Hypermethylation by DNMT1. *Cell Mol.Bioeng.* **7:** 218-224.

Zhou J, Wang KC, Wu W, Subramaniam S, Shyy JY, Chiu JJ, Li JY, Chien S. 2011. MicroRNA-21 targets peroxisome proliferators-activated receptor-alpha in an autoregulatory loop to modulate flow-induced endothelial inflammation. *Proc.Natl.Acad.Sci.U.S.A* **108:** 10355-10360.

Zhu CH, Ying DJ, Mi JH, Zhu XH, Sun JS, Cui XP. 2004. Low shear stress regulates monocyte adhesion to oxidized lipid-induced endothelial cells via an IkappaBalpha dependent pathway. *Biorheology* **41:** 127-137.

Zhu QY, Liu Q, Chen JX, Lan K, Ge BX. 2010. MicroRNA-101 targets MAPK phosphatase-1 to regulate the activation of MAPKs in macrophages. *J.Immunol.* **185:** 7435-7442.

Publications

Original publications

Hahn RT, Hoppstädter J, Hirschfelder K, Diesel B., Kessler SM, Huwer H, Kiemer AK. Downregulation of the glucocorticoid-induced leucine zipper (GILZ) promotes vascular inflammation. *Atherosclerosis*. 2014 Jun;234(2):391-400

Diesel B, Ripoche N, **Risch RT**, Tierling S, Walter J, Kiemer AK. Inflammation-induced up-regulation of TLR2 expression in human endothelial cells is independent of differential methylation in the TLR2 promoter CpG island. *Innate Immun*. 2012 Feb;18(1):112-23

Lack of endothelial glucocorticoid-induced leucine zipper (GILZ) induction under atherogenic flow conditions. *In preparation*

Abstract to talks, Poster

RT Risch, K Hirschfelder, J Hoppstädter, B Diesel, H Huwer, AK Kiemer. Der anti-inflammatorische Mediator GILZ ist ein negativer Regulator der TLR2 Expression im Gefäß, Herbsttagung der Sektion Zellbiologie der DGP in Homburg, (11.11.2011), *Pneumologie* 2011; 65-A48

Kessler SM, Pokorny J, **Risch R**, Zimmer V, Diesel B, Lammert F, Bohle RM, Kiemer AK. The non-translated *H19* RNA acts as a tumor suppressor in human hepatocellular carcinoma. Poster presentation at the Keystone meeting “Non-coding RNAs and cancer”, Banff, Alberta, Canada. *Conference proceedings*, 2011.

Acknowledgements

Zuerst möchte ich mich ganz herzlich bei Frau Prof. Dr. Alexandra K. Kiemer bedanken, dass ich in ihrem Arbeitskreis mit diesem interessanten Thema promovieren durfte. Außerdem danke ich ihr vor allem für ihr Verständnis, ihre Geduld, ihren Zuspruch sowie die ständige Diskussionsbereitschaft und die sehr gute Unterstützung in der ganzen Zeit, auch während der Babypause.

Prof. Dr. Claus-Michael Lehr danke ich für die freundliche Übernahme des Zweitgutachtens.

Aus der Arbeitsgruppe von Herrn Prof. Dr. Jörn Walter danke ich Viktoria Weinhold, Beate Schmitt, Christina LO Porto für die Übernahme experimenteller Arbeiten bei der DNA Untersuchung. Besonders gilt mein Dank Herrn Dr. Sascha Tierling für die gute Zusammenarbeit und Unterstützung bei den SNuPE Analysen sowie für die Teilnahme als wissenschaftlicher Mitarbeiter in der Prüfungskommission.

Ein großer Dank geht an die Spender der Nabelschnüre sowie Dr. Clemens Bartz sowie den Mitarbeitern vom Winterberg Klinikum Saarbrücken für die Bereitstellung der Nabelschnüre.

In gleicher Weise danke ich auch den Spendern von gesunden und arteriosklerotischen Gefäßproben sowie besonders Herrn Prof. Dr. Hanno Huwer und seinen Mitarbeitern von der SHG Klinik Völklingen für die Bereitstellung der Proben.

Den Mitarbeitern der Arbeitsgruppe danke ich für die gute Zusammenarbeit. Insbesondere danke ich Sonja Kessler, Astrid Decker, Jessica Hoppstädter, Yvette Simon, der ehemaligen Mitarbeiterin Kerstin Hirschfelder und vor allem Stephan Laggai für den nötigen Beistand bei diesem Abenteuer sowie die schönen Momente während und auch außerhalb der Arbeitszeit. Außerdem danke ich Jessica Hoppstädter, Nina Hachenthal, Britta Diesel, Sonja Kessler, Yvette Simon, Christina Schultheiß, Ksenia Astanina und Stephan Laggai für die sehr hilfreichen Diskussionen und für die tatkräftige experimentelle Unterstützung während meiner Schwangerschaft und darüber hinaus.

Ich bedanke mich auch recht herzlich bei Theo Ranßweiler für die gute experimentelle Unterstützung bei der Isolierung der Nabelschnurzellen. Außerdem danke ich Christian und Alexander Hahn für die gute Unterstützung bei Design und Herstellung der Flow-Kammern.

Tausend Dank gehen an meinem Ehemann Christian Hahn für seine ständige Unterstützung in guten und in schlechten Zeiten und an meine Eltern Margit und Peter Risch, denn sie sind die besten, die man sich vorstellen kann. Außerdem danke ich besonders meiner Familie für ihre ständige Anteilnahme und Unterstützung.